NTNU

Norwegian University of
Science and Technology

Dynamic process simulation of heat recovery steam generator designed for offshore oil and gas installations

Magnus Gule

Master of Energy and Environmental Engineering
Submission date: September 2016
Supervisor: Lars Olof Nord, EPT
Co-supervisor: Rubén Mocholí Montañés, EPT

Norwegian University of Science and Technology
Department of Energy and Process Engineering

NTNU

Norwegian University
of Science and Technology

Department of Energy
and Process Engineering

EPT-M-2016-47

MASTER THESIS

for

student Magnus Gule

Spring 2016

Dynamic process simulation of heat recovery steam generator designed for offshore oil and gas installations

Background and objective

On offshore oil and gas installations the power demand is high and changes over time. The power plant should be flexible to be able to adjust to the needs of the oil and gas processes on the platform or FPSO. Simple cycle gas turbines (GT) are mostly powering the today's installations. To increase the efficiency, another cycle could be added after the gas turbine to recuperate some of the heat in the exhaust gases from the GT, for example a steam cycle.

The Master's thesis work should build on the specialization project completed in March 2016, where the main objective was to design and build a dynamic process models of the full steam cycle in a process simulation software and study the transient behavior (changes over time) for the process model. The Master's thesis will focus on the heat recovery steam generator (HRSG) of the steam cycle to improve on the previously developed model. The main focus should be directed to transients related to load changes but plant start-up and other transients could also be considered. The starting design (geometry, etc.) of the HRSG should be given to the student.

The main objective for the Master's thesis is to develop a detailed dynamic HRSG model to predict the transient behavior during typical offshore transients.

The following tasks are to be considered:

1. Literature study on dynamic process models of HRSGs.
2. Evaluation of different open-source libraries for power plant modeling within the Modelica environment. Alternatives include ThermoPower and ClaRa.
3. Implementation of heat transfer and pressure drop correlations.
4. Further development of the HRSG model from the specialization project.
5. Model validation based on literature or plant data.
6. Evaluation of the HRSG transient behavior.

Within 14 days of receiving the written text on the master thesis, the candidate shall submit a research plan for his project to the department.

When the thesis is evaluated, emphasis is put on processing of the results, and that they are presented in tabular and/or graphic form in a clear manner, and that they are analyzed carefully.

The thesis should be formulated as a research report in English with summary, conclusion, literature references, table of contents etc. During the preparation of the text, the candidate should make an effort to produce a well-structured and easily readable report. In order to ease the evaluation of the thesis, it is important that the cross-references are correct. In the making of the report, strong emphasis should be placed on both a thorough discussion of the results and an orderly presentation.

The candidate is requested to initiate and keep close contact with his/her academic supervisor(s) throughout the working period. The candidate must follow the rules and regulations of NTNU as well as passive directions given by the Department of Energy and Process Engineering.

Risk assessment of the candidate's work shall be carried out according to the department's procedures. The risk assessment must be documented and included as part of the final report. Events related to the candidate's work adversely affecting the health, safety or security, must be documented and included as part of the final report. If the documentation on risk assessment represents a large number of pages, the full version is to be submitted electronically to the supervisor and an excerpt is included in the report.

Pursuant to “Regulations concerning the supplementary provisions to the technology study program/Master of Science” at NTNU §20, the Department reserves the permission to utilize all the results and data for teaching and research purposes as well as in future publications.

The final report is to be submitted digitally in DAIM. Based on an agreement with the supervisor, the final report and other material and documents may be given to the supervisor in digital format.

☐ Work to be done in lab (Water power lab, Fluids engineering lab, Thermal engineering lab)
☐ Field work

Department of Energy and Process Engineering, 15 March 2016

Olav Bolland	Lars Nord
Department Head	Academic Supervisor

Co-supervisor: Rubén Mocholí Montañés (Ph.D. Candidate, NTNU)

Preface

This project was written the summer of 2016 at NTNU, Department of Energy and Process Engineering. I would like to thank my supervisor Lars Olaf Nord and especially co-supervisor Rubén Mocholí Montañés for technical guidance and advices on structuring the master-thesis and not at least programming troubleshooting.

Abstract

In the offshore oil and gas sector combined cycle (CC) technology is a viable alternative to the traditional gas turbines and land-based power supply on both platforms and FPSOs. In 2015 gas turbines accounted alone for 81% of all greenhouse emitted on the Norwegian Continental Shelf. If integrating heat recovery steam generators (HRSGs) to these gas turbines with corresponding steam turbines, power output can be increased by 50 percent compared to a single gas-turbine cycle.

In Europa, modelling the dynamics of combined cycles have been of growing interest since the beginning of 2000, and especially lately with eruptive marked renewables. Most dynamic modelling software are based on conventional drum-based HRSGs, but few have specialized in once-through systems which is desired in offshore operations due of its fast cycle characteristics.

A comparative literature study of different HRSG-skids was evaluated together with different part-load control systems for the steam cycle. A set of open-source libraries were evaluated and compared in detail for modelling of a once-through steam cycle from steady-state data resembling the CC from Oseberg D. Heat transfer correlations (HTC) for the HRSG including ESCOA, VDI and Næss was rated and implemented in a final model built by the library ClaRa and transients simulated through part-load gas turbine operation.

Feedwater and condenser controls were implemented, but the lack of both dynamic and stable heat exchanger models limits the applicability for simulating real transients. Incomplete libraries, lack of documentation and low level of detail resulted a custom heat exchanger being built including heat transfer correlations of Næss. Due to high complexity and instability of the current model, implementing more control systems and detailed steam models seems improbable. Suggested strategies to improve the model further includes removal of visualization components and replace models with lower level of detail including valves, water tanks and pipes, as well as the completion of the an ESCOA heat exchanger model.

Contents

Acronyms and Abbreviations

CCPP	combined cycle power plant
CCGT	combined cycle gas turbines
CC	combined cycle
EGT	Exhaust Gas Temperature
FPSO	Floating Production, Storage and Offloading
HP	high pressure
HRSG	Heat recovery steam generator
HT	heat transfer
HTC	heat transfer coefficient
IC	Initial Conditions
LP	low pressure
OS	open source
TPL	Thermopower (library)
TSP	ThermoSysPro (library)

List of figures

List of tables

1 Background and motivation

1.1 Current status of the NCS power supply

The offshore industry is today completely reliant on flexible and secure energy sources for their day-to-day operations of oil and gas processing. Both offshore platforms and FPSOs (Floating Production, Storage and Offloading) can consume power rates reaching 50 to 100 megawatts for various processes [1]. To cover their need, the majority of the North Sea installations run on simple gas turbine cycles to supply them with mechanical and electric power.

In 2015 gas turbines alone accounted for 81% of all CO2-emissions in the Norwegian petroleum sector (NPS) [2]. With political will to reduce greenhouse gas emissions (GHGs) and the coherent increase in carbon-tax in 2013, the Norwegian offshore industry is urged to develop less emissive alternatives.

The two most feasible options evaluated to date are implementing combined cycle technology or deploying HVDC power-cables on the seabed connected to the onshore power grid. Statoil announced in 2015 the installation of a HVDC cable to the newly developed Johan Sverdrup field [3], with secondary plans to electrify nearby oil and gas fields like Edvard Grieg, Ivar Aasen, and Gina Krog. Since 2003 both Statoil's Troll and BP's Valhall platforms have been partially operating on onshore electricity [1].

Nevertheless, electrification is primarily considered for the largest fields where production has not peaked or lifetime is still long. Many technical challenges, requirement of heat, on top of the high investment costs, don't always make it electrification justifiable nor attractive to the majority of smaller oil and gas fields which is in the investment order of below 10-20 billion NOK.

Figure 1 illustrates the remaining investments for all fields on the NCS taken July 2016 [4]. It does not include Johan Sverdrup since it is already completely invested. Capitalized and colored callouts show existing fields operating with combined cycles, and others with HVDC cables in plan or operating. It also shows that the large majority of operating fields have less than 10-20 billion NOK left in investments.

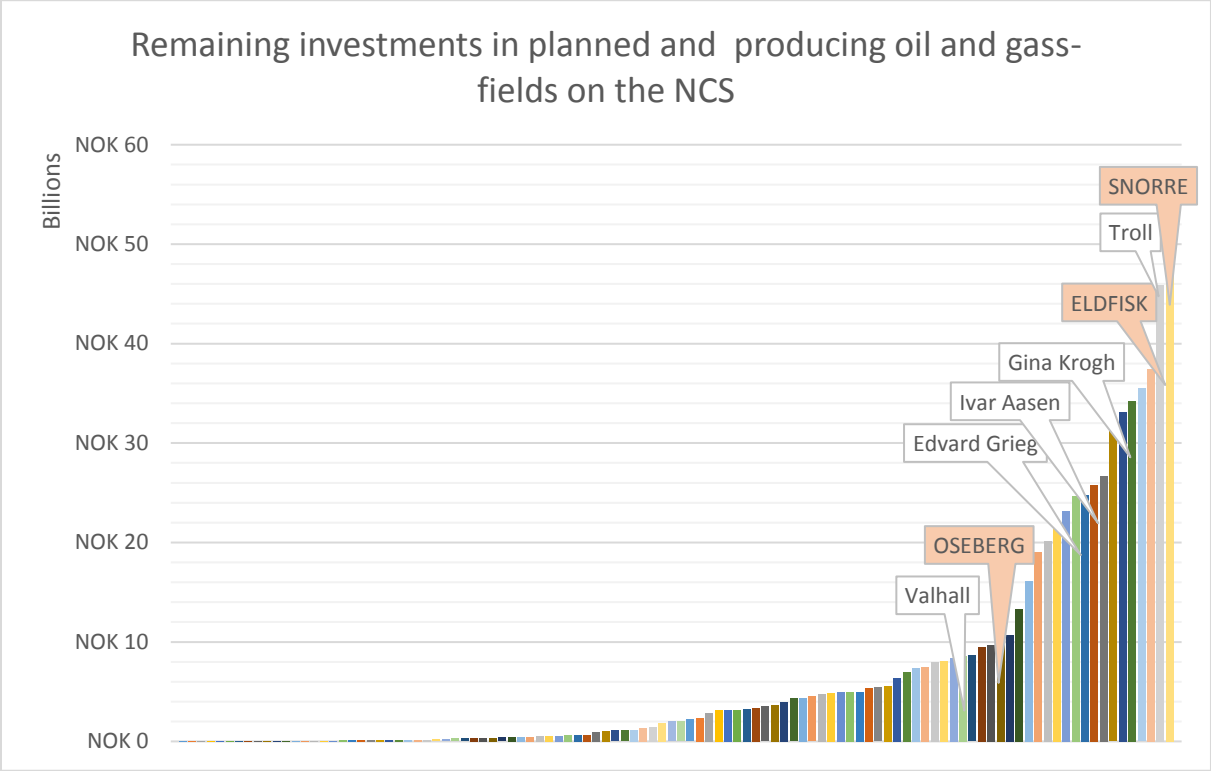

Figure 1: Investment plans on the NCS by August 2016

Combined cycle gas turbines (CCGTs) are seen as viable alternative and with potential for retrofit installations and shorter installation time. The Johan Sverdrup HVDC cable contract entitled to ABB was valued at $155 million. As a comparison the combined cycle investment of a Oseberg D configuration lies in the order of $20-30 millions, where $10 represent the HRSG and steam cycle with one gas turbine operating [5]. It should be emphasized that investment cost alone is not the only reason for justifying installing of HVDC nor CC, but that the trend for investing lies in the largest fields.

CCGTs has since 1991 been implemented on a total of three platforms on the NCS. These include, Snorre, Oseberg and Eldfisk, which has various combinations of heat recovery producing both heat and power from their cycles. Challenges regarding offset operation conditions, flexibility, space and weight requirements and the access to make-up water remains the primary issues for the implementation of new CCGTs offshore.

Norway was the first country in the world to introduce a carbon tax on petroleum-operated activities in 1991. The tax is set to cover all emissions related to combustion of gas, oil and diesel on the Norwegian continental shelf, and on release of CO2 and natural gas. The CO2 Tax Act on Petroleum Activities has then since changed, and is today at a rate of 1.02 NOK per standard cubic meter of natural gas, which for combustion gives the equivalent of 436 NOK per ton of CO2. [2]

Even though, since Norway is also part of the EU Emissions Trading System (ETS), which imply additional fees of 55-80 NOK per CO2-equivalent (2016). When combining these two taxes, companies on the NCS need to pay up to 500 NOK per ton CO2, which is considerably higher than other sectors in Norway and carbon prices in other countries.

In 2007 emissions taxes for NOx was also introduced. The NPS (Norwegian Petroleum Sector) account for about 35% of the total NOx emissions in 2015.

1.2 European CC power and the need of modelling

Today, the European power grid experience large fluctuations in power production from weather-dependent renewables like solar-based photovoltaics and wind-based power turbines. To accommodate for these fluctuations, traditional power plants like coal-based steam cycles and combined cycles (CC) needs to adjust their power output more frequently. Regulating the steam production of these plants over smaller time intervals exert stresses on the steam cycles and may reduce lifetime or break components if not controller correctly. Thus, modeling how combined cycles behave during transient operation is vital to ensure safe and reliant power production.

Naturally, the initial approach to understand the power plants are through development of computer-models. Both private companies and public institutions have developed multiple software packages capable of simulate the behavior of steam cycle components. Though most of these packages come licensed from private companies, quite a few research projects in Europe have released their libraries for

free or as open-source [6-8]. These libraries, and others, are subject for evaluation in building a dynamic model of an offshore combined cycle, which is be the main objective for this thesis.

Previous project thesis by Gule [9] introduces the opportunities for existing and new offshore combined cycles, as well as the emission reduction due to higher efficiencies CC gives compared to simple GT cycles which are the main source of power on remote platforms and FPSOs (Floating Production, Storage and Offloading) in on the Northern Continental Shelf.

It should be emphasized that offshore combined cycles differentiate themselves from land-based CCPPs by a number of factors. The primary driving forces onshore is usually stability and high performance, while offshore part-load regulation, resilience to harsh weather conditions and repeated cycling. Also platforms and FPSOs are subject to strict space and weight requirements that will limit the overall efficiency due to small heat recovery units, or HRSGs. [10].

Thus, dynamic simulation is an essential step to achieve desired knowledge under which various kinds of constrains related to the system design, plant operation and environmental impacts [11].

This thesis evaluates available open-source libraries for modelling and simulating dynamic steam-based power production. The evaluated libraries are ThermoSysPro, ThermoPower and ClaRa, with including comments on non-complete or discontinued libraries that inherent relevant combined-cycle (CC) components. Though, based on the same base coding language, Modelica, none of the libraries serves the full detailed requirements for an compact offshore steam cycle design. This is though natural since the libraries in general are built to their specific needs of the developers themselves, and

What previously used to be steady-state based modelling for plants running at its optimal conditions, has now shifted towards understanding how optimal performance can be achieved through a wide range of various load-levels. Focus on transient operation conditions of combined cycle plants have gradually gained interest since the

beginning of 2000, where most publications focus on existing combined cycle power plants with drum-based heat recovery steam generators (HRSGs).

Dynamic power plant simulation libraries offers tools to model and calculate transient operational behavior of both existing and planned power plants. Outcomes of performing dynamic simulations on a power plant models, could be:

- Reduction of minimum load
- Increase of the load changer rate
- Reduction of the start-up and shut-down time
- Evaluation of process quality during transient power plant operation

1.3 Objectives

The primary task of the thesis has been to model a detailed offshore combined cycle and simulate the steam cycle at predetermined operational points using data from GT PRO from Thermoflow as reference [12]. Heat transfer- and pressure correlations in the heat recovery steam generator (HRSG) has been investigated thoroughly with various open-source libraries using the dynamic process simulations software Dymola [13]. The target was to determine which libraries could represent the suggested offshore combined cycle described, and thus simulate and evaluate transients in the steam cycle system due to load changes in the gas turbine.

Evaluation are based on of thee open source (OS) libraries with the listed criteria:

- Available documentation, sources and examples of CC modelling.
- Level of detail regarding specifically HRSG properties.
- Available heat transfer- and pressure drop correlations for the HRSG.
- Modulation and possibility to implement self-developed models.

The resulting model were developed using a combination of multiple libraries, and various modules and modifications were presented that is included in the final steam cycle.

1.4 Limitations to work

- Detailed transient behavior of the gas turbines is not included. Transient and part-load data are based on steady-state operation points from GT PRO.
- Neither CO2 or NOX emissions are considered.
- Start-up sequence, hot or cold-startup of the CC is not simulated.
- Water treatment, chemicals, nor make-up water is covered.
- Detailed pressure drop correlations where not implemented due to the primary focus of heat transfer correlations on the gas side of the HRSG.

2 Development of HRSGs

HRSGs have since the dawn of the industrial age been implemented in the industry for multiple purposes. In general, they act as a heat exchanger where hot exhaust gas exchange its heat with water flowing inside pipe bundles. This generates pressurized steam, which is further utilized in electric power generation through a steam turbine or as a heat source to other processes with heat exchange. Such tube bundles come in various configurations and geometries, depending on the source of heat, which is normally based on fossil fuels like coal or natural gas.

In coal plants, tube bundles have been used to generate steam since its very invention, but has only in recent decades been utilized to extract heat from exhaust gas in gas turbine cycles. The primary differences lies in temperature range in which coal and gas turbines operates. Coal powered steam plants can reach well above T>1000°C where heat exchange is primarily driven by radiation in large parts of the boiler. The heat transfer gradually shifts towards by a mix of convection and conduction as it cools further up in the boiler and stacks where it is captured by tube bundles intercepting the flue gas flow. Also, the furnace walls in a coal plant exchange heat with integrated steam pipes, which can be a more complex arrangement than we find in gas turbine based HRSGs.

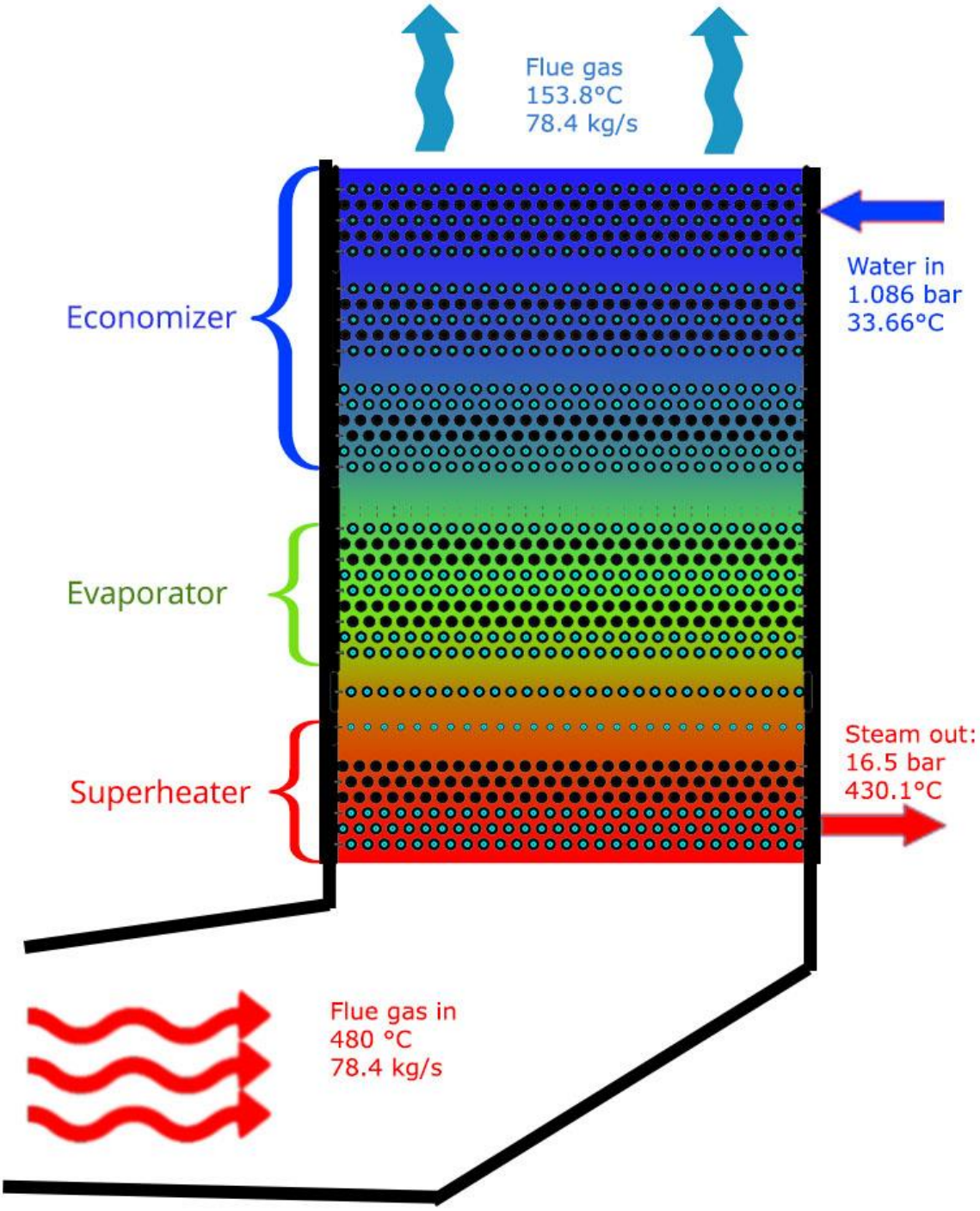

Figure 2: Simplified figure of a vertical Once-through HRSG.

Gas turbines exhaust gas on the other hand lies in the domain of 450-600°C when configured with combined cycles [14]. In this range, convection dominate, and thus a larger contact surface is necessary for heat extraction. For this reason, extended fins are welded on the tube bundles to increase the surface area to the exhaust. In coal

plants, fin configurations are less implemented due to fouling (clogging) of ash and particle deposition between the fins. Even though soot blowing is performed with regular intervals to control the fouling factor, bare tubes are still favored in most power plants.

In gas turbine combined cycles (CCGTs) natural gas or liquid fuel are burned and thus deposition is lesser a problem and can be handled with fewer maintenance intervals.

2.1 Buildup of a HRSG system

The breakthrough of in combined cycle power began in the 1970s when gas turbines could deliver high enough inlet temperature levels to support heat extraction exiting exhaust gas [14]. Since then, steady improvements in gas turbines efficiency has increased the turbine inlet temperature (TIT) making them more susceptible to heat recovery with HRSGs. In 2007 land based CCPPs represented an installed capacity of about 800GW, which is about 20% of the worldwide capacity, mostly running on natural gas or liquid fuels [14]. Low investment costs, short start-up times and flexible operation conditions are some of the properties combined cycle's exhibit that have made it a widely accepted technology for power production.

The majority of land-based CCPPs are based on HRSG configurations including drum-based circulation of the steam cycle. The drum has various purposes, but primarily separates the circulating steam and liquid water before it enters the steam turbine as superheated steam.

Even though once-through systems (OTSG) does not utilize drums directly in their steam cycle, it is important to understand the function of the drum as a control mechanism in most conventional sub-critical steam cycles. The Benson OTSG cycle, which will be discussed in further chapters, also uses a separating unit, and can be seen as hybrid between conventional drum-HRSGs and the pure tube-bundle based once-through cycle by IST. For this reason, taking the basis with the conventional drum-HRSG helps us understand the benefits of using a once-through system for

offshore combined cycles, and why most new CC plants plan to install once-through steam generators as their topping cycle [15].

2.2 Drum based CCPPs

A vertical drum-based single pressure steam cycle is illustrated in figure 3. The water cycles through multiple sections of tube banks, each having its own distinct temperature regions determined by the exhaust from the stack of the gas turbine. The sections are separated into an economizer, evaporator (also called boiler) and superheater.

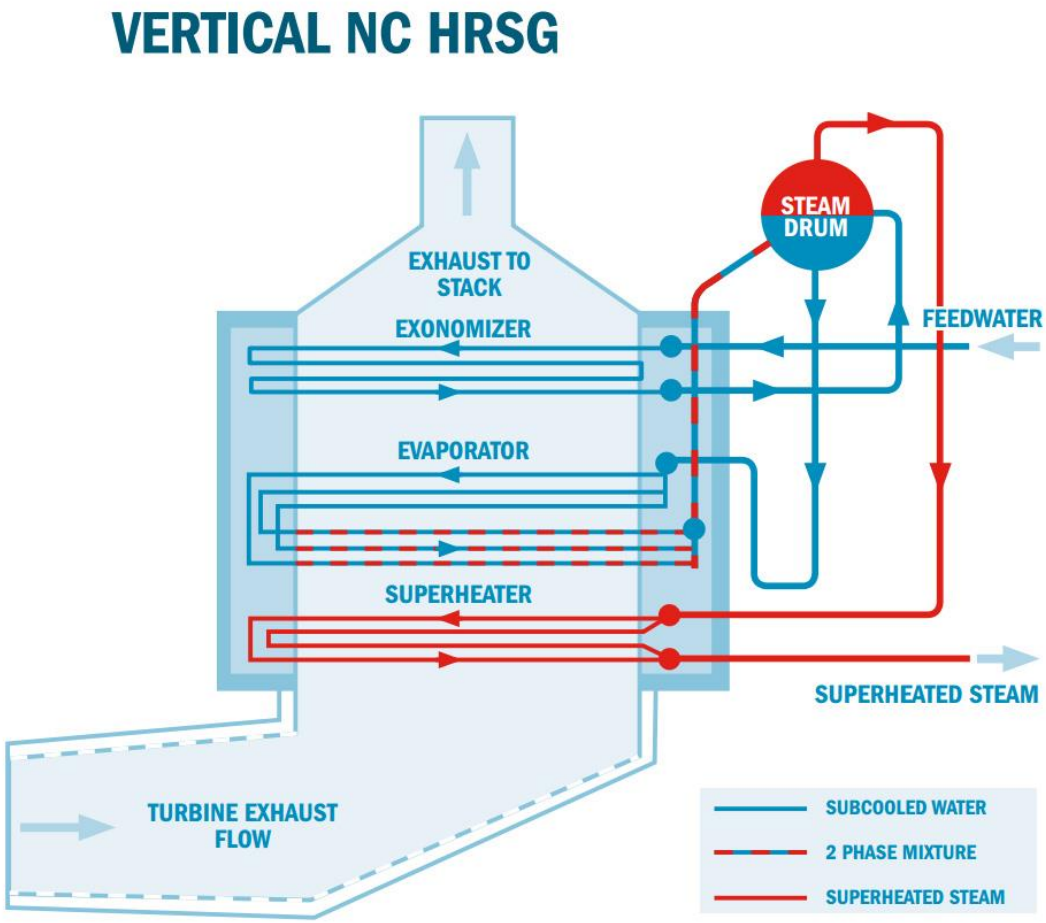

Figure 3: A simplified, single pressure, vertical natural circulating HRSG configuration by IST [16].

The economizer heats the water up to a few degrees below saturation temperature, and consists of the latter part of the HRSG before the exhaust is discharged. The output temperature of the water is dictated by the pinch-point (ΔT_p) in combination

with the approach temperature, which is illustrated in the T-Q diagram in figure 4. The approach point is built into the economizer by design to avoid potential boiling, since this is unwanted for a number of reasons discussed in further chapters.

After being heated close to saturation, the water enters a steam drum, where it exchange heat with the evaporated steam built up in the upper part of the drum. The pre-heated water then gets fed into the evaporator through the bottom of the drum. The hydrostatic pressure made from the elevation of the drum can be used to circulate the water naturally through evaporator, exploiting the density and height difference, and thus eliminate the need for pumps. Whether pumps are needed depends entirely on orientation and configuration of the HRSG, where pipe bundles can be horizontally or vertically oriented.

Next, the evaporator heats the water at the saturation temperature which is kept approximately constant through the boiling process. The heat flux here is the largest through the whole evaporation process because of the high evaporation enthalpy of water. This is further emphasized in the TQ-diagram 4. When operating at design conditions, the evaporator section normally generates fully superheated steam when returning into the drum. To separate low quality steam, the flow is passed through water interface in the drum so that only purely superheated steam exits at the top of the drum tank. This is of particular importance in load-changes and start-up to avoid carry-over into the superheater. As will be pointed out in upcoming chapters, non-superheated water entering the superheater section can be devastating and cause tube

failure in the HRSG.

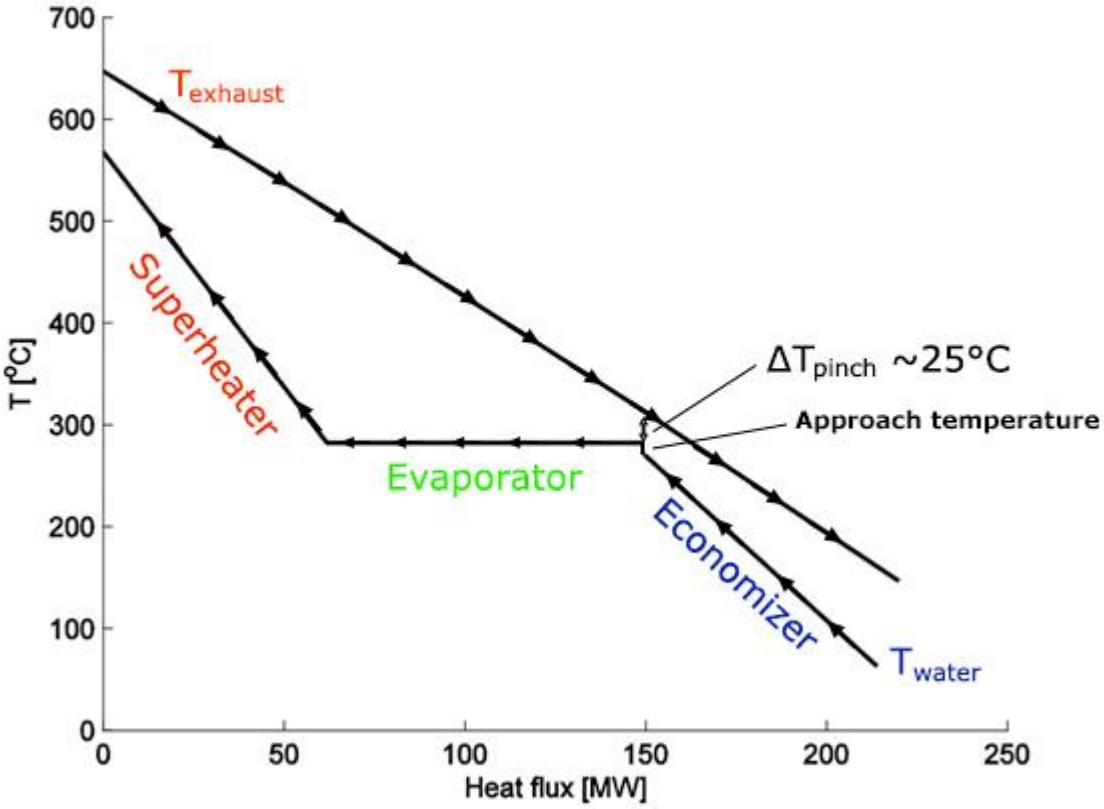

Figure 4: Single pressure TQ-diagram through the HRSG

The evaporated steam enters the superheater, which normally has a different tube and fin configuration than the evaporator and economizer. This is due to the different heat transfer properties of the gas-tube-water interface at each section. The heat transfer coefficient, or U-value, vary vastly depending on water phase, and thus the tube sections is designed to optimally transfer heat in each section. Details on the HRSG heat transfer properties are discussed in chapter 2.9.

2.3 Pressure levels and efficiency

It should be noted that sectioned HRSG design (with economizer, evaporator and superheater) is built for subcritical steam cycles, where drum-based HRSGs have been the dominant design on most land-based CCPPs. To increase the efficiency, more heat has to be recuperated, and thus multiple pressure cycles is utilized to at different saturation temperatures. Most land-based CC plants use three pressure

levels, which is a good compromise between HRSG efficiency and the investment costs of the HRSG. Efficiency increase as the ΔT between the exhaust gas and the water/steam flow is minimized, and can be illustrated as the minimal area between the two lines. The TQ-diagram in figure 5a) show two pressure levels, which compared to a single level follows the exhaust line closer, and thus recovers more heat, producing more steam. The pinch-point ΔT_{pinch} marks the narrowest point temperature difference in the HRSG, and vary by design by 8-35K, depending on size of plant and number of pressure levels. Land-based HRSGs can be designed with lower pinch-values, due to less restrictions to space and weight requirements, which is otherwise a challenge on offshore compact combined cycles. Efficiency on offshore combined cycles only reach around 50%, while land-based power plants has exceeded 60% with more advanced HRSG designs. [17]

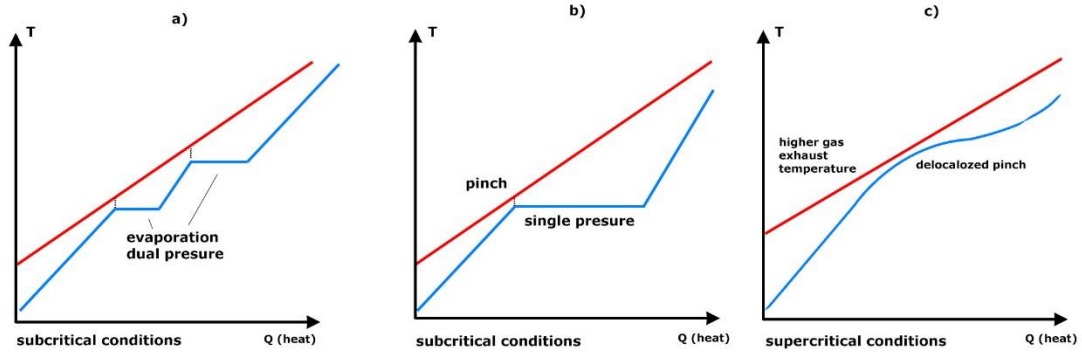

Figure 5: TQ-diagram of subcritical and supercritical HRSG. Based on figure from Dechampes [18]

Gas turbines inlet temperatures (TIT) have incrementally improved over the years with thermal resistant materials, and thus paved the way for higher steam pressure levels in the HRSG [18]. But higher pressures exert more stresses on the HRSG components like the steam-drums, headers and tube bundles. Higher pressures introduce thicker drum walls, which is again increase the weight and the need for expensive steel-alloys to withstand the large temperature gradients throughout the shell of the drum.

2.4 Once-through steam generators

To counter this, once-through steam generators (OTSG) for combined cycles was introduced in the 1990s [10, 19]. The design is well known within most coal plants, with high temperature, high pressure steam cycles. It allows for supercritical operation, which yields lower ΔT, because of no distinct evaporations zone, illustrated in Figure 5 c). Though most land-based OTSGs advocate with supercritical operation conditions and thus high efficiency as its most prominent feature, the system also exhibit many features even for subcritical conditions, and thus in use for compact offshore configurations.

Two leading designs of combined cycle OTSG systems are presented.

2.5 IST simple OTSG system

The simpler tube bundle design is manufactured by IST (Innovative Steam Technologies) [19], who deliver primarily vertical once-through steam generators. It is made up of one continuous, thin-walled tube bundle, without defined economizer, evaporator or superheater. It removes the need for many components like the steam drums, downcomers, blowdown systems and separate fin configuration and variable tube diameter design, common in conventional HRSGs [19]. It can operate dry, without steam or water inside the tube bundle, even at full GT-load. To make this possible, the tubes are made of high nickel Incoloy 800 or 825 alloys, which exhibit high corrosion- and temperature resistance. The tube bundles are horizontally configured, allowing them to thermally expand, sliding freely within flexible tube sheets holding them up. Fins are stainless steel alloy of 409SS or 316SS, which is suited for offshore conditions with high levels of sodium chloride [19].

Running dry is a critical feature for offshore operation conditions, allowing for fast gas turbine startups and shorter maintenance intervals for both cycles. The IST Vertical IST OTSGs built since 2001 are fully modularized, which means that its tube bundle sections are installed by stacking them upon each other, reducing erection time and installation cost. A the U-bends of the tube bundles inspections can be made through integrated maintenance doors on both right and left side of the

OTSG. Since the majority for IST OTSGs have approximately 50 circuits of tubes in each module, losing or shutting down one circuit only affect performance by degradation less than 1% [19].

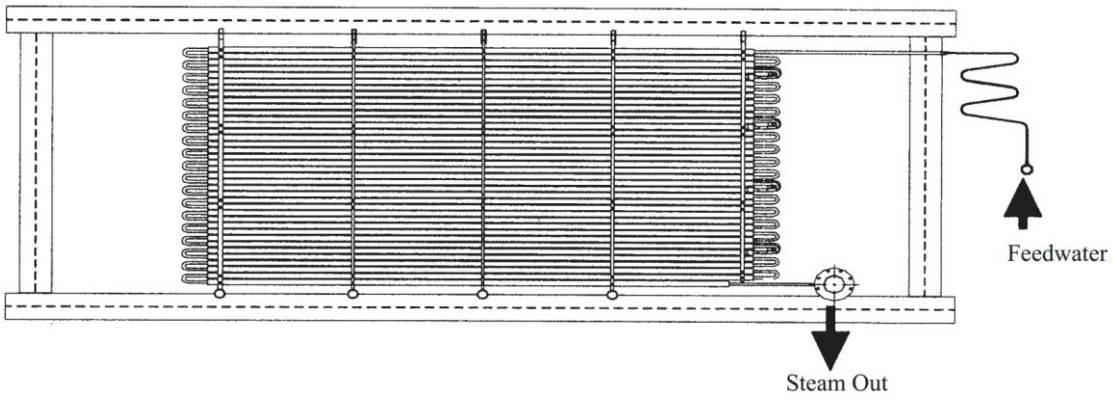

Figure 6: Vertical exhaust flow, horizontal steam flow once-through tube bundle by M.F.Brady by IST [19]

2.6 Benson Once-through Steam Generator

The Benson ® once-through steam generator (OTSG) was originally patented by Mark Benson in the 1920s by Siemens, who initially manufactured this type of boiler. Today it represents the most common implementation of once-through evaporators worldwide, used in both waste-heat recovery, coal and gas-fired power plants [20].

NEM-Group is one of many OTSG manufactures that has acquired license to the Benson ® design patented by Siemens [15]. The tube design is partially sectioned and can be described as hybrid between conventional drum-HRSG and the IST once-through design. These include a separate once-through boiler (OTB) and a superheater, with a steam-separator between the sections. The separator either redirects non-saturated steam back to the once-through boiler headers or to blowout, depending on design and manufacturer.

Headers on the end of the U-bends split the flow into a set of parallel horizontal tubes, and is located outside the gas flow. [21] Tubes are bent at the tube-header welds thus allowing for linear thermal expansion and shrink, shown in Figure 7. This accounts for vertical HRSG tube design in general (both IST and Benson).

In horizontal HRSG configurations, with vertical tube bundles, the water and steam can circulate naturally without the installation of pumps. This is exploited through the density difference of water when boiling in vertical tubes, which is widely used conventional drum-based HRSGs and in the horizontal Benson OTSG from Cottam Development center [20].

However, vertical HRSGs need forced water circulation due to the horizontal flow direction of the bundles. Thus, feedwater- and forwarding pumps are installed before the economizer and the evaporator respectively. Horizontal boiling cause flow instabilities, and the inner tube periphery is not uniformly wetted like with vertical tube boiling. While steam bubbles form at the top, liquid water takes up the lower portion of the tube. The difference in heat transfer coefficient in steam and water, leads to thermal stresses across the tube cross-section, and has to be compensated with flexible tube headers at the end of each tube layer [22].

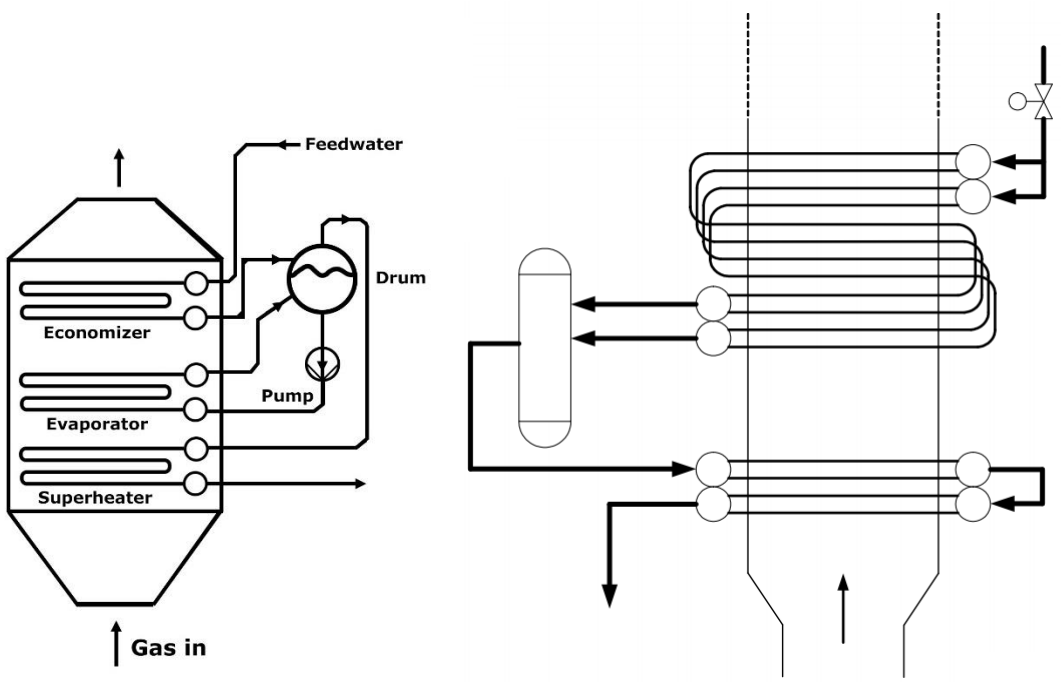

Figure 7: Left: Conventional vertical drum-based HRSG design.
Right: Schematic of NEM Benson Vertical OTSG Boiler and superheater are distinguished.

Franke [20] describes that counter-current yields the lowers pressure drop and needed heat exchange surface on the tubes. However, this configurations yields stability problems which can only be eliminated installing flow restrictors. Parallel flow on the other hand exhibits flow stability but at the cost of larger heat exchange surface and

increased pressure drop. Thus, a combination of both is often used to design the vertical OTSG, shown in figure 8.

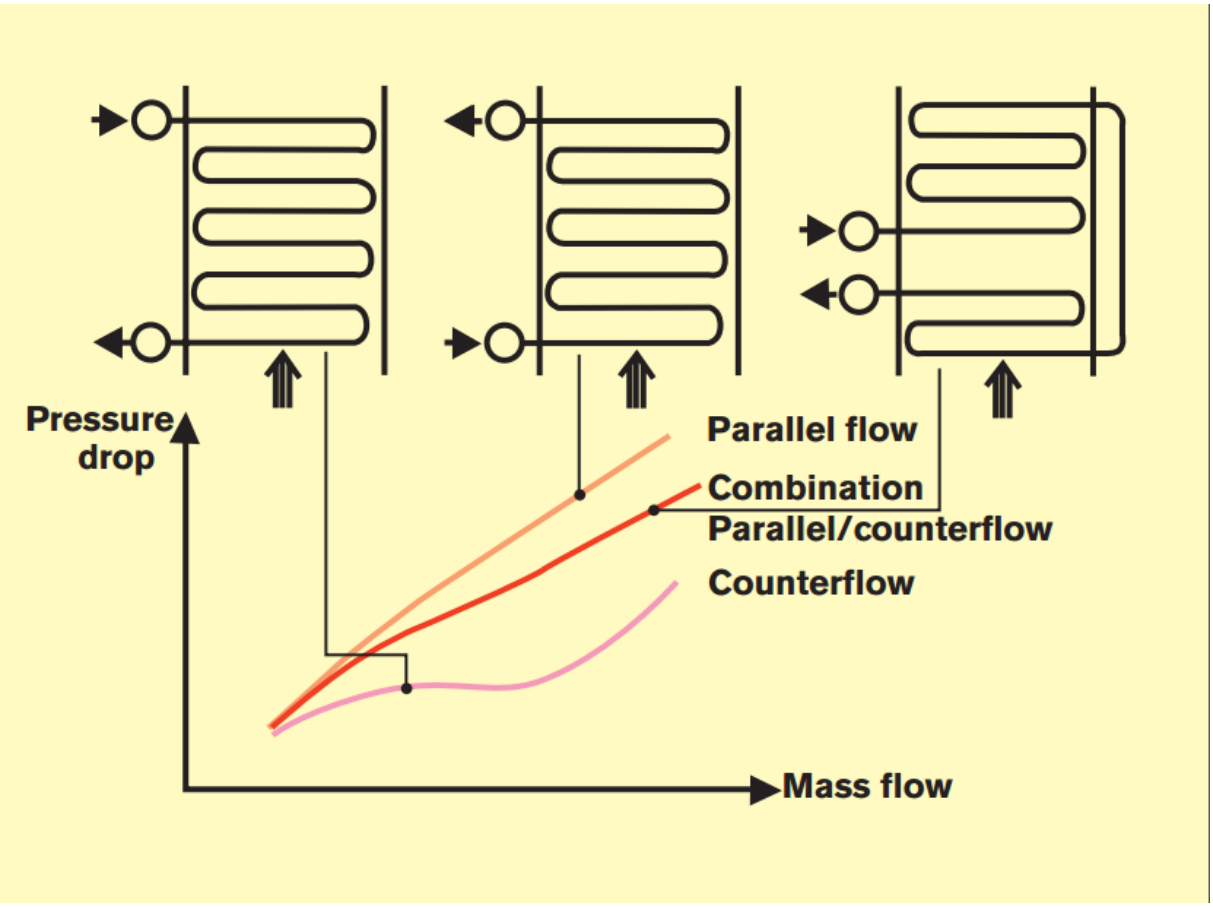

Figure 8: Flow stability in once-through boilers for vertical configuration [20]

2.7 Offshore design considerations

Space and weight requirements are highly prioritized on offshore CC. Quick maintenance to minimized down-time is especially critical. Therefore, dual gas turbine with one HRSG is common configuration to keep the cycles operating, so e.g. one gas turbine can set for maintenance, which is this case-study for the Oseberg D combined cycle.

The primary constrains in fast cycling and load variations of existing CCPPs are the allowed temperature and pressure transients of the steam turbine and the HRSG. Start-up transients in once-through are faster compared to drum-based HRSGs which gives better performance characteristics

Allowable temperature transients in a once-through steam generator is higher compared to drum based HRSGs. This enables for significant increase in overall plant flexibility during start-up, whether it is cold or warm-startup.

In marine environments the heat exchangers are influenced by the build-up of salts in the tube bundles. During by-pass or shutdown of a conventional HRSG, build-up of moisture in the HRSG can potentially accelerate corrosion with certain types of metals. This is why be stainless steel on fins and high-nickel alloys on the tube bundles are suggested by both IST and NEM Group's in their respective OTSG configurations.

Once-through for onshore power plants is considered for supercritical operation giving, better TQ-curves, compared to triple-pressure steam cycles. Triple pressure drum-based HRSG plants with steam pressures of 80-130 bar is common, and with the transition to 160bar and above, the once-through evaporator become advantageous because of better fitting TQ-curve shown in figure 8.

Once-through HRSGs is primarily used with higher main steam pressures and to withstand high thermal flexibility of the tube bundles [14].

Offshore operation run mostly off-design, and thus capability to regulate quickly is more important than optimal efficiency. Weight and space restrict the steam cycle to one pressure level, which is normally subcritical due to limits to weight of the tube bundles withstanding high pressures.

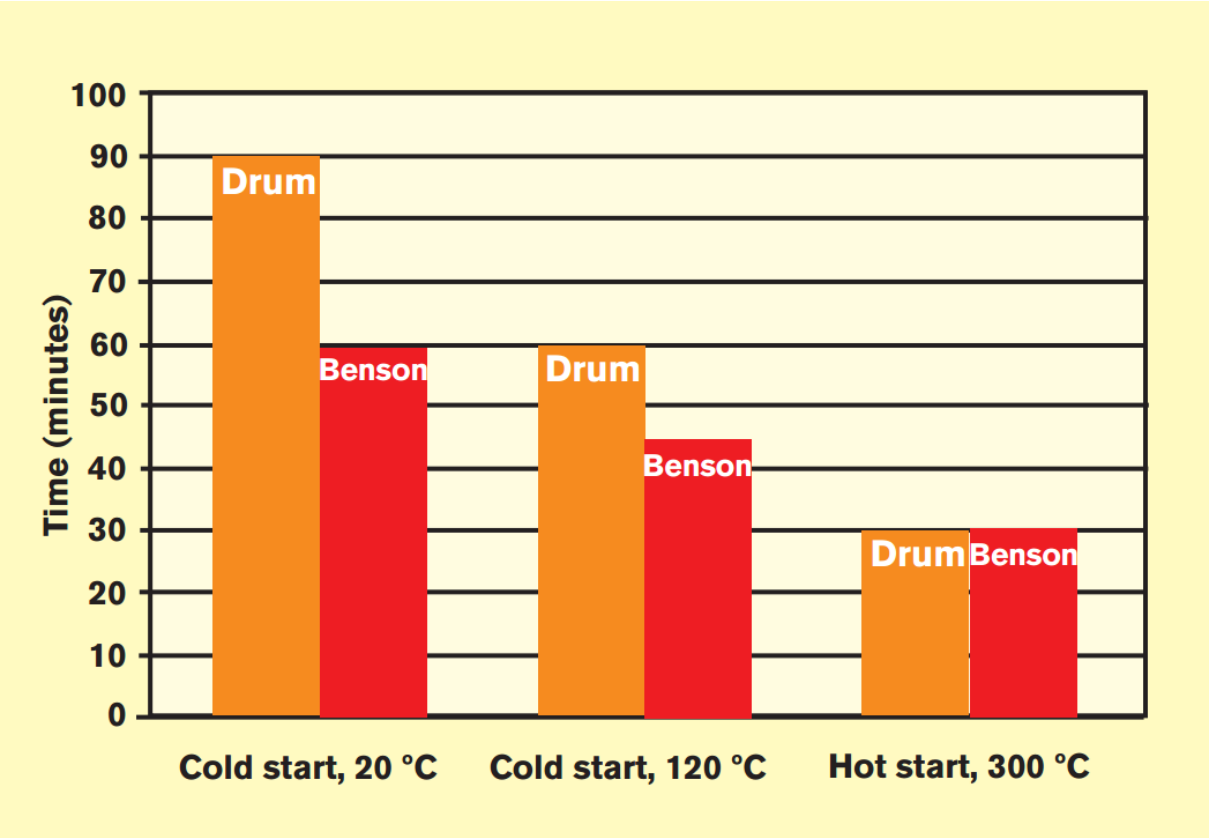

Figure 9: Comparison of Benson type HRSG versus drum HRSG type start-up times, Franke et al. [20]

2.8 Fin design and tube arrangement

Both Fontaine and Franke state that trends for vertical HRSG designs are more common in Europe, and that horizontal design dominate in America [20, 21]. European manufactures dimension tubes with smaller diameter, thus reducing the wall thickness and thermal stresses during cycling.

Vertical HRSG design are less vulnerable to gas side deposition and fouling than horizontal HRSG designs.

Horizontal evaporator pipes in vertical HRSGs are cycling tolerant systems, as the design permits the tubes to expand and contract freely and independently of one another [23]. In contrast evaporators in horizontal HRSGs with vertical pipes are set up vertically in a rigid harp structure supported by their own weight. This gives larger wall thickness to the tubes compared to vertical HRSGs resulting in high thermal inertia in the bundles.

Vaporizer tubes are arranged in serpentine pattern [24]. Thus in a vertical HRSGs the swell effect will establish itself relatively fast thoroughly the tube bundle, compared to horizontal HRSGs where this effect is more gradual and can even cause backflow in the evaporator.

External heat transfer surface and heat transfer coefficient is not necessarily directly proportional throughout the HRSG. Increased fin density only improves the heat transfer if the corresponding water/steam-side heat transfer coefficient doesn't limit the overall heat transfer.

This can be exemplified in the superheater where the fin density is relatively low or completely bare tubes are installed. Due to high resistivity of the steam-side heat transfer coefficient, increased external fin surface will not improve the overall heat transfer noticeably. For this reason, fin density is being proportionally set to the internal heat transfer coefficient at the specific section, where the evaporator have the densest fin configuration, followed by the economizer and lastly the superheater. Note that the superheater fin density should also decrease if radiation contributes largely to the heat transfer, like in coal plants. This is though not the case for most combined cycles. Thus, the overall product of the heat transfer coefficient and the surface area reflect the real U-value, illustrated by table 1 and the corresponding equation.

Table 1: Average HTC values for a HRSG.[9]

Section of HRSG	Exhaust gas side	Water in economiser	Water in evaporator	Steam in superheater
Heat transfer coefficient (h_i) (W/m^2K)	50	500	2500-10000	1000

$$\frac{1}{U_0 \cdot A_0} = \sum_{n=1}^{i} \frac{1}{h_i \cdot A_i} + \frac{\ln\left(\frac{d_o}{d_i}\right) \cdot d_i}{2 \cdot \lambda_{tube} \cdot A_i} + \sum_{n=1}^{i} R_{f,i}$$

Thus, the fin density should be designed optimally to avoid excessive weight increase in the HRSG since not all the sections will utilize the extra surface area equally.

3 Control, automation and regulation

Control systems are vital during transient operation conditions like startup, shutdown, and part-load regulation of the combined cycle. It ensures safe and reliable power supply with the changing demand due to variable production rate and utilities on the offshore installation.

Once-through steam generators simplifies the control system vastly compared to traditional drum-HRSG cycles. Not all the control strategies here will be included in the once-through model

3.1 Gas turbine control

In the gas turbine, control of the variable inlet guide vanes (VIGV) together with fuel flow admitted to the combustor determine the turbine inlet temperature (TIT), and thus the exhaust gas temperature in the HRSG stack. Today, modern gas turbines have up to three VIGVs allowing for high exhaust gas temperature down to approximately 40 per cent GT load [14]. However, the exhaust temperature is varies irregularly, whereas the mass flow vary more linearly with load change. Thus, gas turbine exhaust boundary characterized through variable mass flow, temperature and flue gas composition. However, changes in gas properties like conductivity and heat capacity caused by exhaust composition change is negligible and thus can be assumed to be constant throughout most simulations.

Flatebo [25] showed that temperatures and massflow relative to the design point varies with decreasing gas turbine-load. Data from GT PRO with a GE LM2500+RD(G4) gas turbine is used as reference in figure 10. The massflow exhaust data and EGT (Exhaust gas temperature) has been extracted using WebPlotDigitizer and included as tables in ClaRa flows [26]. Further have the EGT been calibrated to the nominal operation point of 480°C EGT of the user-defined gas turbine of 25MW in our combined cycle. The assumption is that the 33MW GE LM2500+RD(G4)

exhibit the same part-load behavior as the user-defined gas turbine, and thus can be used to simulate similar gradients in part-load scenarios.

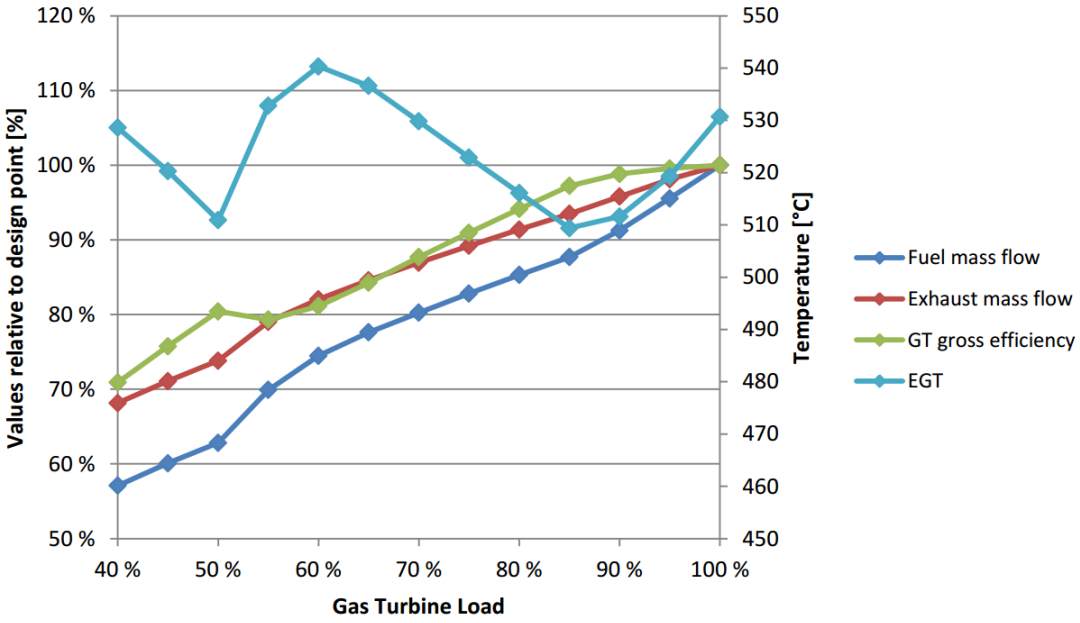

Figure 10: LM2500+RD(G4) steady-state off-design load values. [25]

When regarding figure 10 it becomes clear that the uneven EGT will cause irregular steam production in the heat exchanger with load-changes. This is why well-developed DCS (Distributed control systems) [27] in the steam cycle are of high importance to compensate for fluctuating heat uptake in the HRSG.

Through separate control systems are installed for the hot and cold startup procedures and shutdowns, these will only be covered, and the main focus is normal operation part-load changes. Only data from load changes ranging from to 100% to 60% GT load are considered.

It is further assumed that changes in ambient factors like humidity, temperature or atmospheric pressure is negligible during transient operation scenarios modelled in this thesis. This is also explained by Kelhofer and will not affect changes in short timespans [14].

3.2 Steam cycle control

Once-through systems exhibit a unique simplification of the DCS when compared to conventional drum-HRSGs. The removal of drums and drum-level control has the largest impact and makes the start-up and load change characteristic faster with once-through steam generators. Below follows the sensor and control blueprint of the IST once-through steam cycle: [16]

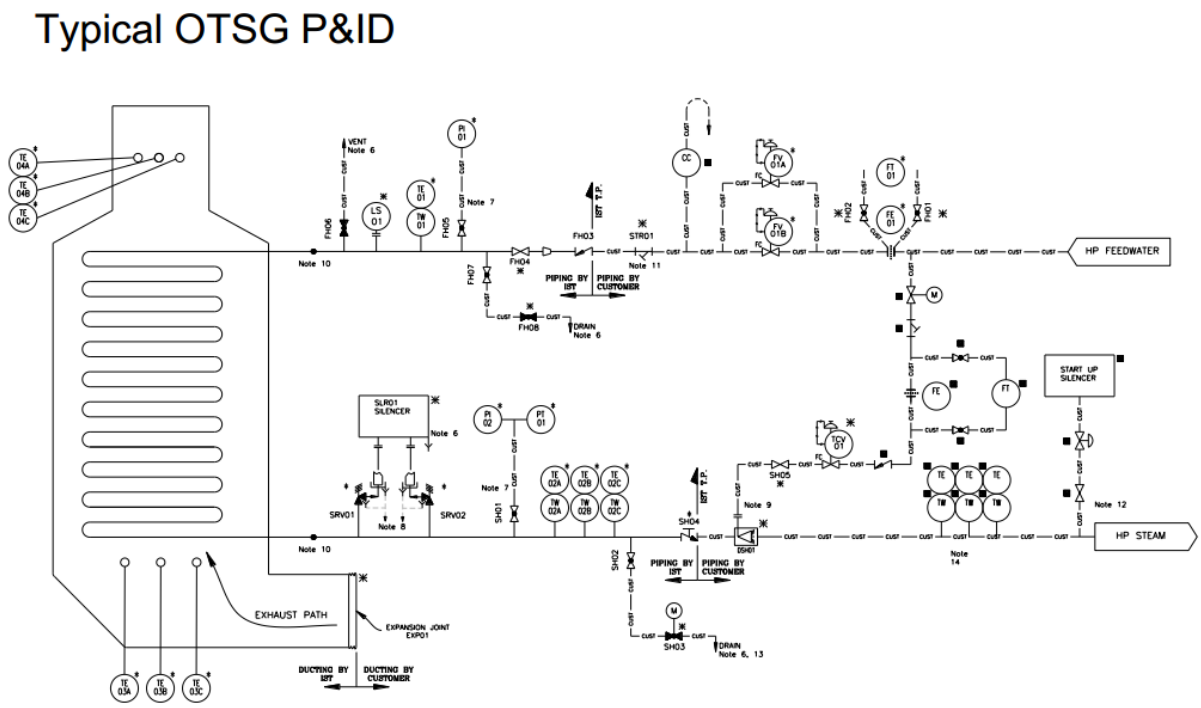

Figure 11: IST control system for once-through steam cycle.

Though the IST control-system schematic can seem complicated at first glance, most of the sensors and valves are installed for venting, drainage or in backup for crosschecking parameters if errors should occur. Circular icons are sensors, and multiple sensors are set in sequence as either failsafe, or to monitor parameter gradients. Note that many controls and sensors are notated with "CUST", indicating that these depend on the individual customers need and existing equipment. During this chapter, only control systems for part-load change will be covered, while direct start-up or shutdown procedures will only be explained in the context of load-change where necessary.

Control systems essential for part-load regulations are:

- Feedwater control, with failsafe bypass valve.(prescribed by GT-load)
- Live steam control using attemporator. (connected to the HP feedwater)
- Level-controls in separator and condenser.
- Multiple temperature gradient sensors before and after attemporator. (disgussed in detail later)

Figure 11 also depicts mechanisms necessary for start-up and shutdown, and preparation and maintenance of the steam cycle, which include vent valves and drainage valves before and after the OTSG stack.

The load is normally operated to meet the demand dictated by the electrical grid, which offshore is set at 60 or 50 Hz depending on infrastructure and gas turbine generator locally on the platform or FPSO.

Most systems are computer based for a whole range of operational tasks such as logging real-time data, making statistics, even provide management information of the economy of the plant, and advise on the intervals between cleaning, inspections and other maintenance work. These automated control systems are built on hierarchic levels, such that gas turbine and steam cycle parameters are automatically following procedures in start-up, shutdown and through load-changes. Process computers provide sequencing events, optimize the heat rate and operation of the plant and advise on intervals for inspections and maintenance.

3.3 Load control

After a gas turbine load change, the steam turbine load will adjust automatically with a few minutes delay dependent on the response time of the HRSG.

Individual frequency control on the steam turbine is not usually installed, because it requires continuous throttle control and results in poor efficiencies both part- and full load. Since the gas turbine supply approximately two-thirds of the total power output, and react quickly to frequency variations it compensates for the delay in steam turbine response without falling out of set frequencies. Supplementary firing is

normally not provided on offshore combined cycles, and thus independent steam load control is not necessary [14].

Frequency control will not be included since the heat characteristics of the HRSG is the main focus for this thesis.

3.4 Separator level control

The separator ensures carry-over do not occur during start-up or part-load change which can lead to quenching of the superheater, which can be devastating since most superheaters are not designed to withstand such stresses. Carryover can also contain deposits from improper chemical treatment of the water [28]. This ensures the steam turbine only receives pure steam, which otherwise could break the turbine blades and reduce their lifetime [29].

In once-through systems, dependency on drum-level control opening for a simplified feedwater control strategy. This is the primarily reason for the advantageous fast start-up characteristic of the OTSG.

Feed water control of the once-through HRSG distinguishes between two modes of operation, namely separator level mode and once-through mode. The separator water level is held constant during initial start-up procedure, while switching to once-through mode when the HRSG load exceeds 30% nominal load [23]. This is illustrated in NEM Groups start-up shown on figure 13 [30], where the separator separate unsaturated water down to blowout, or to recirculate into the evaporator shown in the Cottam Benson horizontal design. Since the separator only is relevant during start-up and refill of the OTSG, its function during normal operation can be neglected, as superheated steam from the boiler bypasses directly into the superheater, and the recirculation or blowout circuit is closed [23, 30]. The absence of any separator data from the upcoming steady-state GT PRO model further supports its irrelevance during normal part-load operating conditions [5]. However, a separator will be implemented anyway for general testing of the system in chapter 10.

3.5 Vertical and horizontal once-through separators

Figure 12 shows a simplified steam pathway of the evaporator for a Cottam horizontal flue gas flow OTSG [20].

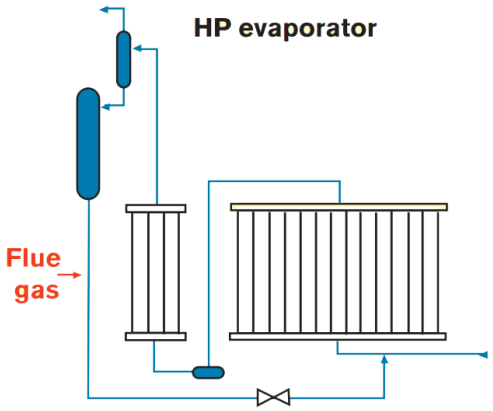

Figure 12: Cottam Once-through evaporator schematic for two stage separator [20]

Here, preheated water from the economizer is distributed equally through the parallel tubes in one single pass. The last section in the evaporator produce superheated steam during nominal conditions, which gets separated into liquid water from the superheated steam and redirects it back into the headers of the evaporator.

Alternatively this is sent to blowout [30] as with NEM Groups configuration depicted in figure 13. On the contradictory, the horizontal OTSG utilize the natural circulation to feed the excess separated water back to the evaporator header without the use of a recirculation pump, which could be used on vertical boilers.

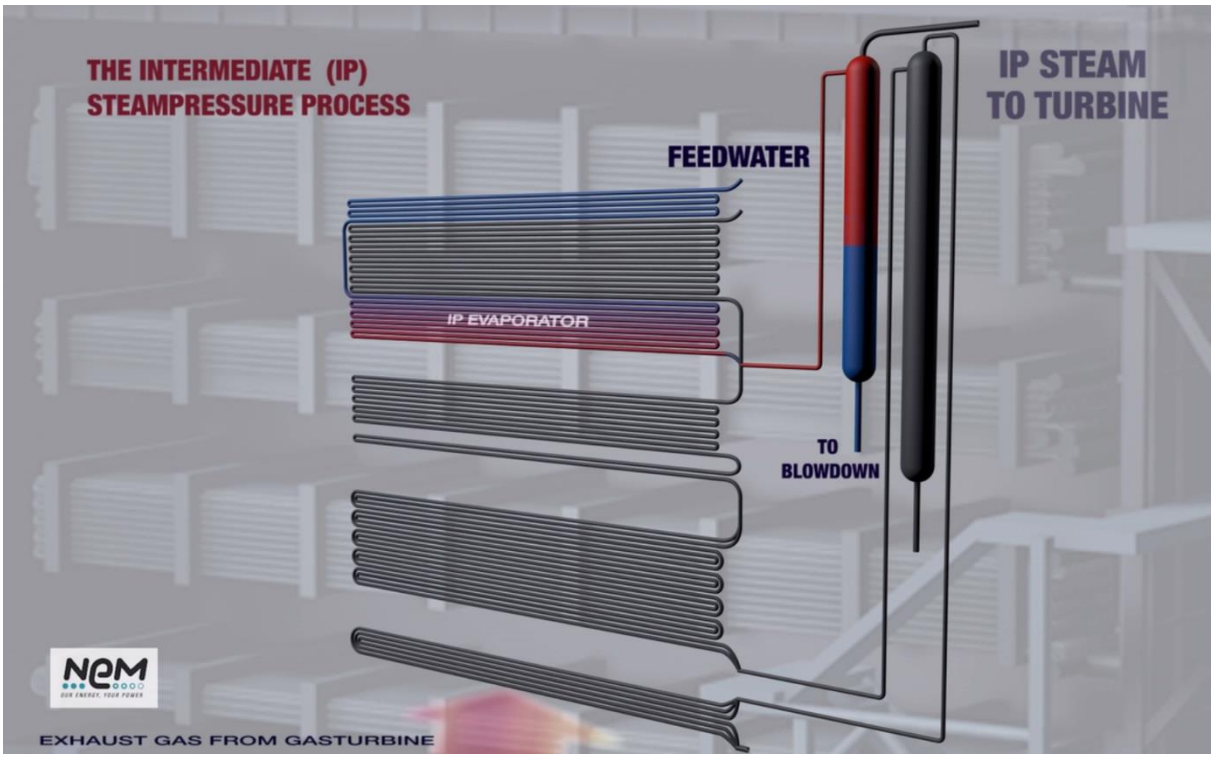

Figure 13: Start-up conditions to HP and LP OTSG with Benson-type [30]

Figure 13 shows the startup procedure of a NEM Group Vertical OTSG. The feedwater initially flows through the evaporator and enters the separator as liquid water and going to blowout. As the tube bundles heat up more steam produces, increasing the pressure in the separator redirecting the flow upwards into the superheater at the top. The water-level is thus stabilized, and the whole separator will contain only superheated steam during nominal operation.

3.6 Feedwater control

In conventional drum-HRSGs the feedwater control valve is adjusted through a *three-element control system*, by the drum level, live-steam flow into the superheater and feedwater from the economizer into the steam-drum [14, 23]. Upper and lower limiters are also included in the controller to prevent carryover or running dry. In multi-pressure steam cycles, the total number of controllers restrain the transient speed and causes slower start-up characteristics. Dechamps (1994) [31] state that expanding the control models does not necessarily provide better performance over time because this adds to the complexity and leads to increased inertia and startup

times. This is due to the moving evaporation zone during shifts in part-load changes in the boiler, and the correction of swell and shrink of the water that can be quite lagging take time before stabilizing flow.

Brady describes that transients in the IST design are accommodated with a feed-forward control, with prescribed feedwater flow values as a function of the gas turbine exhaust temperature and flow rate [19]. Its proclaimed as a single point of control for the OTSG and the predefined operation conditions are set through he DCS which is connected through the feedforward and feedback control loop, which monitors the transient in gas turbine exhaust load and outlet steam conditions respectively. When a transient is monitored, the feedforward control sets the feedwater flow to a predicted values based on the turbine exhaust temperature, such that steady state superheated steam conditions can be produced [32].

The feedwater temperature must also be controlled corresponding to the acid dew point [14] but will not be further investigated or implemented in the coming model.

Detailed explanation of the once-through HRSG controllers are further explained in chapter 12.

3.7 Live-steam temperature control

Theoretically, the design of the steam cycle should be targeted on the natural characteristic of the HRSG to attain the correct steam temperature when the flowrate is at nominal values. This means that the spray water only needs to be used when the gas turbine is being brought up to load or when it operates at off-design conditions. In practice this can only be attained to a limited extent, because the natural characteristic of the HRSG changes over time due to factors such as fouling of the tube surfaces, which affects the total heat transfer in the HRSG. Therefore operating with continuous spraying is quite common, allowing the steam temperature to be adjusted both up and down. This is essential if the temperature needs to be increased and not just act as a limiter through the cycle, which is needed depending on the load-change.

To accommodate for such peaks spray-water attemporator are normally used between the superheater and steam turbine. It sprays a cool water mist into the superheated vapor, distributing the evenly lowering the temperature and slightly increases the mass flow. The spray attemporator in figure 14 is taken from the IST P&ID schematic, where the spray-water is directed from the tank after the economizer. Multiple temperature sensors provide exact values downstream of the nozzle to ensure stabilized values [33].

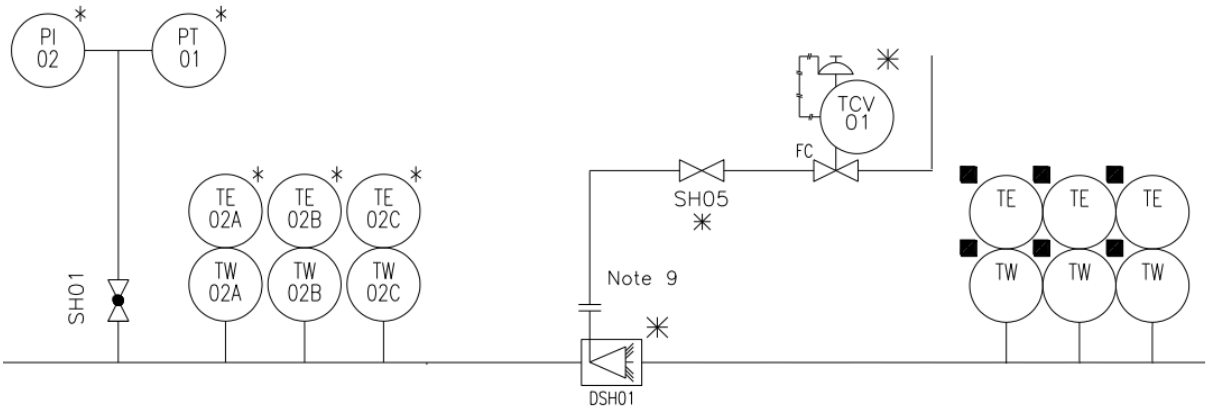

Figure 14: Spray attemporator from IST once-through cycle. Both temperature and pressure sensors are included.

Nominal spray injection value are suggested by the ClaRa library to be set at 1/30 of nominal steam inlet flow [34].

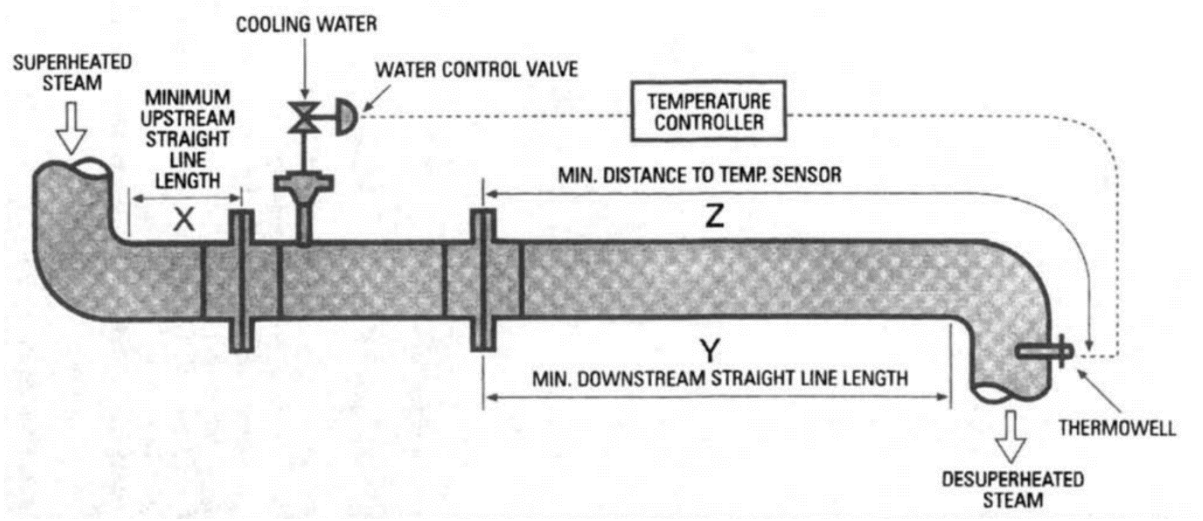

Figure 15: Illustrated steam attemporator by Lindsley [33]

3.8 Live-steam bypass valve

Down to approximately 50% the steam turbine is usually operated by a sliding pressure control. Below this value the pressure is kept constant by closing the steam turbine valves, or redirecting the steam through a bypass valve. This gives more flexibility during startup, shutdown turbine trip, or quick changes in load. However, in normal part-load transients, sliding pressure control is sufficient.

3.9 Level control in feedwater tank and condenser

The hotwell level is controlled by adjusting the condensate valve after the pump. It is controlled by a series of PI-controllers which calibrate for the deviation in flow in and out of the condenser in combination with measured water-level. Water level is maintained by a adjusting the valve followed by the condenser pump.

Feedwater tanks have level limiters, where drain valves will open if it is too high. Likewise, makeup water is admitted, normally through the condenser, if the level is too low. This will increase the condenser level, and in turn the feedwater tank level [14].

Injection of makeup water and drain valves is placed on various locations dependent on the custom configuration of the steam cycle. More details on the actual controller is described in the model.

3.10 Sliding pressure control

The sliding pressure control lowers the admission pressure in order to control the flow into steam turbine. This will initially maintain the volumetric flow rate without introducing throttling losses. It reduces the control stage inlet pressure with maintained temperature at part-loads which results in more stable volumetric flow. Johnson also state that sliding pressure control results up to 40 percent less power consumption than partial arc control when running on 50 percent cycle load [35].

Below 50 percent load the live steam pressure is held constant by a valve at the steam turbine inlet. However, this give increased throttling losses and increased stack losses. Thus, sliding pressure operation is best suited for high part-load efficiencies. Hence, the total power output of the combined cycle is adjusted through the gas

turbine control (VIGVs and fuel flow) and sliding pressure control. This regulation is commonly used in conventional steam plants with supplementary firing. (Kehlofer chapter 8. Page 216:[14])

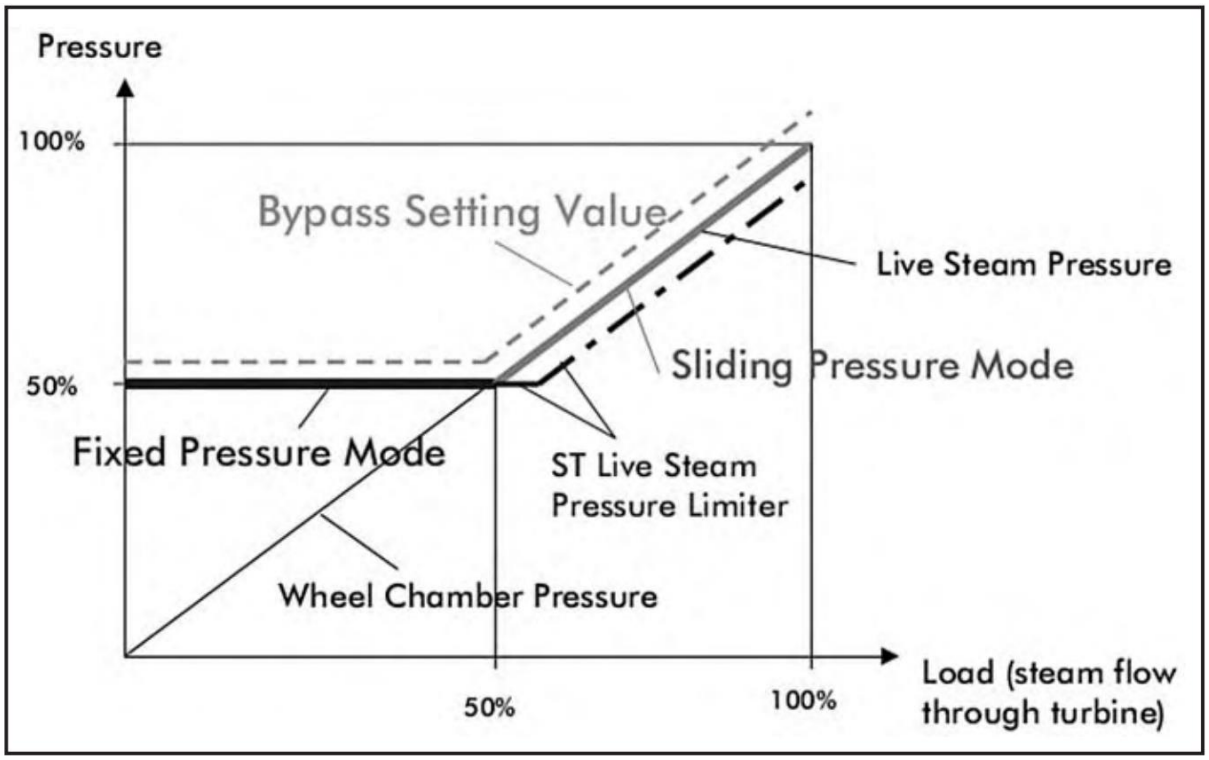

However, reducing the boiler pressure reduces the mean temperature in HRSG, resulting in lower efficiencies in the steam cycle. A pressure gradient is developed. This has traditionally been compensated with introducing impurities like silica oxide into the cycle. Nevertheless, this makes the sliding pressure control slower compared to partial arc control and instant load changes are not possible.

Instant load changes is possible with partial arc control, but sliding pressure control gives higher part-load efficiencies [35].

3.11 Partial arc control

Partial arc admission can be though of as an effective means of controlling the admission area to the turbine, whilst maintaining the pressure. It consists of staging valves that controls the steam admittance into the turbine control stage with multiple valves, usually 4, which operates in special sequence. It is built up of stationary blades divided into a number of sections of arcs each controlled by a valve,

which are circumferentially distributed around the turbine for regulating steam admission flow.

Valves in each arc regulate the steam flow and are shut down sequentially. When the first valve is fully closed, the second one closes and finally the two last ones [36].

Because of the sequential closing of the valves, a relative large part of the total mass flow is throttled with the first valve, meaning 25 percent of the total mass flow. Hence, the throttling losses are high when a valve starts to close, but decreases as the flow diminishes. When the two first valves have been closed, the remaining two valves close simultaneously in order to keep the shaft force even (part 16 in figure 16). This behavior is the same as for normal throttling control.

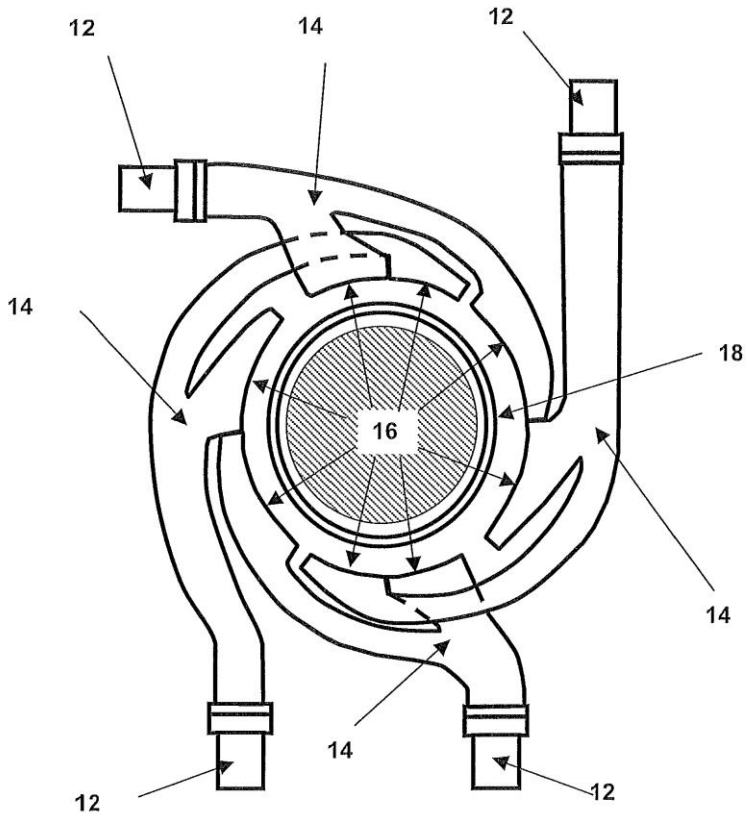

Figure 16: Partial arc control. Courtesy by Alstom technologies

Compared to a single valve control, the partial arc deliver less throttling losses when operating at part load.

4 Dynamic modelling procedure

The procedure needed to build a dynamic model differentiates much from what a steady-state model demands. It requires a wider understanding of the how certain components behave and in what order they should be placed to make a stable and reliable model. This chapter goes through some of these details in understanding what makes a model stable and unstable, how initialization is done and what boundary conditions apply to various models. However, most learning come from experience with dynamic modelling and thus a custom summary presented in figure 17.

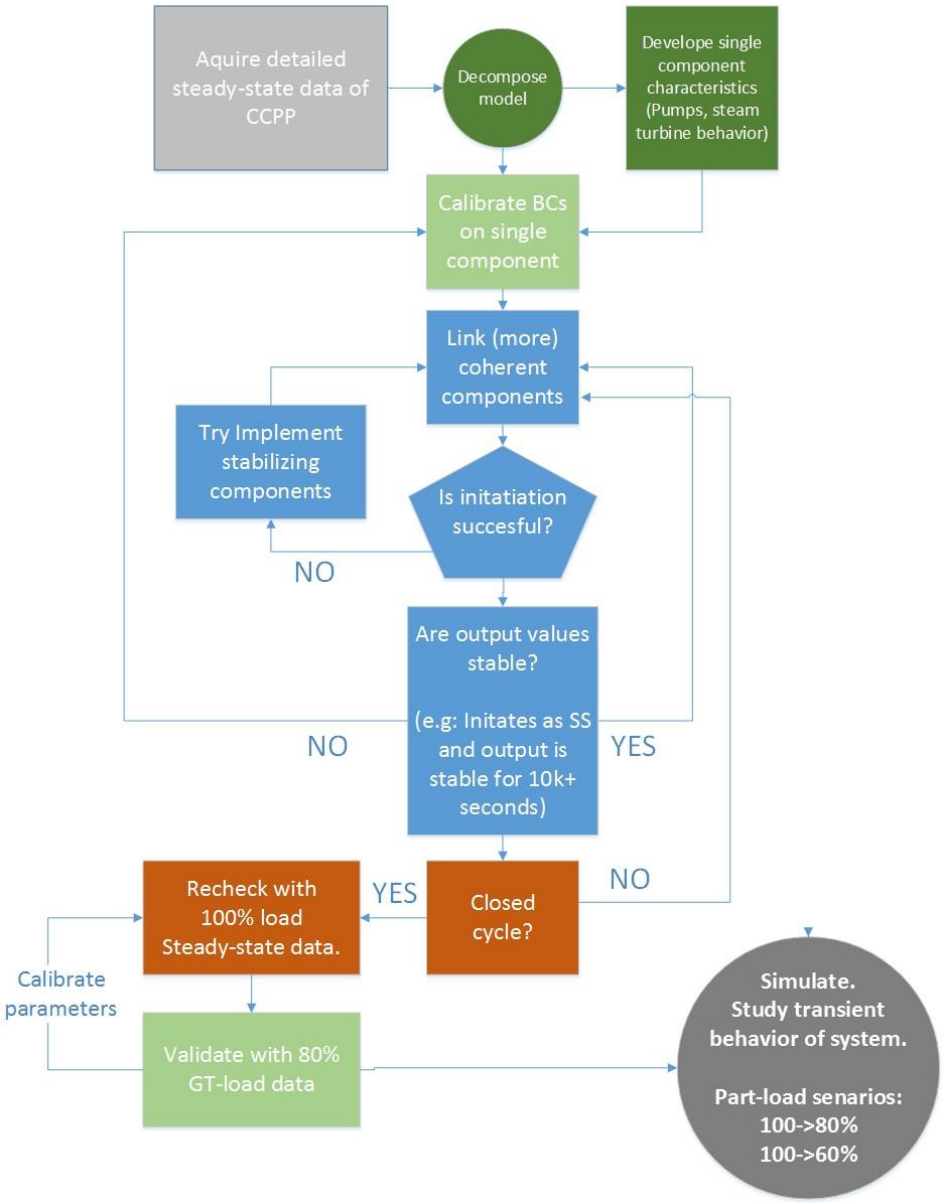

Figure 17: Simplified overview of dynamic modelling procedure based on experimental practice.

4.1 Modular approach

Each component in the model can be generalized into its isolated characteristics needed in order to build the whole model. Decomposition of each element can be set into generalized set of vectors and variables suggested by Dechamps [31], which is an:

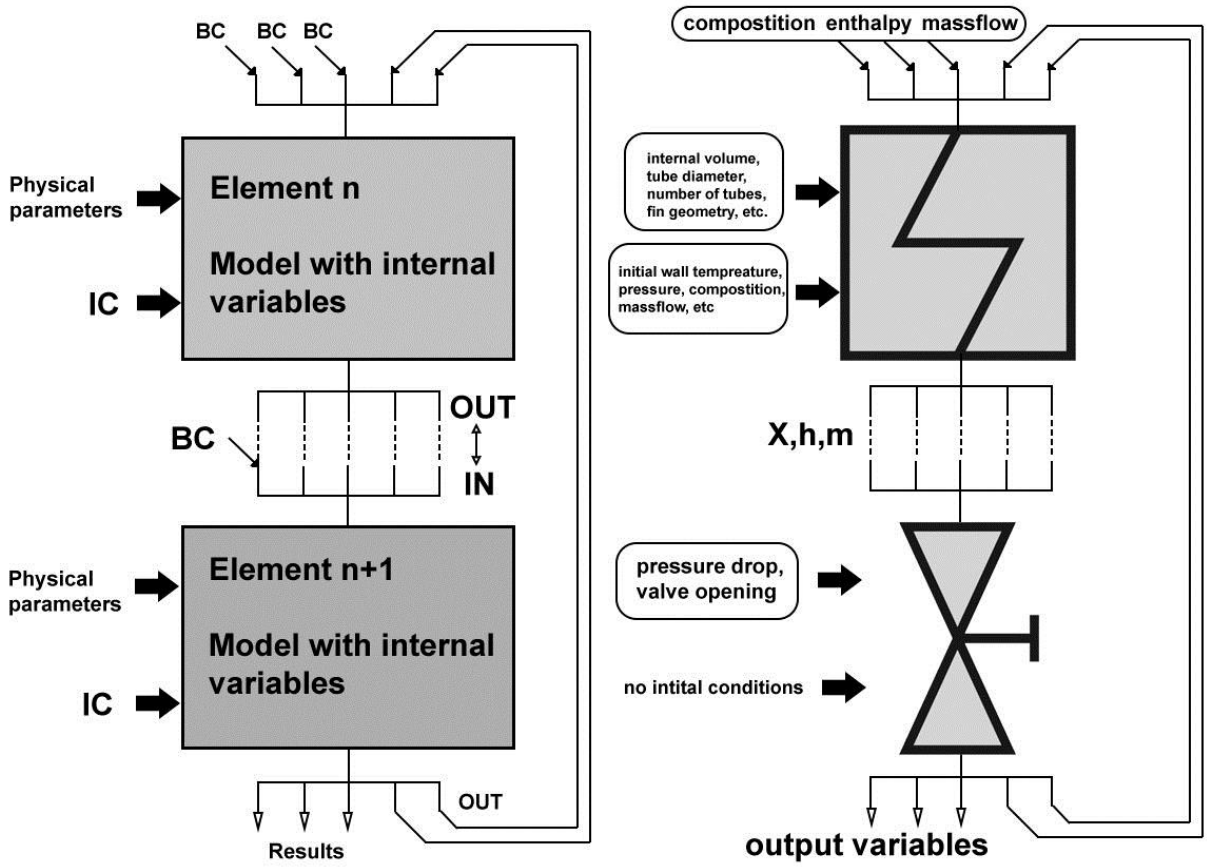

Figure 18: Modular approach method illustrated redrawn from Dechampes [37]. To the left is a generalized view, while the right with some example components. BC: boundary condition. IC: Initial condition.

- Input vector, (or boundary condition - BCs) which the components requires to calculate its performance mathematically.
- Output vector (which is produced by the component)
- Vector of necessary parameters, characterizing the components size, geometry, properties, and more.
- Internal variables, or mathematical models doing the intermediate calculations specifically to that model.
- Initial vectors to start the system (can be interpreted as input vectors)

The vectors (or in general BCs hereafter) are then linked to the other coherent connected components (like steam generators, valves, heat exchangers, etc.). Since each component has a boundary layer set at the inlet, outlet or both, nearby component with the same inlet vectors can be connected, illustrated in figure 18. However, connecting the elements is with arbitrary boundary conditions

4.2 Boundary conditions types and requirements

The logic behind building up a dynamic cycles is based on the much of the same logic as Kirchoffs potential (voltage) and flow (current) laws. In a simplified view, one can see boundary conditions or elements in the cycle a set of potentials (pressure) or mass flows (currents) that makes up the equation-set of closed steam loop. Setting the correct type of boundary conditions (BCs), or more precisely state variable, is vital to initialize single components before combining them to others. Thus, defining BCs with pressure or mass flow is not arbitrary, although standalone components can use both when tested individually.

An example is that the steam turbine is dependent on the front and backpressure of the turbine to calculate its power production. Other parameters set in the steam turbine rely on both inlet and outlet pressure to be known to perform the calculation. In the Kirchoffs analogy the pressure on both side produce a massflow of gas going through the steam turbine which has resistances in form of impeller blades, moment of inertia in the shaft, and other flow restrictors. Opposite, defining inlet and outlet state variables as mass flow will fail calculate the pressure ratio over the turbine, which is needed to calculate the other characteristics and to create the output.

However, when connected the steam turbine to other elements, the intermediate connections between them gets linked, forcing both boundary conditions to match, overwrite or be calculated based on the other one.

The modelling convention is to use massflow inlets and pressures in outlets for a components connected in series. Water needs three state variables to be defined, while gas needs two, assuming ideal gas law, which is the standard case.

Combining the various boundary conditions with selected steam cycle components is not arbitrary, and vary between the libraries. The dependency on what BCs each component require to initiate is not straight forward, and can be easier with some libraries than others.

Another problem emerge when linking components (like pumps, steam turbine and condenser) results in increased dynamic behavior and thus instability of the boundaries originally set between them The original steady-state behavior set by the BCs is suddenly affected by the new BC which used to be static, but are now dynamically dependent. A new characteristic has developed between the two or more components connected, and will stabilize given none conditional-steady components are included. This problem emerge normally when the system expands and include more and more components, and can result in tiresome troubleshooting finding the source of the instability. Causes can be depend on time-constants, stable and unstable components, which will be further discussed.

4.3 Steady and non-steady components

For producing a dynamic simulation model, the first thing is to divide the components of the power plant into steady and non-steady. One can distinguish these with the change rate of the component answering to a change in the thermodynamic boundary conditions (e.g change in temperature) reaching a new state of equilibrium [38]. To clarify, table 3 shows the classification of the steam cycle components into steady and non-steady for the models used in this thesis:

Table 2: Classification of power plant components into steady and non-steady [38]

Steady components	Non-steady components
Steam turbine	Heat exchangers
Pump	Steam pipe
Valve	Mixing point
Compressor	Feed water tank
..	..

Any system transient can be characterized by time constants, which indicate the time it takes for the system to reach its equilibrium in response to an interference in the parameters. Steady components have significantly smaller time constants in comparison to the non-steady components, which means low influence to the dynamic behavior.

Dechamps defines such constants in the various parts of the HRSG with the following equations in Table 4 [31].

Table 3: Time constants for numerical stability in the HRSG [37]

Type of HRSG time constant for..	Time constant [s]	Nominal Order of magnitude τ
External gas HT	$\tau_g = \frac{H c_{p_g} \dot{m}_g}{v_g u_g S_e}$	0.1
External HT with metal	$\tau_{m,g} = \frac{M C_m}{u_e S_e}$	100
Internal HT with water	$\tau_w = \frac{\dot{m}_w c_{p_w} l}{u_i A_i V_w}$	1
Internal HT with metal	$\tau_{m,w} = \frac{M C_m}{u_i S_i}$	100

H	height
v_g	gas speed in one dimension
S_e	External heat transfer surface
u_g	heat transfer coefficient for gas
u_i	heat transfer coefficient for water side
C_m	mixture velocity gradient (s-1)
V	real fluid speed (not 1D speed)

The stability of the numerical methods are revealed by evaluating the time constant, τ. Sampled numbers are based on normalized values to the closest order of magnitude ten for each parameter in the equation. Low numbers indicate more the potential for instability in the equations. Instability increase with the number of control volumes calculated as opposed to the heat exchangers as a whole.

The libraries discussed further on has different ways to tackle the continuity of steam/water through the cycle, which will come to view when evaluating the ThermoSysPro library.

5 Solving the equation sets

Computation of the system can be done in two ways: Sequentially or in a system of grouped non-linear equations using global methods.

Sequential computation is the simples approach and solves the elements sequentially, one after the other. The method has some drawback though. If the system has feedback-loops implemented (as with a cycle, illustrated by figure 18), the first element asks for the result in the second one, which are not computed yet. For this reason, the result from the preceding time increment (Δt) has to be used, thus introducing a time lag into the system. Therefore, sequentially computing is only applicable if the time-step is substantially smaller than the smallest time-scale of interest in the system.

Alternatively the non-linear equations can be *grouped up* and solved with a more arbitrary time step

However, dynamic simulation programs today often self-determine how to solve the equation set, based on the most time efficient calculation methods.

5.1 Discretization and numerical methods

Since some of the components in the system (like heat exchangers) cannot be solved by a unique set of non-linear algebraic equations, they need to be spatially discretized into a finite number of elements or slices, where they are solved linearly. All of these elements gives a deeper level of detail and needs to be solved for every space and time increment, which gives each discretized element a set of differential equations.

The combined set of linear- and non-linear equations are solved using numerical methods, which fall into two broad methodologic categories:

5.2 Explicit solving:

This method depend that a previous point in time has already been calculated for its current state to be solved. Starting the solver, this means using the initial conditions. Mathematically speaking the point at time $t + \Delta t$ is dependent on the solution of the system in time t. As the name indicate this method don't need an iterative procedure, but has an explicit set of equations that gives the solution. However explicit solving has an upper limit to how big the time increment Δt can be before the system gets numerically unstable, which is directly linked to the physical properties of the system. Depending on which explicit scheme we use, there will always be a time-limit and step-limit related to this instability.

To exemplify: The HRSG has its limit represented as the time it takes for the gas to cross one discretized slice in the heat exchanger. Depending on the gas speed, which is normally in the order of 10-20 m/s, a reasonable slice-size would be in the order of a few centimeters. Fontaine explains that it makes little sense to spend a lot of time for time-intervals in the order of milliseconds in the system, since the time interval of interest is often in the order of tenths of seconds or even in minutes over long transients [24].

5.3 Implicit scheme

Implicit methods do not depend on the calculation at time t to calculate its current state $t + \Delta t$. This solution is unconditionally stable for any size of time step and is in general the preferred for transient calculations for its robustness and unconditional stability [39]. The downside using implicit schemes is that the truncation error increase with larger time step.

There exist intermediate methods using both explicit and implicit scheme, where the most known are Crank-Nicolson method and Galerkin [40], but the stability criteria are in the order only two to three Δt more than the explicit schemes, and thus not comply with the time intervals of interest in a HRSG. Nor the large computational time needed to solve the iterative procedure.

Dymola uses various modifications of the implicit DASSL solver, which self-determine the optimal method for the whole equation set. [13]

5.4 Homotopy

During the initialization phase of a dynamic simulation problem, it often happens that large nonlinear systems of equations must be solved by means of an iterative solver. The convergence of such solvers critically depends on the choice of initial guesses for the unknown variables. The process can be made more robust by providing an alternative, simplified version of the model, such that convergence is possible even without accurate initial guess values, and then by continuously transforming the simplified model into the actual model. This transformation can be formulated using expressions of this kind:

$$\lambda \cdot actual + (1 - \lambda) * simplified$$

Where lambda is the homotopy parameter going from zero to one, and *actual* and *simplified* are scalar expressions, which formulate the system equations, and is usually called a homotopy transformation. If the simplified expression is chosen carefully, the solution of the problem changes continuously with lambda, so by taking small enough steps it is possible to eventually obtain the solution of the actual problem.

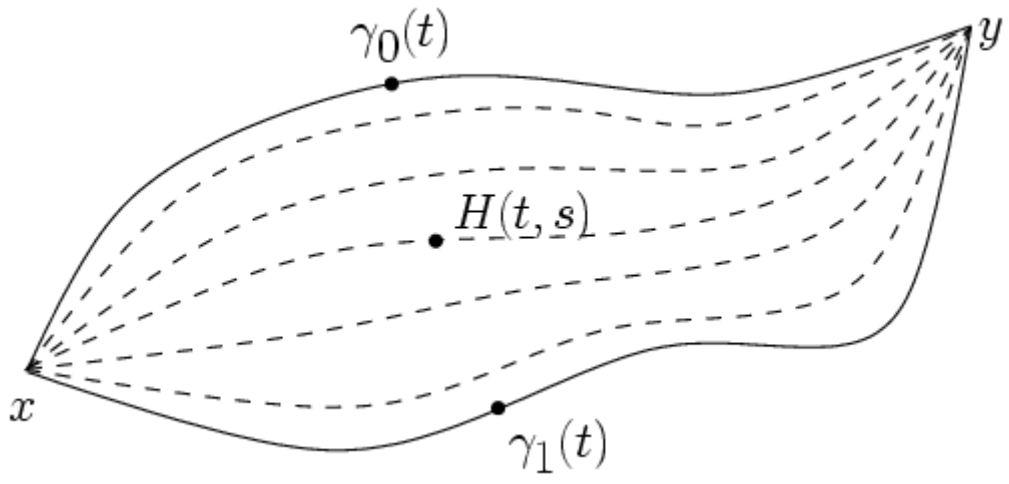

Figure 19: The dashed paths shown are homotopic relative to their endpoints.

In fluid system modelling, the pressure/flowrate relationships are highly nonlinear due to the quadratic terms and due to the dependency on fluid properties. A

simplified linear model, tuned on the nominal operating point, can be used to make the overall model less nonlinear and thus easier to solve without accurate start values.

Note that the homotopy operator shall not be used to combine unrelated expressions, since this can generate singular systems from combining two well-defined systems.[41]

By default, all libraries in Dymola uses homotopy which can be globally turned off or on for all sub-components in the model.

6 The Vertical Benson OTSG model

The case design is a section based vertical Benson OTSG with distinct superheater, evaporator (boiler) and economizer. The parameters are scaled by partially known parameters from the Oseberg D combined cycle and a suggested design by Lars O. Nord using commercial software GT PRO, developed by Thermoflow [12]. Known parameters include OTSG inlet and outlet temperature, pressure and mass-flow, and a predefined percent-based pressure drop across each section. Closely related work by Flatebø [25] and Folgesvold [42] used similar base-parameters in their combined cycle design also supervised by Nord. Part-load steady-state data at 80 and 100 percent are summarized in the appendix, and table 4 below give the base parameters for the cycle.

Jordal et al. stated using GT PRO simulations for part-load and full load steady-state is considered and reflect the performance of existing technologies [43].

However detailed, a set of assumptions in the dataset must be made in order to coincide with the available model libraries investigated in the next chapters.

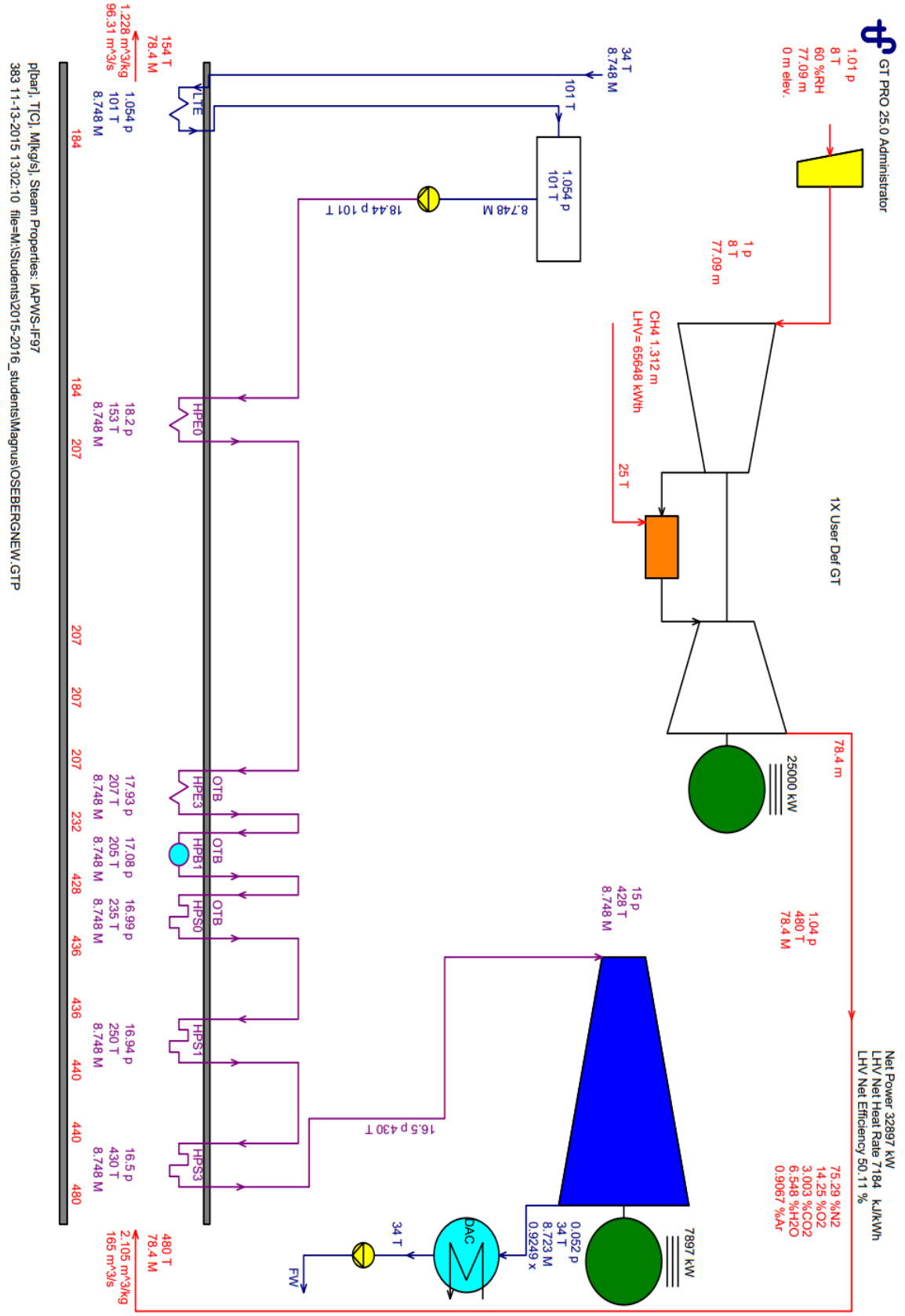

Figure 20: Overview of the nominal design-condition of the GT PRO data.

Table 4: Scaling parameters of the combined cycle mode of GT PRO

Gas turbine load		100 %	60 %
Model Type	[-]	User defined	User defined
Exhaust mass flow rate	[kg/s]	78.4	65
OTSG inlet gas temp	[°C]	480	450
OTSG outlet gas temp	[°C]	154	143
OTSG steam ΔP_{loss}	[bar]	1.94	2.08
Inlet steam turbine temp	[°C]	428	413
Outlet steam turbine temp	[°C]	34	28
Power output ST	[kW]	7897	5984
Power output GT	[kW]	25000	15000
Combined cycle output	[kW]	32897	20984

The deaerator is an integrated part of the condenser, which was selected in the GT PRO build options when data was generated. For the further modelling, the deaerator will merely act as a feedwater tank.

6.1 Approach temperature

GT PRO documentation also state that no approach temperature is included in the steady-state data, indicating that water leaving the economizer is at saturation point at design point [44]. The approach temperature is built in the economizer by design to suppress potential boiling which can lead to water hammering and unwanted tube-to-tube differential expansion [29, 45]. In vertical HRSGs the hydrostatic head can compensate by pressure increase but is normally not high enough. Alternatively, the external heat transfer area of the economizer is designed so that boiling will never occur at any part-load.

Nevertheless, setting the approach temperature 5-10K below saturation is done when the cycle has been properly calibrated and validated towards the data.

6.2 Location of the steam-separator

The most noticeable about the GT PRO data is the absence of the steam separator in both the graphical data output and elemental description. The help-files in the software describe the Once-through Benson sections as one single continuous coil connecting the last economizer (HPE0), evaporator (HPB1) and first superheater (HPS0), and makes no mentioning of the characteristics of the separator, nor size of it [44].

However, recalling chapter 3 the separator do not play any vital role during normal high part-load transitions, and that the blowback or recirculation valve is most likely closed at this operation mode. Consequently, the once-through evaporator practically acts as a continuous tube bundle split into various number of parallel passes of depending on section, connected by headers in the tube end. Figure 21 [9] from previous work shows the tube-stack of each section in detail.

Thus, it is assumed that a Benson separator is located between the first superheater HPS0 (OTB) and HPB1 (OTB) described in figure 21. This is the last row of the OTB and whether the last row is included or not is insignificant regarding heat transfer before separation.

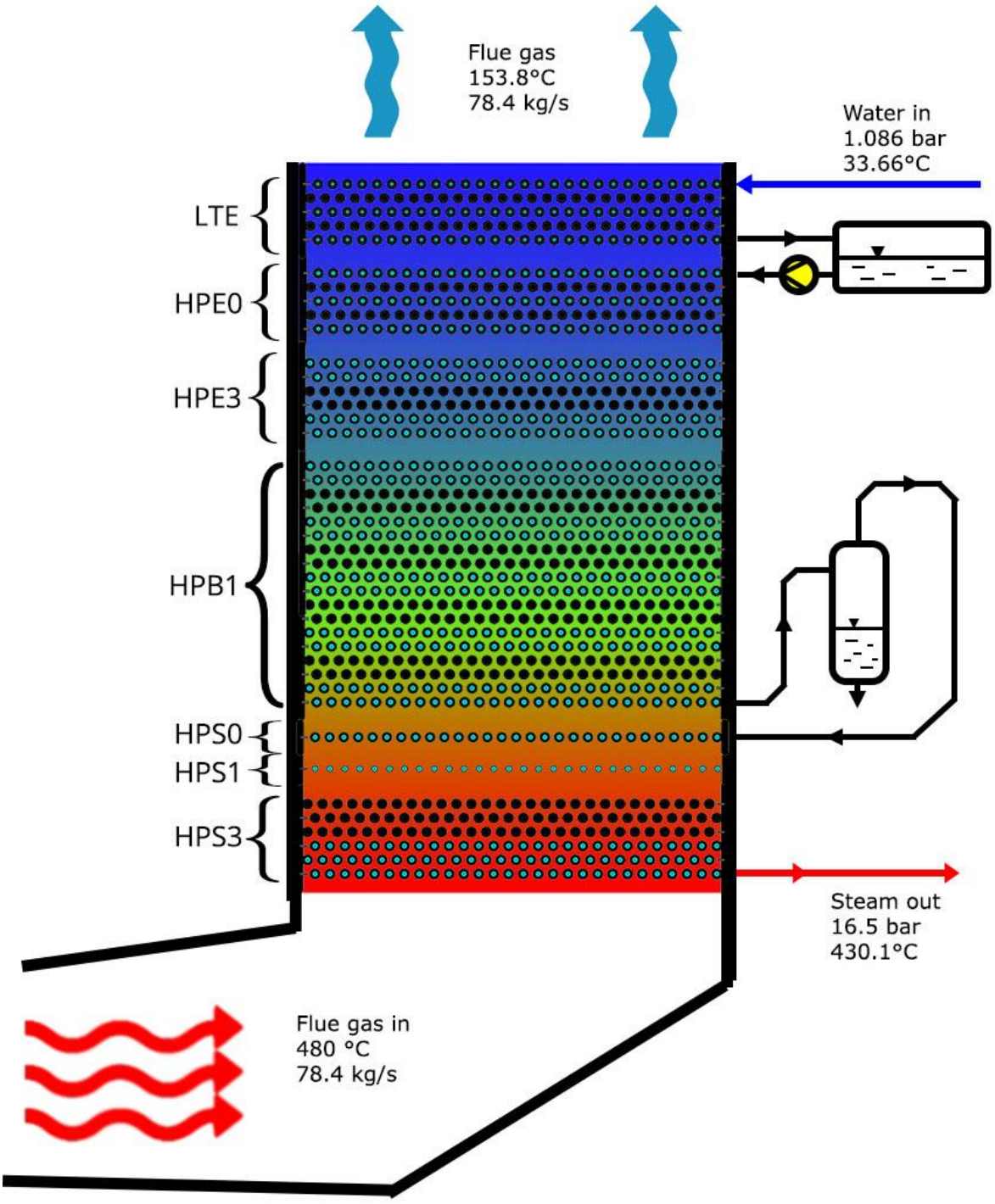

Figure 21: Simplified sketch of the OTSG showing alternate tube passes. White dot indicate flow outwards and black center inward flow.

Possible options for both reinject unsaturated water back into the HPB1 or to blowout will be tested within the library packages if present. It is expected that the separator will act as a buffer tank to the dynamics of the steam cycle and help initialize the model and work as an indicator for the needed water flow in the steam cycle when stabilizing.

6.3 Flow path and tube rows per pass

How the headers split the flow into parallel tubes in the OTSG play a major role in the total heat transfer absorptivity, section pressure drop and part-load characteristic act on the steam cycle. The first economizer has one row per pass, while the last superheater has three rows per passes. In the once-through evaporator, there are two rows per pass, but this changes in the transition to both the economizer and superheater.

Some inconsistencies in the tube row data has been accounted in HPE3, HPB1 and HPS0, showing 5.876, 15.62 and 0.5095 tube rows respectively. All being part of the OTB, and both HPB1 and HPE3 having two rows per pass, it is assumed that the summarized rows (22.0055) represents the whole OTB and can be set to 22 rows (11x2). All sections exhibit the same fin configuration. Errors are highlighter in detailed graphical HRSG pages of the appendix.

It has been confirmed that the heat transfer values for the summarized OTB correlates with the external heat transfer surface through back-calculations using ESCOA HT-correlations, which has been found in multiple papers. Further corrections to the external , The usage of ESCOA is merely based on the structure of the GT PRO output data, since these correlates with the procedural calculation found in papers using them [46, 47].

Correlations themselves will be discussed in further detail in chapter 11.

6.4 Inconsistency in Reynolds numbers

Based on the output format in GT PRO, one can predict that the heat transfer correlations are most likely based on the ESCOA correlations, although it has not been officially confirmed by any documentation from GT PRO. The ESCOA heat

transfer correlations are the only ones found to utilize gas mass flux in kg/m^2-s as an intermediate calculation for further dimensionless numbers like Reynolds, Prandtl and Nusselt.

Calculation the gas mass flux and further the Reynolds numbers shows that the resulting numbers deviate from the output of GT PRO. All numbers up to the Reynolds formula has been validated with insignificant deviation and good correspondence with the existing numbers.

$$G = \frac{W_g}{N_w L(S_t - A_0)}$$

$$Re(d_0) = G \cdot \frac{d_0}{\mu}$$

Here S_t is the transverse pinch length, A_0 the obstruction area in front of the OTSG, and N_w number of parallel tubes in width, L tube length and W_g gas mass flux.

The only variable able to change the Reynolds number is the characteristic length, which is shown to not correspond to any particular length throughout all section calculations. Table 5 shows a summary of the best most prominent characteristic lengths. Also Reynolds calculations based on max velocity has been tested, whereas the best results show length close to d_t including bare tube diameter plus two times the fin thickness.

Table 5: Reynols number calculated with various characteristic length

	HPS3	*HPS1 (BARE!)*	*HPS0 (OTB)*	*HPB1 (OTB)*	*HPE3 (OTB)*	*HPE0*	*LTE*
GT PRO Reynolds number	10681	10029	12169	13301	14647	9782	10528
GT PRO d_0 [mm] traceback calculation	33,75	35,26	35,67	34,02	32,68	27,18	28,20
$Re(d_0)$ external tube diameter	10052 -6%	9013 -11%	10646 -14%	12416 -7%	14234 -3%	9144 -7%	9486 -11%
$Re(d_v)$ volume equivalent diameter [48]	11419 +6%	9013 -11%	12965 +6%	15120 +12%	17335 +16%	10627 +8%	10909 +3%
Re(d_t) bare tube diameter plus two fin thickness [49]	10685 0%	9013 -11%	11316 -8%	13198 -1%	15131 +3%	9864 +1%	10233 -3%

To remain consistent the same defined characteristic length needs to be applied to all. The most established methodology convention is to use the bare external tube diameter reference length [49] [47, 50, 51]. However, with finned tube banks characteristic length is suggested modified in multiple papers because of the various fin density and geometry. Frass [52], Næss [49] and Kawaguchi [48] have all discussed this in their respective research papers.

Table 6: Suggested characteristic length in various papers.

Kawaguchi	$d_v = \sqrt{n_f \cdot s_f \left(\left(d_0 + 2 * h_f \right)^2 - d_0^2 \right)}$
ESCOA [46]	d_0
VDI Atlas	$l' = \frac{\pi}{2} \sqrt{d_0^2 + h_f}$
Næss [49]	$d_t = d_0 + 2t_f$
Schmidt/FDBR (FD) [52]	$l' = \frac{A_{tot}}{\pi}$

If the Næss characteristic length is being used, it shows good agreement, with the exception of the bare tube diameter row in HPS1 which is a continuous error through

all the calculations. Unable to correct for this value in any tested characteristic length suggest that the GT PRO averages or simplifies this specific tube.

It should also be noted that be the errors previously described in the OTB would maybe affect how the Reynolds may be calculated as well. This is unknown because of the "black-box" nature of the GT PRO. With this uncertainty is hard to know the exact correlations used, and qualitative guesses suggesting either Næss' d_t characteristic length d_0 used by ESCOA is the best choices thus far.

Furthermore, it is clear that the final model will suffer from the error already calculated in the Reynolds-numbers which both heat transfer and pressure drop correlations depend on in the models now being evaluated.

7 Evaluation of the libraries

In the Modelica, C-based objective language, there is a large amount of different libraries to use for modelling different domains including mechanical, electrical, thermal and fluid mechanical translation. The conversion of energy and flow between the different domains is what makes Modelica very applicable to especially dynamic simulation which easily becomes complex with even the smallest power cycle systems. With the existence of both open-source (OS) and commercial libraries it can be hard to evaluate which should be chosen for the different modelling tasks, while at the same time exhibit robustness, quality of documentation and with level of detail.

Reviewing the different open-source libraries indicate that the quality and limitation of each one reflects the specified research program it was purposefully made for by the developers themselves. However, some have extended their library content to domains like electrical, mechanical components together with the thermal and fluid components which is published as multi-purpose open-source library to the public.

Especially large emphasis has been taken toward existing heat transfer correlations of the include HRSG modules in the libraries evaluated, and has been the decisive criteria for constructing a OTSG model with high level of detail.

7.1 Open Source versus Commercial libraries

In general, commercial libraries are more maintained than the open-source libraries and offer exclusive support and feedback to the clients. However, this advantage comes at a cost of licensing which lead many researchers to developing models themselves from existing open-source libraries. The cost can often be in the order of ten-of-thousands of NOK per license, and it thus become imperative that scoop of study is included highly within the detailed models of the library, with only minor modifications necessary.
On the contrary, open-source is per definition free, and can be further contributed and improved from individuals of different fields of study. Both types have pros and cons that has to be individually examined for its specific features, which is often decisive when choosing from a wide variety of libraries.

Regardless of license type, most of the source-code in both type of libraries can usually be investigated directly to understand the underlying calculations of the models. The Modelica language is highly flexible in the context that both commercial GUI-software like Dymola and its open sourced counterpart OpenModelica can use the same libraries. OpenModelica is based on a long-term development from the non-profit organization OMSC (Open Source Modelica Consortium) where most of the board members origin from research referred to throughout this paper, both from universities, institutes and private companies [53]. The libraries included with the OpenModelica software stem from a collection of maintained and non-maintained libraries, where three out of the four investigated libraries are included in the latest OpenModelica package [54]. Any user registered at the OMSC webpages are free to contribute and upload their libraries in the OM package.

7.2 Evaluation criteria for

All the evaluated libraries contain dynamic modelling of thermal water and gas systems for and is available under the Modelica License Version 2.0. An overview of the investigated libraries are set up in table 7, including some indications of their content:

Table 7: Initial comparison of libraries.

	Thermopower	ClaRa	ThermoSysPro	SiemensPower
Origin country	Italy	Germany	France	Germany
latest version	3.1	1.1.0	3.1	2.2
Dev. Status and last major update	Continuous, Sourceforge, march 2011	Continuous, claralib.com, Aug 2016	Beta, June 2014	Discontinued, march 2012
Compatible with MSL* version	3.2.1	3.2.1	3.2.1	3.2
Documentation	Built in, in-code, external, conference papers	Built in, in-code, web-documentation library.	None, conference papers and examples	Partially, built in, in-code
Quality of documentation number of papers written	Good. 10+ papers.	Good. Approx 5-10 papers	Preliminary good. Less than 5 papers.	Low
HRSG tube and fin level of detail	Low, simplified	High, modular	High, static	High, non working
Gas HT correlation options	Constant HTC. Flat tube.	Modular. VT-Atlas, Nusselt, …	Rigid. Babcock and Willox. Tabulated.	Rigid. ESCOA (non-complete)
Primary application domain	Thermal power plant	Coal steam plant with CCS.	Horizontal drum-HRSG CC	-
Initial HRSG evaluation	Lacking detailed geometry	Complex. Only for coal plant,	Conditionally good	None working models. Unstable.

*MSL: Modelica Standard Library

Listed below are some guide lines set for evaluating the desired features and properties necessary for building the once-through steam cycle model:

- Extensive tube bundle fin geometry in the HRSG model. Include heat transfer correlations with variable h.t.c. on both water and gas side of the heat exchanger.
- Level of detail in tube arrangements in HRSG. Fin-corrections. Number of tubes and arrangements of these.
- Flow-pattern options (cross-flow/co-current/counter-current parallel flow)
- Changeability of dynamic conditions of the HRSG, including choices of using dynamic mass, heat and pressure balances with different conditions. Discretization options of heat transfer and pressure drop (cells, fluid volumes, number of tubes, etc) and correlations of these.
- Ease of use, documentation, compatibility towards other libraries and validation towards the steady-state data as well as documented sources.

7.3 Inadequate documentation

Documentation is a first indicator of whether the library has the necessary included components to model a once-through steam cycle. It is either integrated into the library through commented code or help-files, or linked to papers on the internet. One of the three main libraries evaluated and tested did not have any documentation released yet, which has been further confirmed through mail correspondence with Baligh El Hefni, who's the main developer of ThermoSysPro.

Opposite, the library can seem to have been over-documented, and have components missing or later removed in its development. SiemensPower 2.2 seemingly had a complete library with documentation inside its source-code of the ESCOA heat transfer correlations, the same used in the GT PRO data. However, after thoroughly examination of the source-code, none of these correlations existed within the parameterized models ready for input and connections.

In short, the Siemens Power library, both version 2.1, 2.2 and OMCtest was not further evaluated since recursive model builds failed in 10 out of 12 package branches, indicating errors on multiple levels throughout the library. Initial debugging of the flue-gas model code indicated that there might only be minor variables and compatibility issues which could be fixed. However, compiling the model in Dymola after the initial corrections, errors on multiple dependency levels arose as a result,

since Dymola checks the module levels sequentially. Thus, it is unknown how deep the error chain grows, and brings uncertainty to further debugging.

Discarding the SiemensPower library, it shows that finding an applicable library is not straight forwards elimination process. Poor documentation is a general problem throughout all OS libraries as will be discussed further. This means digging into the source-code is the only real way to know the characteristics of the built-in models coming with the libraries.

8 Improving previous Thermopower model

Thermopower is an open-source library developed at Poleticnico di Milano, for dynamic modelling of thermal power plants and energy conversion systems. It has been continuously developed since 2002 and is based on the Modelica Standard Library, which makes it backward compatible within older Modelica versions [55].

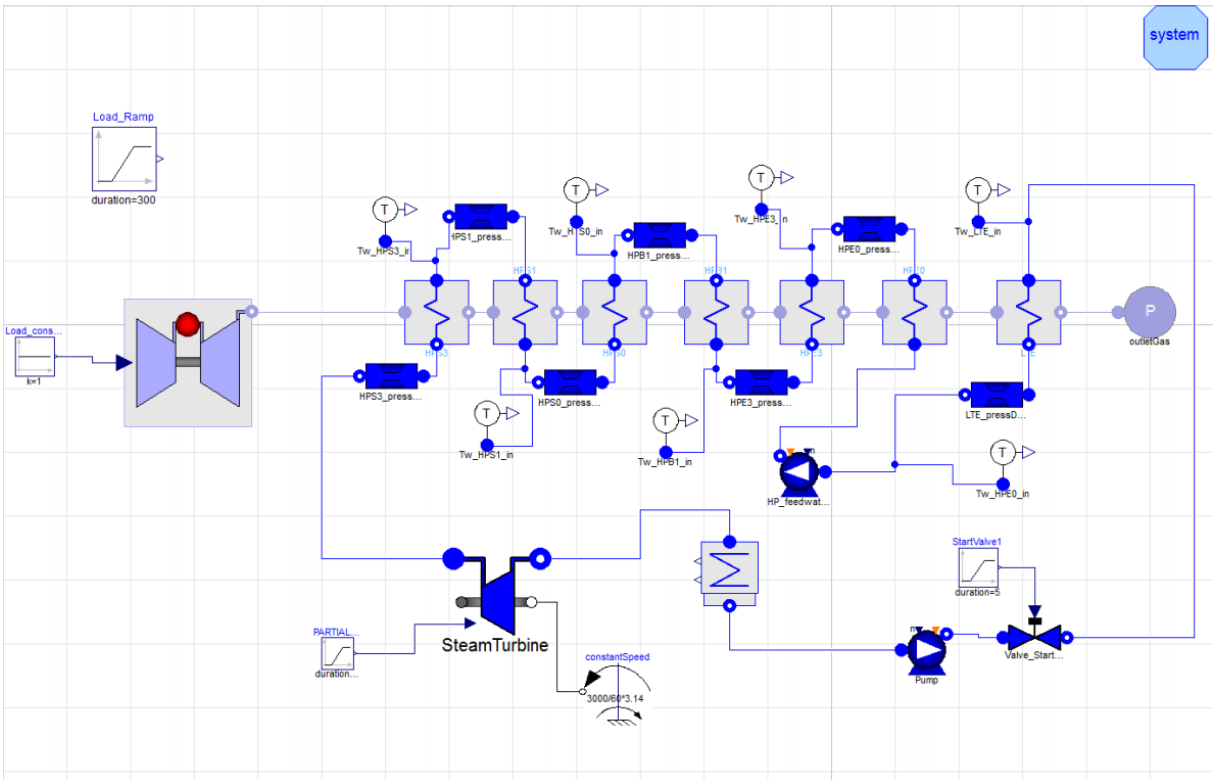

Figure 22: Preliminary Thermopower model of GT PRO data.

Previous work by Gule [9] carried out the initial modelling of the same GT PRO data with Thermopower, and the library's features and properties were also documented.

Listed below are some remarks for improving the current model, and limitations to Thermopower's current version.

Static heat transfer coefficients

Although some papers have justified the simplification of constant heat transfer coefficient [56], it has been highly advised to use heat transfer correlations for both inside and outside of the tubes, which is also the prime objective of the thesis. Heat transfer dependency on Reynold, Prandtl, and other dimensionless numbers are the requirement for further detailed modelling of the once-through heat exchanger.

Lack of horizontal tube flow with tube bends and fin configuration

Both horizontal and vertical flow patterns are arbitrary not defined, since horizontal pipes tend to produce stratified flow, as vertical give wetted perimeter. Hydraulic pressure drop and calculation is neither calculated, and merely based on roughness of the inside of the tube calculated by Colebrooks equation [7]. The external heat surface is simply set with an area value, with no geometrical parameters of fin height, width, length etc., which makes external correction factors to be set within the externally defined surface area.

Bridge ClaRa HRSG model to Thermopower

However, other modules in the Thermopower exhibit detailed features, like partial arc control in the steam turbine, detailed gas turbine model, valves with detailed characteristics and pumps with flow and efficiency characteristic curves. With the established knowledge in the library, it is desired to continue the model by integrating models from other compatible libraries.

The ClaRa library, which will be discussed in further detail in chapter 10, contain a Thermopower-ClaRa water/steam flow adapter, able to convert the flows between the IPWS-97 library of Modelica and the TIL Media library of ClaRa. This opens up for using heat exchanger models from ClaRa directly in Thermopower.

ClaRa primarily made for coal plant

Initial investigations of the ClaRa library show that no included tube-bundled heat exchanger exist suitable for the detailed OTSG. Through mail correspondence with

developer Lasse Nielsen, it is suggested that a dynamic flame-room model integrating slag, coal fuel and exhaust gas may replace the heat exchanger. Simplifications using no coal input fuel and slag mass flow was set, making in act as a pure exhaust heat exchanger.

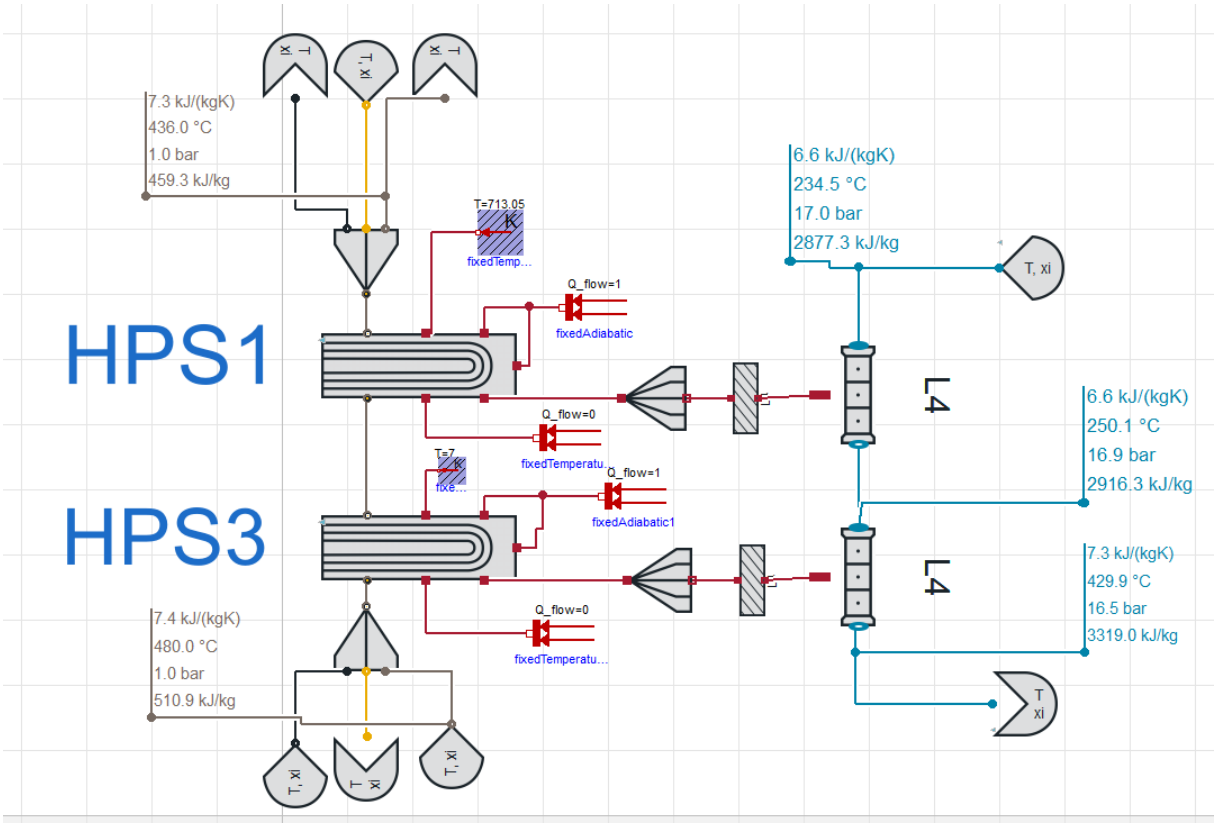

Figure 23: Initial once-through model using flame-room burners as tube bundles.

However, with multiple heat ports, large amounts of unnecessary calculation output, and setting heat-ports adiabatic with various boundary conditions, made connecting the initial OTSG sections a delicate procedure. With over 6700 equations needed solving after just two heat exchangers, the focus shift towards ThermoSysPro which is dedicated towards pure HRSG power plant modelling.

9 ThermoSysPro

The library is developed in France by Baligh El Hefni and Daniel Bouskela at the EDF R&D [57] and aims to model and simulate both static and dynamic thermal power plants. Compared with the already discussed libraries, beside the Siemens Power 2.2, this is the only library coming with an out-of-box ready HRSG-module (dynamic heat exchanger) with extensive tube fin configuration options, including

cross-flow and dynamic heat exchangers properties, while still being open-source, and with working models. The library claims to be validated against several cases in power plant modeling, e.g. nuclear, thermal, biomass and solar domains [57]. The library has continuously been in development since 2011 and has not officially been releases though found in the OpenModelica package.

The library contains different domains of power plant modelling for 0D-1D static and dynamic modeling of thermodynamic systems, which includes disciplines such as thermal-hydraulics, combustion, neutronics and solar radiation.

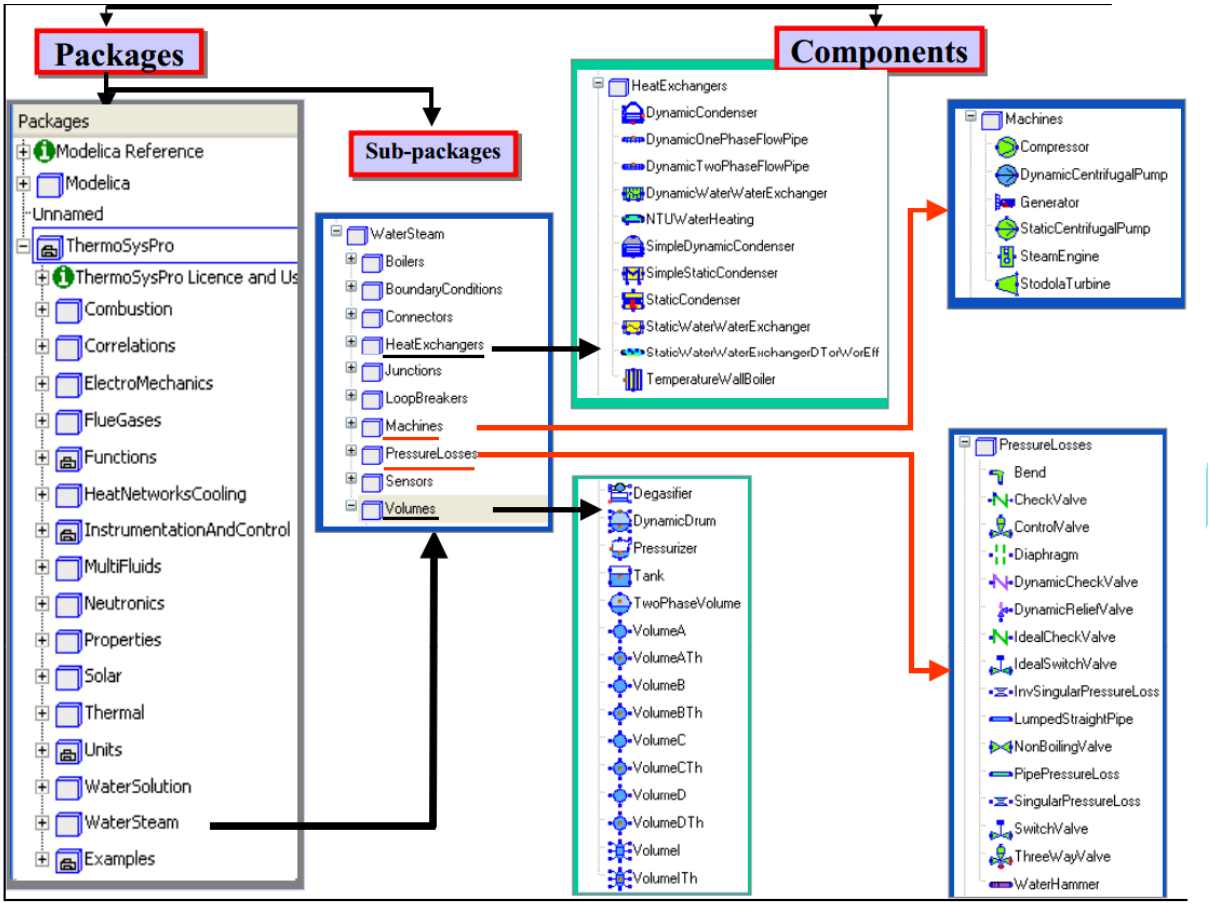

Figure 24: Package structure of the ThermoSysPro library

The library structure is similar to both ClaRa and Thermopower where components are subdivided into application domains, each corresponding to a connector type [58]. It supports both incompressible and compressible flow and can handle reverse flow like the other libraries, and utilize the Modelica Standard IPW-97 library for calculating water/steam properties.

9.1 Two-phase cavity model

The tube bundles in ThermoSysPro are modelled as non-adiabatic two-phase volumes, with either vertical or horizontal cylindrical geometry. Accumulation of both mass and energy are considered in each mesh cell of the volume, including the inertia of the fluid. The grid scheme calculations are based on finite volume method, just as Thermopower, which has been described in detail in previous work [9].

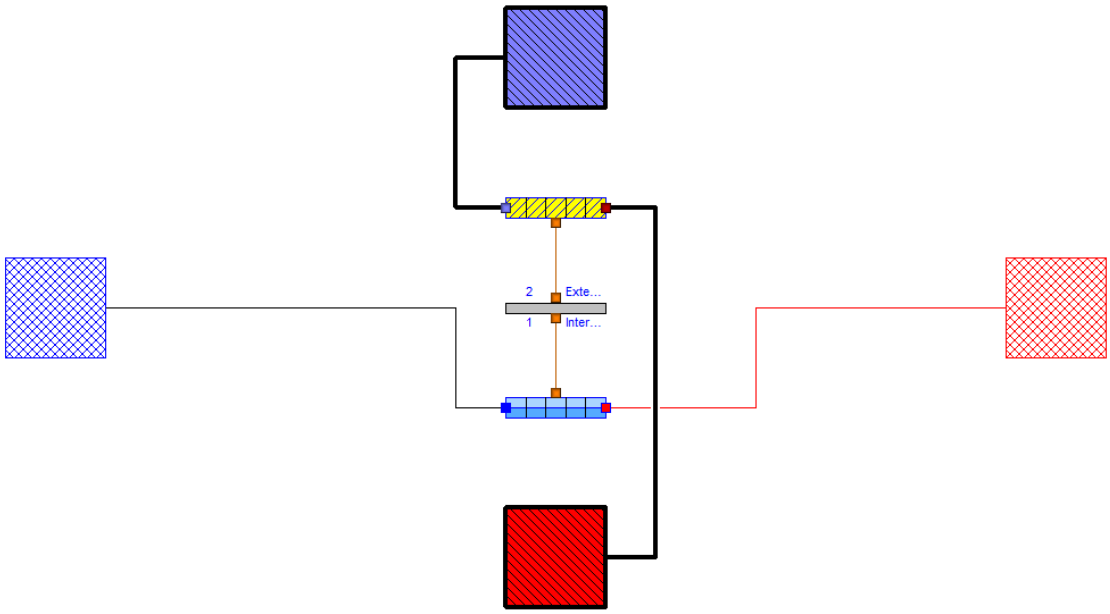

Figure 25 Dynamic Heat Exchanger model in ThermoSysPro

The model build-up is similar to the Thermopower heat-port connection principle, but all parameters are built into the StaticWallFlueGasesExchanger (yellow) and TwoPhaseFlowPipe (blue) depicted in figure 25. A metallic wall with specific heat capacity connects the two volumes through heat ports.

A special feature is the options to manually include inertia, advection and dynamic mass balance in the two-phase pipe flow model. Initialization can be done either through steady-state or through predefined enthalpy or temperature skids defined for each discretized volume. In Thermopower only initial enthalpy values can be defined.

9.2 Initialization procedure

The modular approach explained in chapter 4.1 has been used together with the flowchart in chapter 4 figure 17 to model the OTSG piece by piece. Keeping the heat

exchanger chain low enough, no particular initialization values are needed because Dymola helps set the automatically if none are defined. Growing in number, both initialization from the parametrization options in the heat exchanger model and using externally scripts are necessary to run the OTSG model isolated.

In short, using externally set initialization values increase the workload and the values has to be calibrated when end boundary conditions are changes. While both Thermopower and ClaRa will do with an all-in-one click for both translation (compilation) of the model to C, initialization and simulation, ThermoSysPro needs to do all these operations manually. To systematically update parts of the model for calibration, multiple scripts can be used to structure the initialization order but will also increase the workload for every iteration.

Dymola has options to update the initialization values after the model has been simulated. Unfortunately, when used in ThermoSysPro it will cause errors in the initialization mesh of the heat exchangers, over-defining it with valued not valid for the model. Though some of the values are improves, all the values have to be edited before the next simulation.

The slow initialization and simulation procedure is ThermoSysPro is thus one of its main problems increasing the workload of the model.

9.3 Intermediate volumes and flow-multipliers

Some type of components cannot be directly connected because of their dependency of particular state-variables in either connection points. To quick fix for this to ensure that almost any component can be connected in series, mixer volumes are set in place between them. The mixer volumes act as boundary conditions for all state variables of the flow, and helps e.g. the steam turbine initialize with a set backpressure at time zero.

In the included CCPP example, these type of intermediate mixers are set in front and back of steam turbines, and between steam drums and heat exchangers in some cases. They act as stabilizing agents buffering the current state of the flow between two components, which otherwise could make inconsistent flow pattern and cause singularities in the calculations, because of poorly set initial conditions. A bad set

initialization can cause the element to cause backflow or produce unrealistically high or low output of values, causing other elements to fail in the chain.

Ideally, such components should not be necessary if the initialization procedure was properly integrated in the components, and input of arbitrary state variables would warn the user or just be alternatively calculated based on the state variables given.

However, this not being the case, a last unknown component used in the attached CCPP example was flow multipliers. These were implemented in front of the steam turbine and after the condenser in the CCPP example without any particular documented purpose, if any.

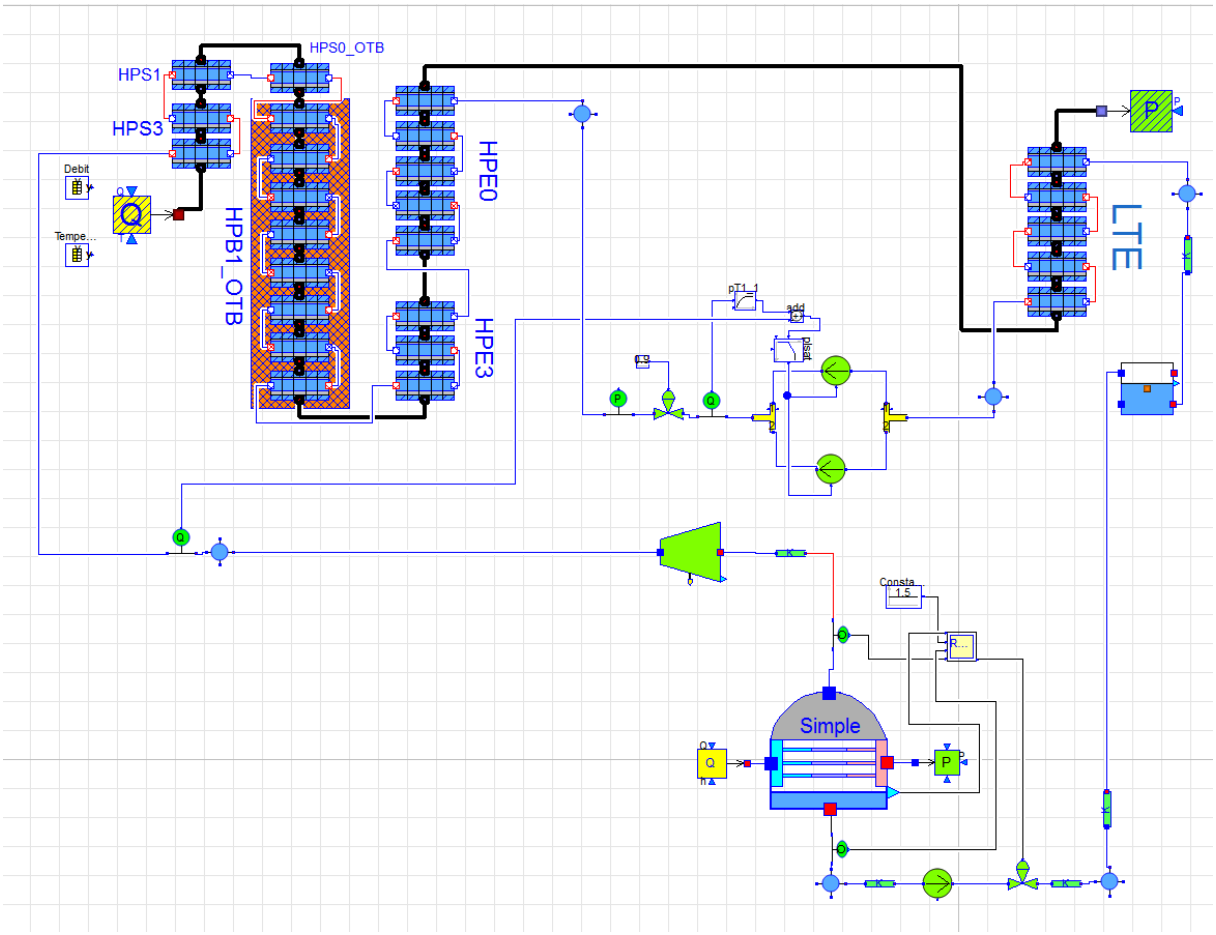

Figure 26: Preliminary OTSG steam cycle in ThermoSysPro

As a result of the high initialization workload, usage of mixer volumes, and the unknown purpose of the flow multipliers maybe necessary to the model, it was natural to re-evaluate the advantages of using ThermoSysPro over the other libraries.

This drove the motive to take an extra look at the ClaRa library module layers, for which ended up actually becoming the core library for final steam cycle built in the coming chapter.

10 ClaRa

ClaRa (Clasius-Rankine) is an open source library of power plant components written in Modelica. It is primarily based on modelling of coal-fired power plants with carbon, capture and storage (CCS) modules, but is capable to simulate heat recovery power plants like combined cycles as well [38]. Both once-through and drum-circulated boilers are supported, and the library is structured in layer dependencies just like Thermopower and ThermoSysPro – however on a much more detailed level and with easily replaceable modules. It includes components like pumps, fans, turbines, furnaces, electric motors, mills, valves, piping and fittings, as well as storage tanks and flue gas cleanings units. Unlike the other two, it also includes vapor and liquid separation units – modelled as centrifuges – which are the only out-of-the-box pure phase separators beside the traditional drums found in all libraries. Thus, the Benson™ Once-through cycle can in principle be modelled with this separator, using the Level 3 (L3) mechanical steam separator with leveling control [34].

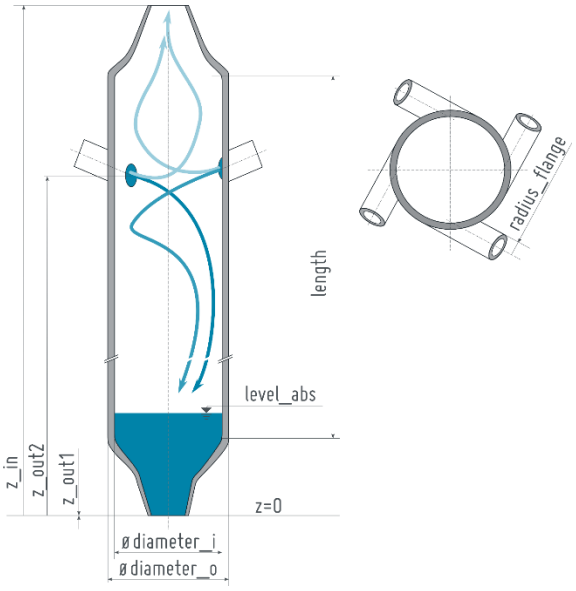

Figure 27: Model of the ClaRa L3 steam separator. [6]

ClaRa provides component models at different level of detail supporting the user in creating models tailored to their specific need [38]. The advantage of this concept is that the physical precision of a complex power plant can be adopted to the given simulation task without an unnecessary excess of computing time. Components of low interest can be set to lower details levels ranging from L1 to L4, describing the which physical effects should be included.

The additional libraries that come with ClaRa include media data from the TIL Media library, as well as functions for pressure loss and heat transfer from the FluideDissipation library. Developers claim that the TIL Media library is faster and more rubust when compared to Modelica.Media which all other libraries depend on [34].

However the IWPS95 water tables is the default option when modelling water based cycles, and is further used it the upcoming models.

The component models are validated towards measured data from existing plants [38]. High-quality models are ensured through collaboration with industrial and academic partners such as

- TLK-Thermo GmbH, Braunschweig
- XRG Simulation GmbH, Hamburg
- Institute for Thermo-fluid Dynamics (TUHH), Hamburg
- Institute of Energy Systems (TUHH), Hamburg

10.1Library structure

ClaRa has a broad range of physics elaborated into the library structure that is well-arranged and user friendly. The figure below shows the top level content of the structure tree:

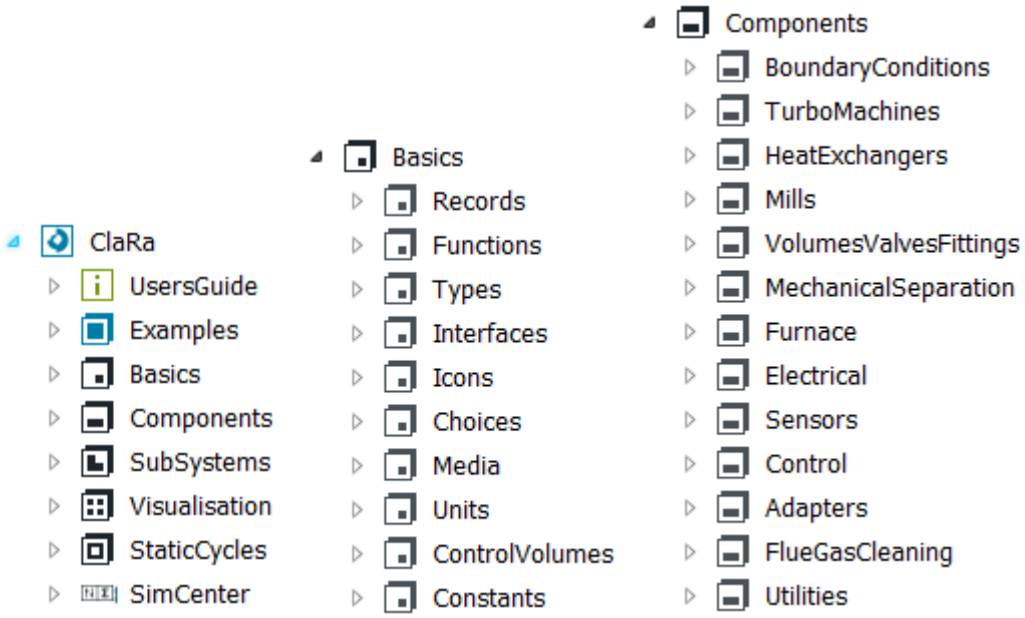

The package Basics provide elements which are fundamental to all models contained in ClaRa. Beside data structures *(Records/Types/Choices),* special *Functions* and *Constants* the package provides *Interface (connector-)* definitions, *Media data*, the *ClaRa unit system* (based on SI units) and the fundamental *Control Volume* definitions.

SubSystems provide models of increasing complexity and are based on each other, as indicated by the little black boxes in the icons.

The Components package provides all basic models necessary in order to build up models for conventional power plants. The package is divided into sub-packages according to the different component categories, e.g. *TurboMachines*, *VolumeValvesFittings* or *Furnace*.

Visualization package contains various elements for displaying and plotting of dynamic simulation data, which is unique to in the context of Thermopower and ThermoSysPro. This simplifies the modelling procedure drastically, since primary parameters for flow and levels can be seen directly in the model without the need to check the simulation data three. The values are also continuously updated during the run time of the simulation. *Quadruples* for example provide a dynamic version of similar displays used in steady state simulators or manufacturer design sheets of

components. These and other state variable displays will be extensively used throughout the modelling procedure.

10.2Levels of detail

The ClaRa library contain models at different levels of detail. What assumptions and structural limitations the model is based on differ from user to user, and the physical effects wanted to be investigated may not be of equal importance throughout the model.

ClaRa has been built to provide a well balanced combination of readability, modelling flexibility and avoidance of code duplication. Consequently, each component in ClaRa is represented by a family of freely exchangeable models, where every component family is grouped into four levels of detail, L1, L2, L3 and L4. Below follows an explanation of the various detail level of the ClaRa library.

Table 8: Level of detail. ClaRa explained

L1: models are the simplest models and based on characteristic lines and / or transfer function. These result in idealized physical behavior and the model definition may be derived either from analytic solutions to the underlying physics or a from phenomenological considerations. Applicability is limited to the validity of the simplification process, and non-physical behaviors may occur otherwise. Examples: *transmission lines model for fluid flow in a pipe.*
L2: Models are based on balance equations. These equations are spatially averaged over the component. The models show a correct physical behavior unless the assumptions for the averaging process are violated. Example: *single control volume for fluid flow in a pipe.*
L3: Models are by construction subdivided into a fixed number of spatial zones. The spatial localization of these zones is not necessarily fixed and can vary dynamically. For each zone a set of balance equations is used and the model properties (e.g. media data) are averaged zone-wise. The models show a correct

physical behavior unless the assumptions for the zonal subdivision and the averaging process over zones are violated.

Example: *moving boundary approach for fluid flow in a pipe.*

L4: Models can be subdivided into an arbitrary number of spatial zones (control volumes) by the user. They thus provide a true spatial resolution. For each zone a set of balance equations is used which is averaged over that zone. The model shows a correct physical behavior unless the assumptions for the choice of grid and the averaging process over the control volumes are violated.

Example: *finite volume approach with spatial discretization in flow direction for fluid flow in a pipe.*

By now, the fundamental equations of a model are defined by setting its level of detail and the physical effects of consideration. However, these equations declare which physical effects are considered, but not how they are considered. For instance, the pressure loss in a pipe may be modelled using constant nominal values or via correlations taking the flow regime and the fluid states into account. These physical effects are therefore modelled in replaceable models that complete the fundamental equations using predefined interfaces, e.g. the friction term in the momentum balance. By separating the governing model definition from the underlying submodels, the *flexibility* of the model is enhanced without loosing readability.

In order to cope with these different needs, the ClaRa library provides component models at the same level of detail but covering different physical effects. They are distinguished by different self explaining names.

10.3Modulated heat exchanger buildup

The heat transfer of the “flameRoomWithTubeBundle” model became the initial approach for testing the included heat transfer correlations of the library and thus, reducing the model to the necessary heat transfers of the tube bundle of the OTSG. The model exhibit the necessary parameters for defining the particular geometry of the OTSG, specifically the tube bundle geometries and additional HT-correlations that can be customized.

From details in table 8 it becomes clear that the fluid volumes needs to be built on at least level 3, preferably level 4 to include detailed dynamic momentum and energy balances for water. The gas side however depend directly on the heat transfer correlations and corresponding pressure drops, and momentum equation can in general be ignored because of the short time timeframe the gas turbine regulate in. A level 2 will probably be sufficient for the gas side.

From the included examples the library, the flame room-module mentioned earlier was extracted, and the structure investigated. A set of different model compositions were then suggested.

10.4Flame room dynamic model

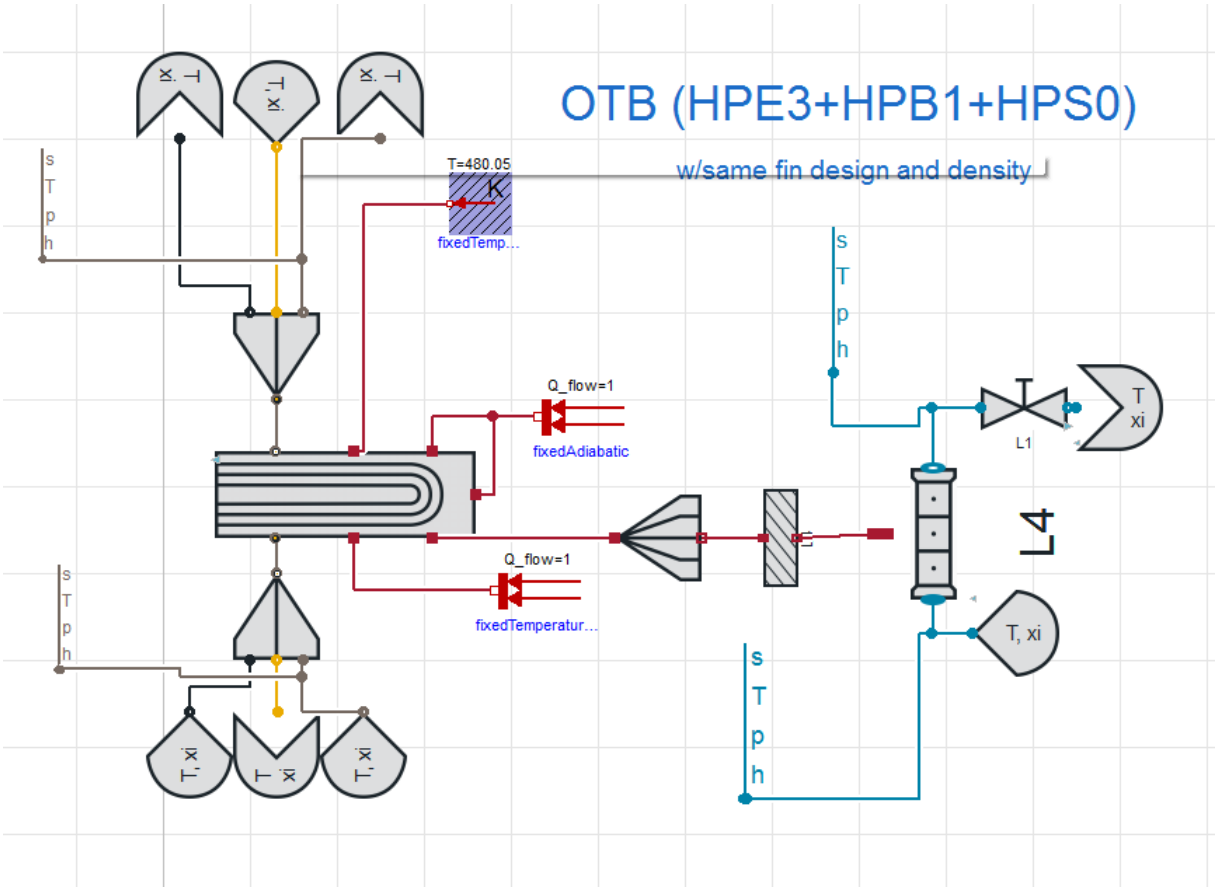

Figure 28: FlameRoomModel in ClaRa with external pipe component connected to the tube bundle

Figure 28 above shows the original once-through boiler combining the tube bundles HPE3, HPB1 and HPS0 which had identical fin configuration and tube diameter. Suggested by developer Lasse Nielsen, a set of heat ports need is set to

adiabatic conditions or, close to adiabatic to avoid singularities which some of them produced. Both radiative and convective heat transfer is regarded in the model through the furnace walls, carrier tubes holding the tube bundles, and through the top and bottom boundaries of the model. The only port active is the heat transfer correlation to the tube bundle, sending

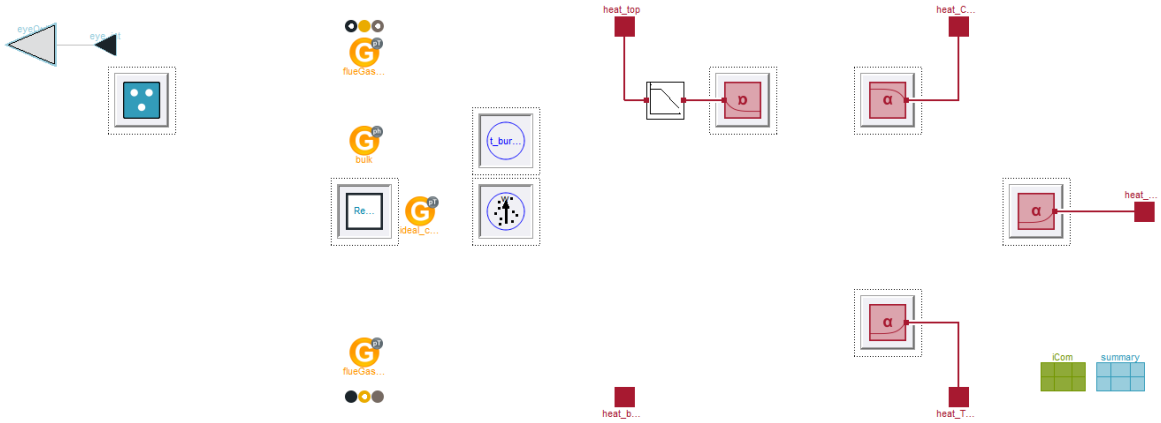

Figure 29: Inside the FlameRoomDynamic_ model_ with_ tube_ bundle

Unlike Thermopower and ThermoSysPro, the library does not need direct port-connections to every module through its calculations. Gas volumes and heat transfer correlations are calculated on using the boundary gas condition values or the averaged bulk properties.

Figure 29 shows the internals of the flame room model with red boxed heat transfer correlation components, four gas zones calculations depicted as yellow G's, a gas side tube bundle volume to the left. The rest is non-relevant modules for the CC being burning time, particle-migration and reactive-zone for the coal.

The gas model used with ClaRa is a composition based one, where the fraction of each gas N2, O2, CO2, Argon and so on, is predefined and put together to form the flue gas model. Default flue gas model contains eight different gasses, in which ash is one of the components. The state properties for each gas in the exhaust is calculated, making it an inefficient way to simulate and a source of error discussed later in the thesis.

11 HTC correlations

There exists a high number of heat transfer correlations for different finned-tube designs in conventional power plants. This comes from the usage of variable geometry on the fins which can be of quadric, circular, rectangular, spherical, serrated design - to mention some. Despite the vast availability of correlations, each of these tend to be limited to different flow conditions, specific designs and regions of variable flow parameters (like Reynolds and Prandlt numbers), which makes the correlations less comparable to regions outside their study.

For this reason the validity of these correlations does not necessarily agree with a general HRSG design, and is limited to the range analyzed with transient operations conditions of a plant, e.g. start-up or shutdown, where vastly different flow regimes are experienced. It is therefore common to apply the regions in which the different HTCs are tested, and with a percent-wise certainty to their results [47].

With this in mind, various heat transfer correlations have been investigated and tested with the ClaRa library.

11.1VDI heat transfer correlations

With the advantages of the family-structured models of ClaRa, testing various external heat transfer correlations inside the flame room model becomes just a few clicks for modification. Geometrical parameters and boundary conditions remain separate from the heat transfer calculating, thus reducing the workload each time a new correlation is tested.

The included heat transfer correlations for the tube bundle is based on both bare and finned tube models, specifically round and quadric tube fins, taken from VDI Heat Atlas [50]. Both are based on industrial confidential data acquired by the authors,

and supports both aligned and staggered tube bundles.

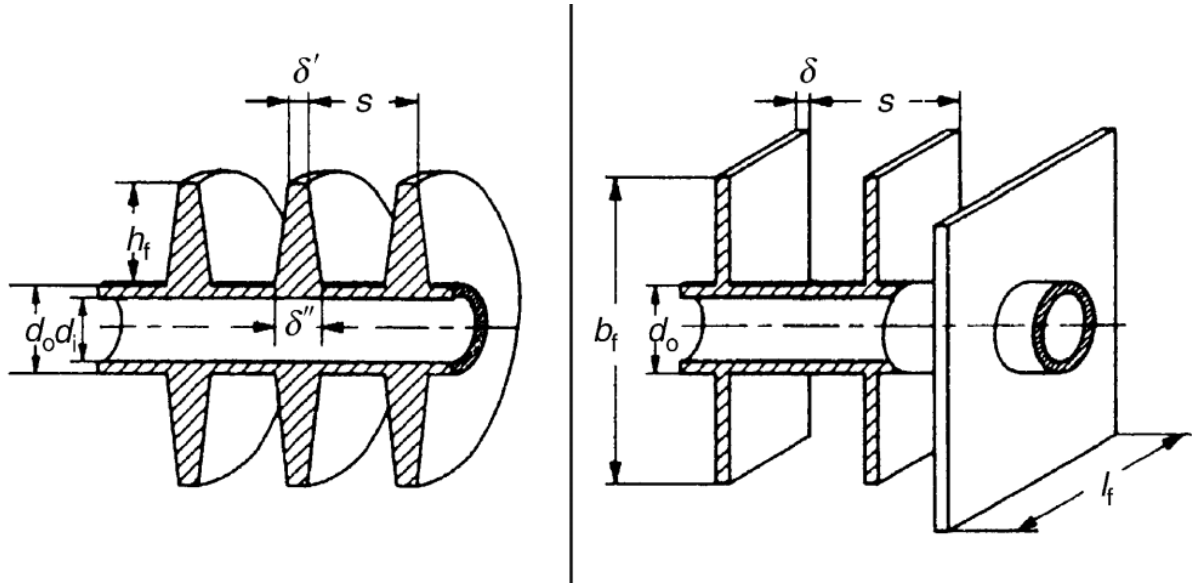

Figure 30: Circular and quadratic fin surfaces by VDI Heat Atlas [50]

The elemental heat transfer calculation is by default based on logarithmic mean (LMTD), but arithmetic mean or inlet or outlet conditions can also be chosen. Below follows the derived equations for a finned tube bank heat transfer

$$\dot{Q} = \alpha\left(A_{bare\,tube} + \eta_{fin}A_{fins}\right)\Delta T_{LM}$$

Assuming uniform heat transfer coefficient for both bare tube and fins, with a defined fin efficiency η_{fin} which has been experimentally derived to

$$\eta_f = \frac{\tanh(\phi \cdot m)}{(\phi \cdot m)}$$

The correlations is similar to Th.E. Schmidt, but have other coefficients and exponents that are being evaluated, which will be looked into later. All Nusselt numbers are based on the bare tube diameter as characteristic length. The equation for staggered tube bundle are as follows:

$$Nu = C_1 \cdot Re^{0.6} Pr^{\frac{1}{3}} \cdot \left(\frac{\mathrm{A_{tot}}}{A_b}\right)^{-0.15} f_{st}$$

The f_{st} coefficient is based on the total number of staggered tube rows (N_r) in the flow direction, which is expressed in table 10. A_b is the bare tube area between the fins, while A_{tot} is the whole external tube surface area. The heat transfer correlation

is valid for an evaluated measurement uncertainty of about ± 10% to ±25%, 1000≤Re$Re \leq 100000$ and $5 \leq A_{tot}/A_b \leq$30. [47]

	f_{st} staggered
C_1	0.38
$N_r \geq 4$	1.00
$N_r = 3$	0.95
$N_r = 2$	0.87
$N_r = 1$	0.87

Table 9: Coefficient for pipe bundle alignment inside HRSG

The fin efficiency is defined through experimental data given by figure 31 its corresponding equation set for quadratic fins configurations.

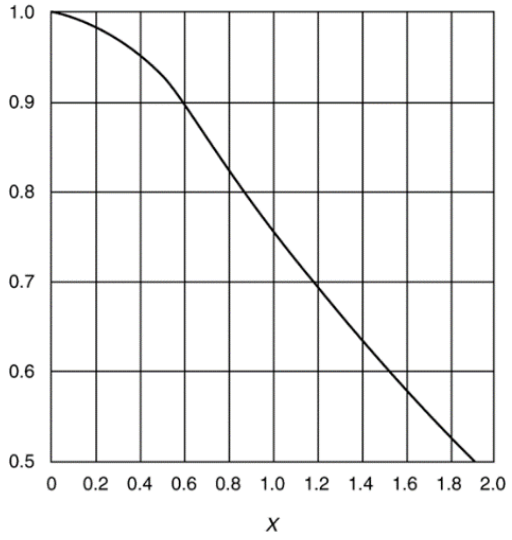

Figure 31: Fin efficiency (eta) as an experimental function of X.

$$m = \sqrt{\frac{2\alpha_m}{\lambda_f \cdot \delta}}$$

$$X = \phi \cdot \frac{d_{tube}}{2} \cdot m$$

$$\phi = (\phi_{st} - 1)(1 + 0.35 \cdot \ln \phi_{st})$$

$$\phi_{st} = 1.28 \frac{d_0 + 2_{h_f}}{d_0} \sqrt{\left(\frac{l_f}{b_f} - 0.2\right)}$$

11.2Improved correlations with Schmidt

The Th.E. Schmidt correlations are built upon a large number of test cases, mostly with annular solid fins. The correlation in cas of staggered tube layout is defined with characteristic length of the bare tube diameter

$$Nu_{d_0} = 0.45 \cdot Re^{0.625} Pr^{\frac{1}{3}} \left(\frac{A_{tot}}{A_b}\right)^{-0.375}$$

Where the correlation is valid for an evaluated measurement uncertainyy of about $\pm 25\%$, $1000 \leq Re \leq 40000$, $5 \leq (A_{tot}/A_b) \leq 12$, and $N_{rows} \geq 3$ consecutive arranged tube rows [47].

The fin surface area in VDI needs to be corrected from quadratic (rectangular fins with equal width and length, depicted in 30), to serrated fin area. Thus implements the Th.D. Schmidt correlation for serrated fins described by Hashizume et.al. [59]. The correlations are quite similar with only small adjustments from what is found in the VDI Heat Atlas regarding the initial fin efficiencies.

The surface area calculated by the quadratic fin area, defined by one single fin is:

$$A_{fin} = 2 \cdot \left(d_0 + 2h_f\right)^2 - 2 \cdot \frac{\pi}{4} d_0^2 + 4 \cdot \left(d_0 + 2h_f\right) s_f$$

where s_f is the fin thickness and h_f is the fin height from the base of the tube. Serrated fins are however defined with fin area as:

$$A_{fin} = 2 \cdot \frac{\pi}{4} (d_s^2 - d_0^2) + (1 - rat) h_f s_f \cdot 2 + \pi \cdot d_s \cdot 2(1 - rat) \cdot h_f$$

where rat is the ratio of unserrated fin to serrated height, better described by:

$$d_s = d_0 + 2 \cdot rat \cdot h_f = d_f - h_s$$

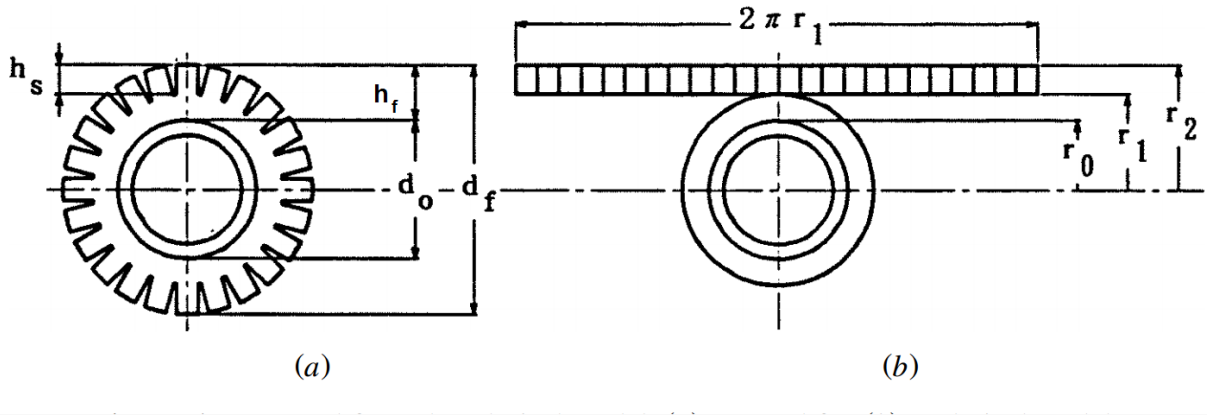

Figure 32: Serrated fin geometry parameters

The fin efficiencies are similar to VDI, with just a few modifications.

$$m = \sqrt{\frac{2\alpha_m}{\lambda_f \cdot \delta}}$$

$$X = \phi \cdot m$$

$$\phi = d_f(1 + 0.35 \cdot \ln \phi_{st})$$

$$\phi_{st} = \frac{d_f}{d_0}$$

Initial calculations with the serrated fin surface area showed deviation in error from the GT PRO of ~5% margin, and was further reduced to -0.02% when compared and corrected with other equations from Weierman [51], Næss [49] and the original ESCOA equations described by Ganapathy [46]. Furhter this strengthen the theory that the ESCOA correlations are the ones used giving the most exact numbers.

11.3K. Shah fin efficiencies

Finding an improved fin efficiency correlation is also needed since the ones of VDI Heat Atlas naturally don't correspond the GT PRO data. K. Shah [60] derived the equations for serrated tubes (or studded fins) on specifically for the use in tube banks.

$$\eta_f = \frac{\tanh(m \cdot \phi)}{(m \cdot \phi)}$$

$$m = \sqrt{\frac{2\alpha}{k_f \delta}\left(1 + \frac{\delta}{w}\right)}$$

$$\phi = \phi_{st} + \frac{\delta}{2}$$
$$\phi_{st} = \frac{d_f - d_0}{2}$$

w serrated fin width

δ fin thickness

d_f tube diameter plus two fin heights

λ_f fin thermal conductivity [W/mK]

11.4Næss correlation

Næss proposed heat transfer correlation based on various staggered serrated fin types from a broad set of studies, comparing with an experimental setup varying tube bundle layout and tube and fin parameters. Characteristic length was set to bare-tube diameter, even though other lengths was suggested depending on tube arrangement and fin type [49].

Calculating the pinch between the transversal and the longitude tube directions in equation below, we get the Nusselt number for the GT PRO conditions.

$$\frac{S_t}{S_d} \approx \frac{P_t}{P_d} = \frac{71.42mm}{78.58mm} = 0.909 < 1.0$$

$$Nu = 0.107 \cdot Re^{0.65} \cdot Pr^{\frac{1}{3}} \cdot \left(\frac{P_t}{d_e}\right)^{0.35} \cdot \left(\frac{l_e}{d_e}\right)^{-0.13} \cdot \left(\frac{l_e}{s_f}\right)^{-0.14} \cdot \left(\frac{s_f}{d_e}\right)^{-0.2}$$

Where P_t is the transverse tube pinch, d_e effective tube outer diameter, l_e net fin height $(h_f - t_f)$, t_f fin thickness and s_f is fin pinch $(\frac{1}{n_f} = s + t_f)$. Næss claims the equations correlate to 95% of the data to within $\pm 4.2\%$, which is the best correlation to general tube bundle configurations found yet.

11.5ESCOA correlations

The primary focus of the thesis have been to implement the ESCOA correlations, which is believed to replicate the GT PRO steady-state data to high accuracy. GT PRO output pattern resembles the exact ESOCA calculation procedure, which previously have been identified through the output variables like gas mass flux, not found in any of the other correlations.

The ESCOA (Extended Surface Corporation of America) equations is maybe the most detailed equations for serrated finned tube bundle heat transfer, and is empirically derived by the producers themselves. The original correlations published in 1978 is presents a table-based calculations procedure for designing a HRSG-setup based on pre-defined heat transfer requirements and desired geometrical parameters.

The original equations from 1979 has gone through multiple improvements and iterations by different researchers including V.Ganapathy [46], Kawaguchi [48], and are categorized into traditional and revised equation sets by Hofmann [61].

$$Nu = \frac{1}{4} Re^{0.65} \cdot Pr^{\frac{1}{3}} \cdot \left(\frac{T_{gm}}{T_{fa}}\right)^{\frac{1}{4}} \left(\frac{d_f}{d_0}\right)^{\frac{1}{2}} C_3 C_5$$

where T_{gm} is the average gas temperature in the discretized volume, and T_{fa} is the average fin temperature. C_3 and C_5 are dimensionless geometrical correction factors calculated based detailed fin geometries, tube spacing, number of tubes and Reynolds number. A complete set of coefficients is set in table 10 which is set for staggered tube bundles.

Unlike the other correlations where Nusselt-number only depends on the geometrical parameters of the fin-tubes and gas flow, ESCOA also depends on approximated fin-tip temperature and fluid temperatures inside the tube. The calculation procedure from the 1979 paper rely on approximated known heat transfer rate, fouling, and thus internal HTC. The fin temperature (T_f) is calculated through the fin base temperature, and fin efficiency (η_{fins}). Fin base temperature is further reliant on the total heat transfer rate and resistances (R) of the inside film, fouling layer and tube wall respectively.

$$T_f = T_{fin,base} + \left(T_{gas,avg} - T_{fin,base}\right)\left(1.42 - 1.4\eta_{fins}\right)$$

$$T_{fin,base} = T_{internal} + \dot{Q}(R_3 + R_4 + R_5)$$

This means that the heat transfer model in ClaRa needs a bridge, or external records, to capture the data between the modules. In ClaRa this record comes a iCom record seen in the experimental ESCOA heat exchanger module in figure 33.

All the internal properties of the pipe and the gas has to be calculated separately, which means a new heat exchanger model has to be generated. Below is an experimental model for the ESCOA HT-correlations, based on pipe L4 fluid flow and L2 gas volume details.

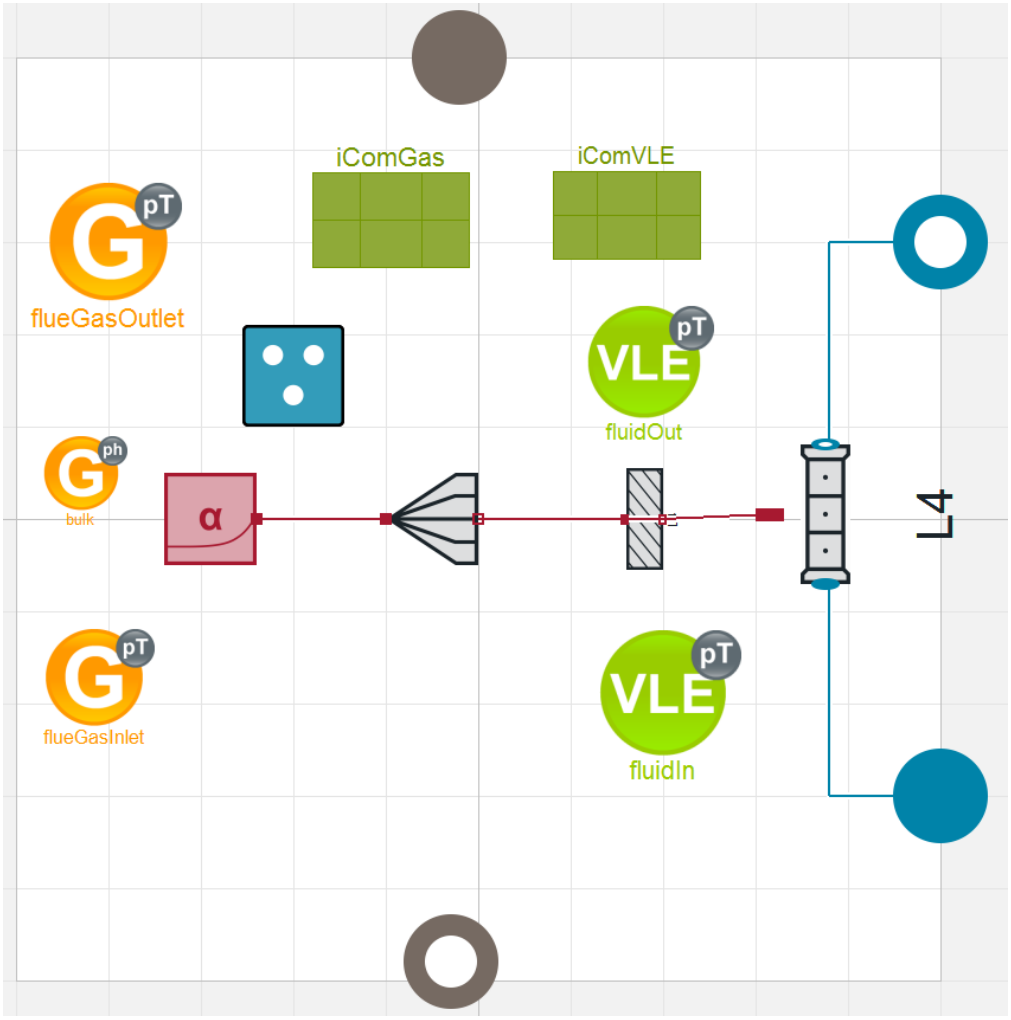

Figure 33: Experimental ESCOA heat exchanger with separate records (iCom) for both fluids.

Table 10: ESCOA coefficients for staggered, serrated tube bundle.

ESCOA coefficients for staggered, serrated tube bundle:

$$C_2 = 0.07 + 8.0 \cdot Re^{-0.45}$$

$$C_3 = 0.55 + 0.45 \exp(-0.35 \frac{l_f}{s_f})$$

$$C_4 = 0.11 \left[0.05 \cdot \frac{P_t}{d_0}\right]^{\left[-0.7 \cdot \left(\frac{l_f}{s_f}\right)^{0.23}\right]}$$

$$C_5 = 0.7 + [0.70 - 0.8 \cdot \mathrm{e\^{}}(-0.15 \cdot \mathrm{Nr}^2)\,] \left[e^{\left(-1.0 \cdot \frac{P_l}{P_t}\right)}\right]$$

$$C_6 = 1.1 + \left[1.8 - 2.1e^{-0.15 \cdot N_r^2}\right] \left[e^{-2.0 \cdot \frac{P_l}{P_t}}\right] - \left[0.7 - 0.8e^{-0.15 N_r^2}\right] \left[e^{-0.6 \cdot \frac{P_l}{P_t}}\right]$$

Although the correlations are detailed and easy to implement directly into code, the conversion from imperial units to SI-units leaves every conversion step vulnerable to errors in the calculation. In the appendix, such a conversion procedure to implement the ESCOA HT-correlations into ClaRa has been initiated but not completed due to the large workload of uncertainty of the resulting equations.

Pressure drop ESCOA

The ESCOA correlations also include pressure drop calculations through the tube bundle, and is also based on the coefficients found in table 10. However, these were not implemented in the experimental ESCOA heat exchanger, nor any other module, due to primary focus on the heat transfer correlations which will have the biggest impact on transient behavior of the OTSG system.

However, the absence on external variables makes these equation easier to implement in their own module, like the previous HTC discussed before ESCOA.

$$\xi = 4 \cdot \left(\frac{d_a + 2h}{d_a}\right)^{\frac{1}{2}} \cdot C_2 C_4 C_6$$

Pressure drop calculations of the whole channel with staggered tube bundles are expressed as:

$$\Delta p = N_r \xi \frac{\rho_{gm} {w_E}^2}{2}$$

where N_r is the number of rows of tubes in the flow direction, w_E is the velocity in the net free area of a tube row, and ρ_{gm} is the average gas density.

N_r	number of rows of tubes in flow direction
w_E	Velocity in the net free area of a tube row
ρ_{gm}	average density of gas

11.6Comparing the correlations

The advantage of all the correlation (beside ESCOA) is that they are all dependent on parameters that exist explicitly on the exhaust gas side of the tube. This means they can be coded into ClaRa as an exchangeable HTC module, which can be with the same dimensioned heat exchanger.

The flame room model used to compare the heat transfer with ideal HTC conditions the inside of the tube, restricting the heat transfer purely to the exhaust side of the model.

Since the ESCOA model was only partially developed, it is suggested from the heat transfer test of the complete once-through boiler (HPE3, HPB1 and HPS0) that the Næss correlation is the closest candidate to resemble to GT PRO data. Numbers from GT PRO are proportionally calculated by their number of tubes in each section.

Table 11: Heat transfer correlation comparison

	Q	Nu	Re	η_fins	HTC_gas
	[W]	[-]	[-]	[-]	[W/(m2.K)]
SCHMIDT	1,30E+07	68,05	11587	0,262	83,20
VDI K.Shah fin eff	1,78E+07	69,33	11961	0,852	85,67
NÆSS	1,80E+07	91,04	11983	0,731	112,55
VDI Rectangular fins	1,82E+07	68,60	12978	0,747	84,83
GT PRO data	1,95E+07	84,50	13555	0,745	109,40

12 Building the ClaRa model

12.1Condenser forward and HP pump model

An ongoing problem has been the dynamics of the pump-models in both Thermopower and ThermoSysPro which have been hard to initialize. ClaRa includes L1 pump models and thus provide the needed simplification to the pump. Selections from GT PRO suggest that all pumps run on constant rotational speed, and thus the pump valves controls the flow through PI-controllers elsewhere in the system.

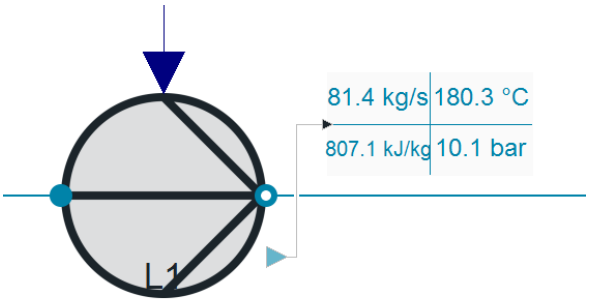

Figure 34: L1 pump model in ClaRa.

The flow rate of the L1 pump depends on the pressure difference and an external driving power connection. Hydraulic characteristic profiles is modelled assuming incompressible fluid properties and is limited to stationary flow with no backflow options.

ThermoPower and ThermoSysPro on the other hand require predefined characteristic performance and mass/pressure curves, which by experience easily disrupts flow and pressure states if initialization is outside its normal operation domain. Simplifying the pump model ended up being the breakthrough needed to achieve a closed and stable steam cycle, which was only conditional at the other library models.

12.2Condenser water Level Controller

Since the pumps are prescribed at constant rpm, the pump valves dictate the flow and thus are the controllers for both the feedwater pump and condenser pump. Apart from level limiters and live-steam temperature control, these are the only vital control systems needed to model the once-through cycle.

The condenser-level control-system is based upon the example included in ThermoSysPro, measuring the incoming vapor and outgoing water mass-flow of the condenser, with reference to a set level-value in the hotwell that can be freely chosen. The controller is part of the publication from Baligh et al. from 2013 [62] EDF/R&D STEP studying large transients in combined cycle power plants. The model is translated from French and is depicted in figure 35.

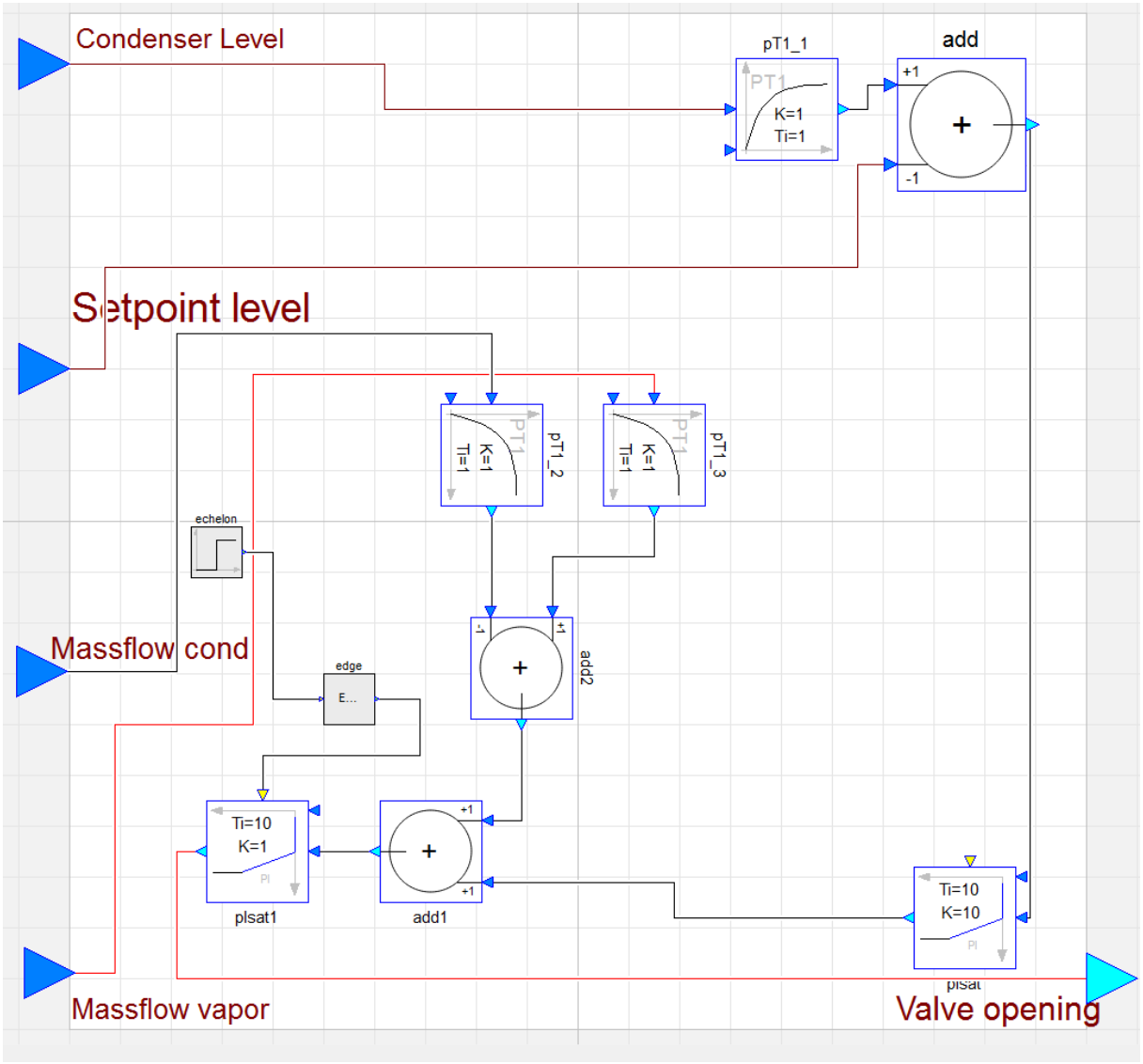

Figure 35: Condenser level controller. Translated from French.

The signals are compared through are first-order transfer functions, accumulating the signal through PI-controllers with integrated limiters giving delay to re-evaluate the new level measurements.

Initial usage of the controller gave good water control in both the ThermoSysPro model and in ClaRa. Since ThermoSysPro and ClaRa library has its own data type for Real type signals, a converter had to be created. ClaRa already include similar adapters for connection water-streams from the TIL Media library to the IPW97 Modelica water library. To make the signal connection-points compatible, one port from both ThermoSysPro and one from ClaRa has to be put in the same model, and a simple equation for the value type "Real" is set. Two adapter has been made to

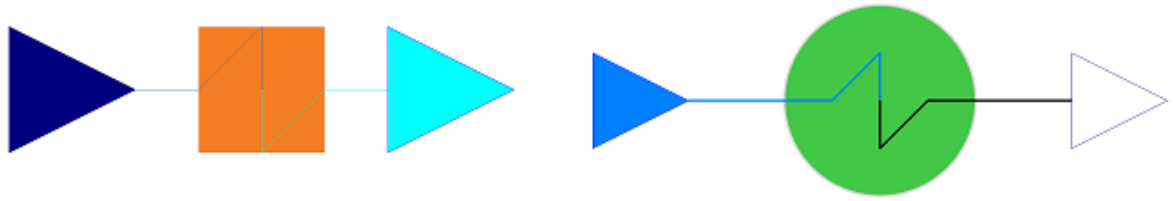

Figure 36: Conversion adapters of Real type ThermoSysPro to ClaRa, and vice versa.

With the new adapter, we can now connect Real-signals from the sensor-components in ClaRa to the input connections in ThermoSysPro, thus utilizing the included condenser level controller.

Condenser efficiency

Depending on the level-controller, it has been tested that the heat transfer is optimal and directly proportional with the incoming mass-flow into the exchanger. Variable parameters regarding the heat transfer, both inside, and outside tube (htc, cooling flow, etc) shows that the capacity of the heat exchanger is not limiting the massflow.

12.3Feedwater PI controller

The OTSG feedwater strategy has been thoroughly described in chapter 3.6 based on the IST control system. In the depicted controller designed in figure 37 the prescribed steam flow y is calculated based on prescribed steady-state load data from 60 and 100 percent GT load. The assumption is that the feedwater is linearly dependent on both exhaust temperature and exhaust mass flow, giving the two linear equation sets. The solution giving $x_1$and x_2 one, describes the coefficient values in the feedwater controller.

№	X_1	X_2	b
1	753.15	78.4	8.748
2	723.15	65	6.765

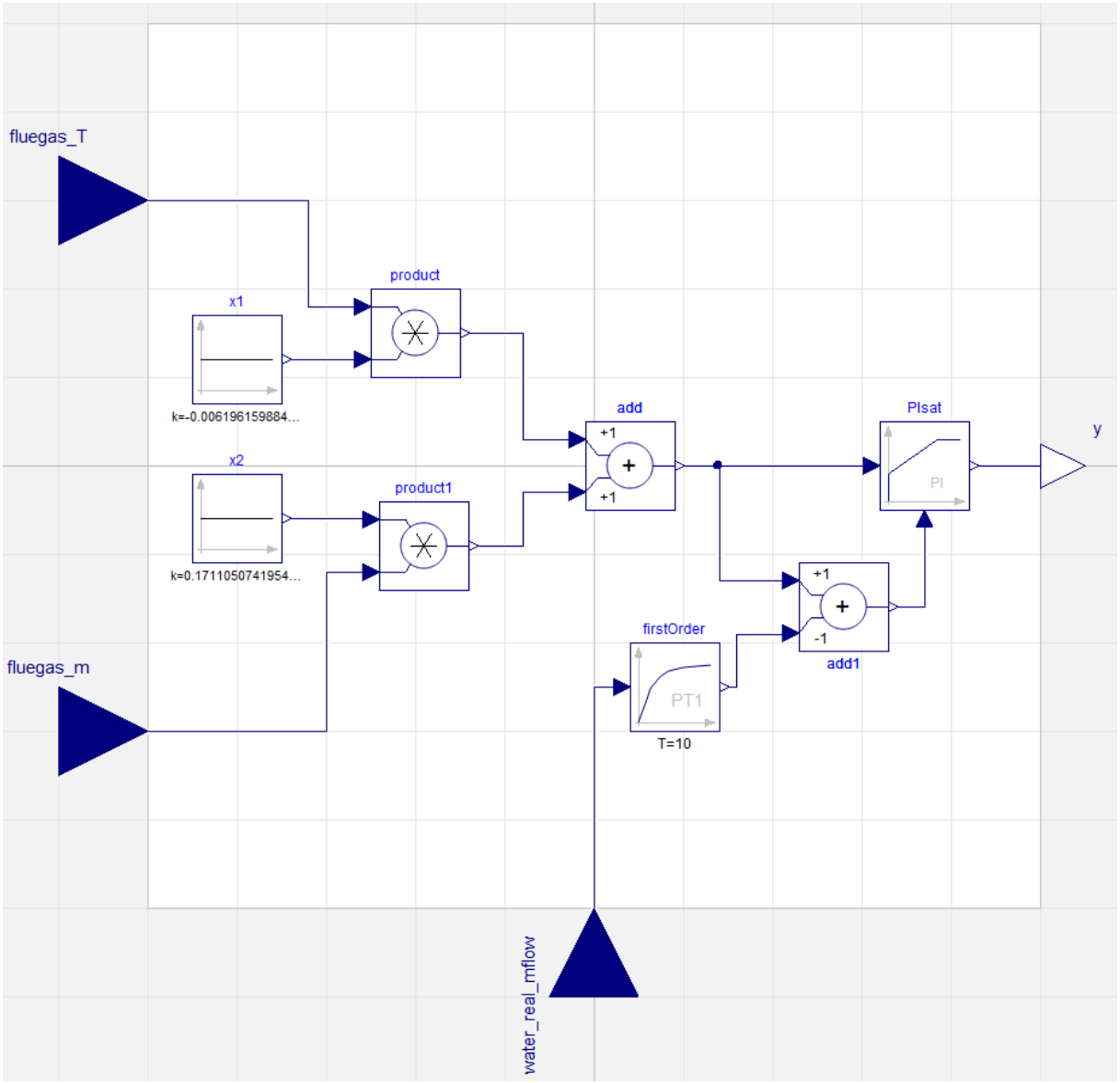

Figure 37: Feedwater controller assuming linear relation between off-design and nominal operation point.

After the valve set-point has been calculated by the linear equation it is compared with the massflow sensor to regulate the valve opening signal through the PI-controller, which is limited from 0 to 1 in output value. Y is the value of the valve-opening after the HP feedwater pump, thus regulating the waterflow into the HPE0 economizer.

12.4Constructing the heat exchanger

The flame-room model included with ClaRa added unnecessary features not relevant to combined cycle model. Although the tube bundle model could be tested for single tube bundle heat exchangers, a set of four different fin configuration sections would be needed. It was thus clear that a simple model had to be made to be able to close the steam cycle for the first time.

Figure 38 a) and b) show a pure L2 and an L2 gas and L4 water volume heat exchanger respectively. Both use the Næss L2 heat transfer correlations on the gas side, which is connected either through a single wall in a), or discretized into an arbitrary number of wall nodes and volumes on the pipe model b).

Figure 38: a) L2 heat exchanger. b) L2 gas and L4 fluid volume

Heat transfer correlations for the L2 two-phase model is based on a horizontal boiler heat transfer model without inertia, dynamic momentum or energy equations. Its fluid properties are averaged over the volume, but is rendered stable at all test performed.

The L4 two-phase model use discretized pipe fluid volumes and includes dynamic momentum and energy equations. Unlike the pure L2 model, the L4 fluid model were unable to initiate in steady-state for any of the OTSG sections. Multiple types of heat transfer from ideal, constant HTC to geometry dependent two-phase flow was tested.

Pressure drop correlations are set to separately to the HT model of choice. For the current model, pre-set static pressure drops are defined for the gas-model, and linear mass flow dependent pressure drop for the steam/water volumes.

However vital the L3 and L4 detail is for simulating the lag in the steam cycle, sudden instabilities in the LTE heat exchanger crossing exhaust temperatures below 180°C rendered the L4 model useless. It is suspected that the problem lies in the flue-gas model of the TIL Media library, since frequent errors have emerged from wrong gas property calculations, even at steady-state conditions without any fluctuations in the cycle. This could though be due to singularities found elsewhere in the model and is thus hard to investigate without debugging the model in detail.

12.5ClaRa Steam cycle

An overview of the whole steam cycle including control systems are shown in figure 39. The once-through boiler is as predicted set as one heat exchanger, and the superheater (HPS) is simplified including the single bare tube of HPS1 with HPS3. A steam separator has been placed between the superheat and thee evaporator, which displays the current condensate of unsaturated water as 0.1kg/s over 8.7kg/s entering the superheater. The steam turbine L1 model operate at constant isentropic efficiency

following Stodalas's cone law including a term for entropy production, with a nominal pressure ratio of about 280.

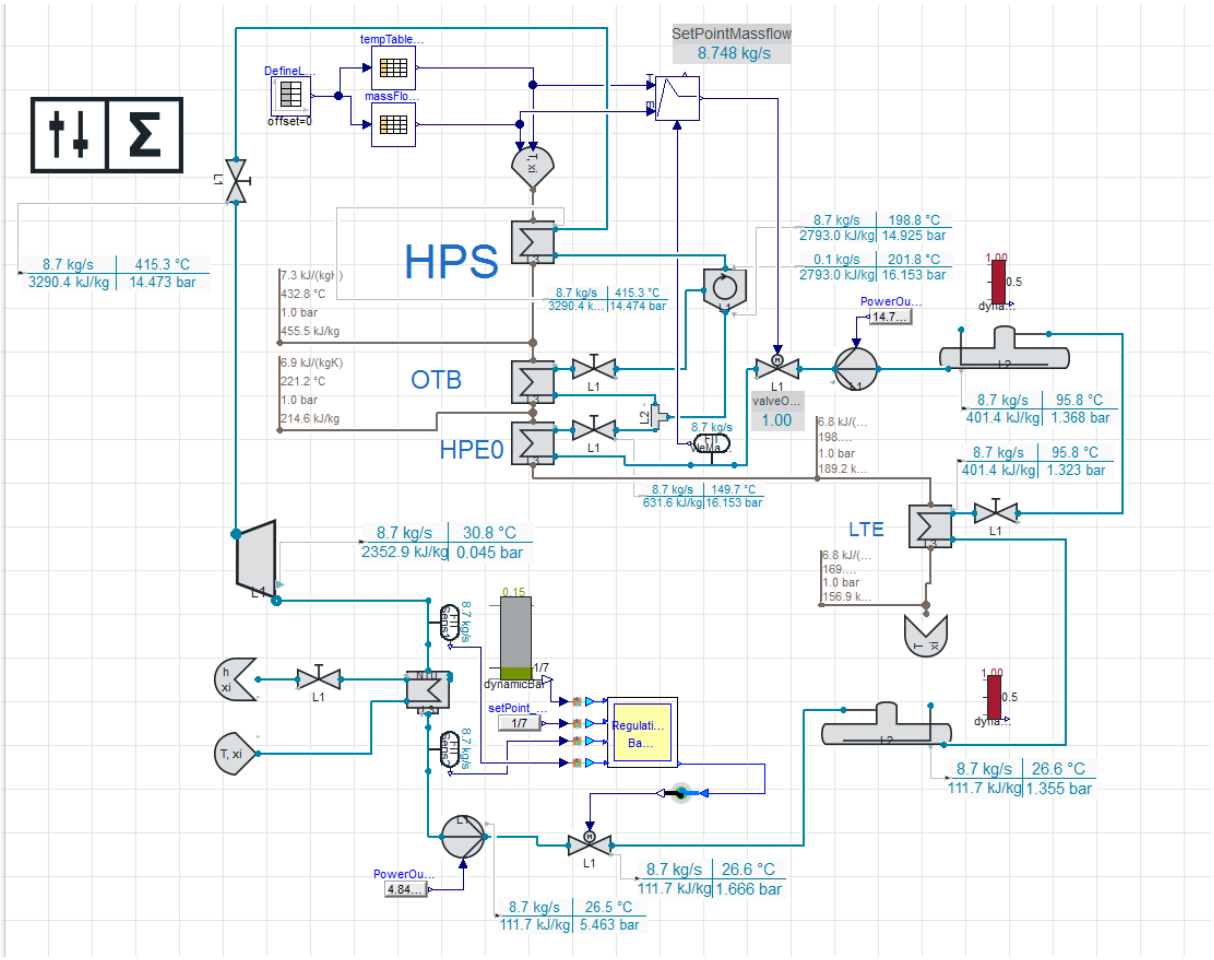

Figure 39: Complete steam cycle at nominal design-load

The gas turbine load is easily input through a timetable dictating the exhaust mass flow and temperature defined by the part-load steady-state curve of the calibrated GE LM2500+RD(G4) output explained in chapter 3.1. Figure 40 visualize the

current set point value generated out of the feedwater controller at nominal load.

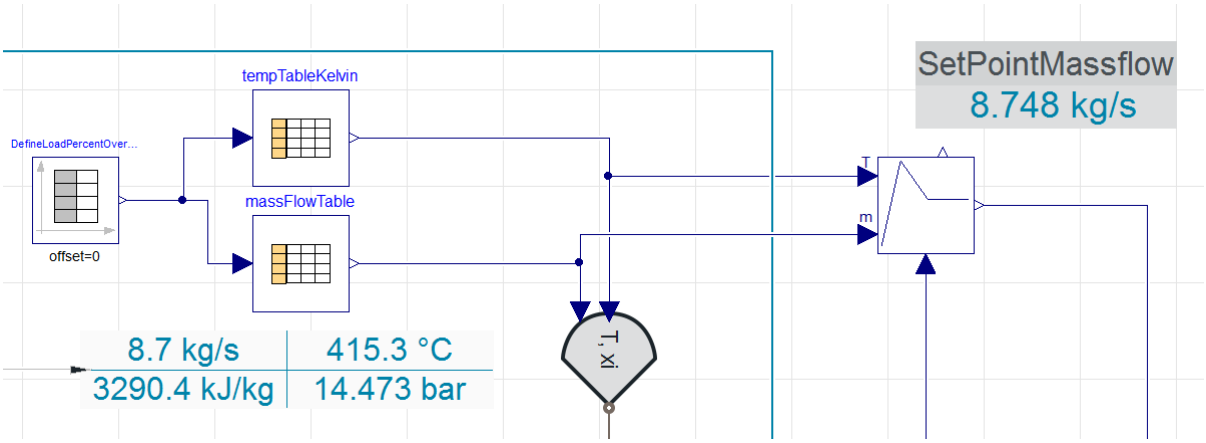

Figure 40: GT load and feedwater controller circuit

A live-steam temperature controller has not been implemented since the model barely initiates at its current number of installed components. Neither are high steam temperatures a problem since the heat transfer of the L2-heat exchangers are unable to recuperate heat GT PRO design point.

13 Simulation results and evaluation

A late error discovery were made in the off-design point of the of 60 percent gas turbine load from the GT PRO data. The GE LM2500+RD(G4) showed large temperature differences in the lower load parts at 60% with over 60°C difference in EGT. The EGT temperatures got recalibrated with at factor of 0.88 to the 60% load to coincide with the GT PRO data. The EGT was further linearly corrected with 0.15 increase reaching 0.82 at 40% load to 1 at nominal load. The exhaust mass flow is within 1 kg/s error to the 60% load point, thus not calibrated. The load-curve is seen in figure 41:

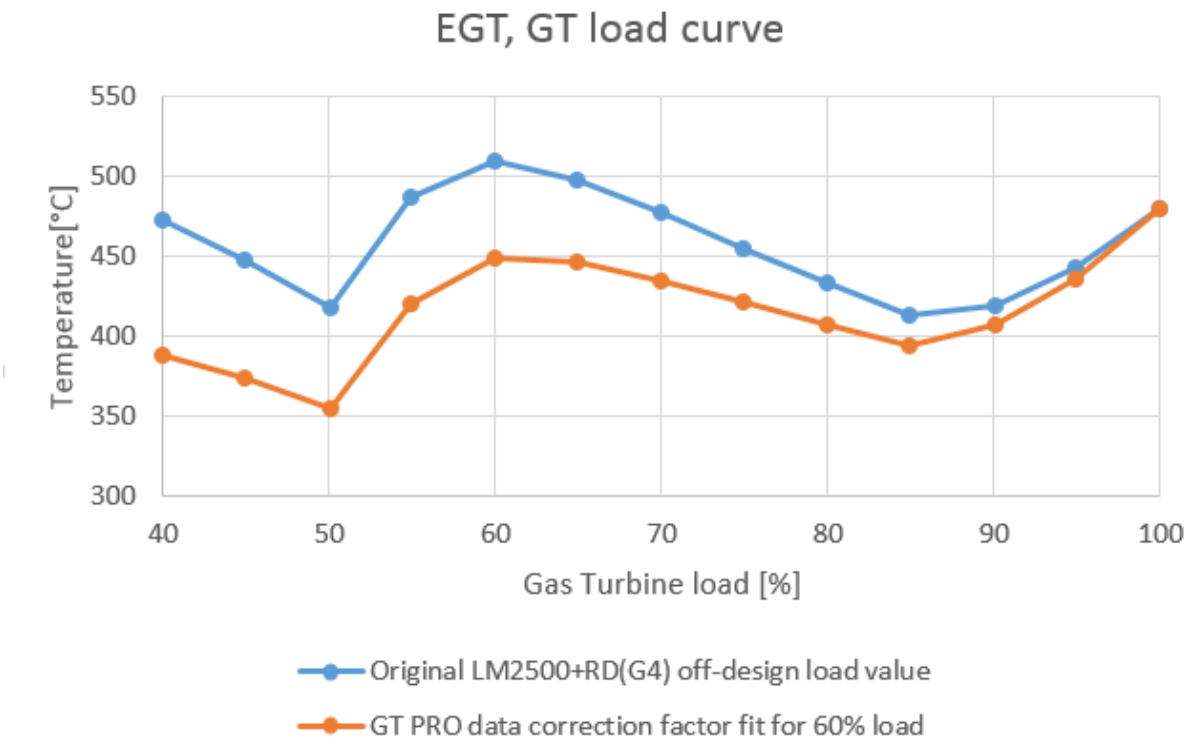

Figure 41:Re-calibrated exhaust gas temperatures

However this is not the correct part-load data, it is the currently best testing the steam cycle with limited time frame. The 60% steady-state exhausted an EGT at 450°C which fits with the new curve.

In an effort to increase the heat recovery rate in the heat exchangers, higher correction factor (CF) in the Næss equations was set. Basically this means multiplying the HTC with a number to increase the heat transfer rate. However, increasing the CF had no effect on the output steam temperature produced in the OTSG, which was less than 1°C. A side-effect however is more unstable heat exchangers in the gas side in during load transients.

Control systems work as expected and the linear feedwater controller deliver feedwater into the HPE0 at rated values. The pressure throughout the OTSG has also been reduced closing into the off-design data live-steam pressure with 10.9bar towards 11.5 bar in the GT PRO data. The error is larger though at nominal load where the pressure is reduced greatly due to the steam separator still recirculating about 1.5% of the primary steam flow.

The simulations will as previously stated have no physical effects of the lag dynamic momentum and energy would have on the system because of the L2 fluid volumes missing these properties. Simulation data will therefore not resemble any actual behavior of the system, given that the EGT-part-load curve is even close to reasonable values.

First test are 10 min 100% load to 60% load change with one gas turbine. The steady-state values of 100% and 60% load are depicted in figure 42 and 43, respectively:

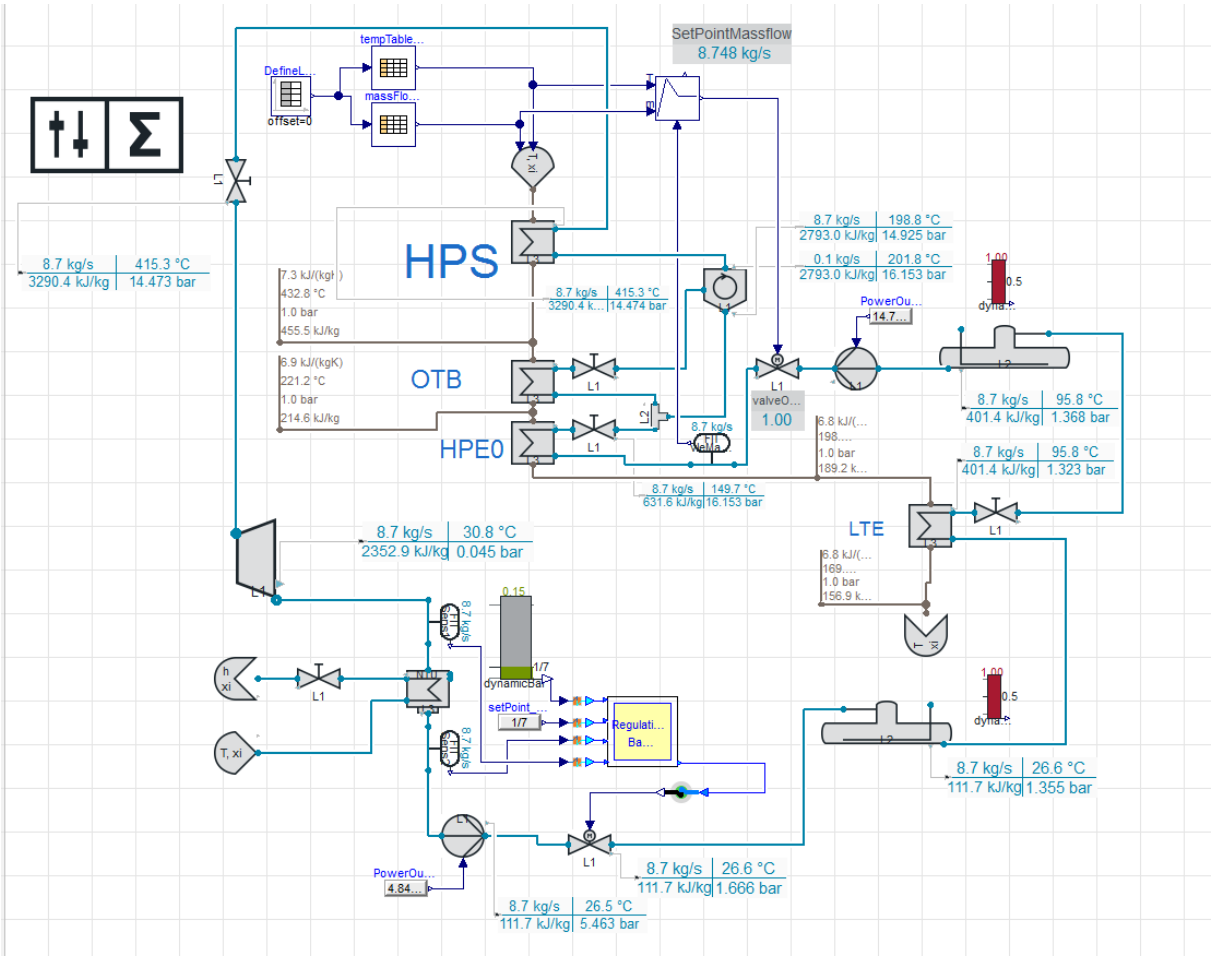

Figure 42: Steady-state nominal load (100%)

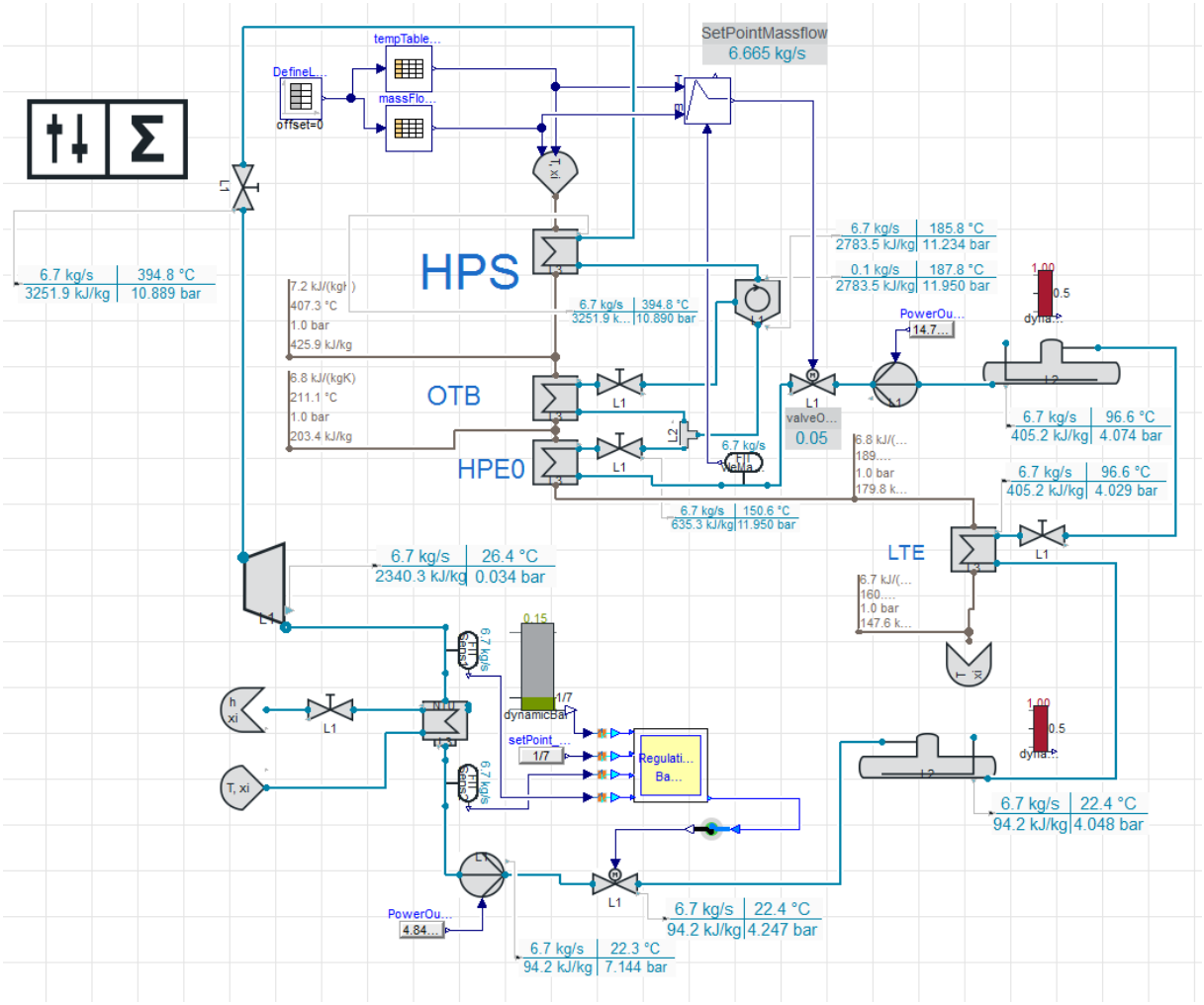

Figure 43: Steady-state of 60 percent gas turbine load.

The heat transfer values of nominal load in the model give the live steam temperatures expected at 60% load, 415°C. Furthermore is the output steam temperature from the OTB 60°C lower than expected at part-load at 190°C when . This indicates that the heat transfer properties of the exchangers needs to be improved, or rather changed if it were to meet the GT PRO data at all.

For the transient results, we see as expected no late oscillations in the steam turbine due to instant reaction to EGT and exhaust mass flow. The separator recirculates

large amounts of water when the load is reduced, but also helps stabilize the cycle since the OTSG cannot recuperate enough heat to produce the steam.

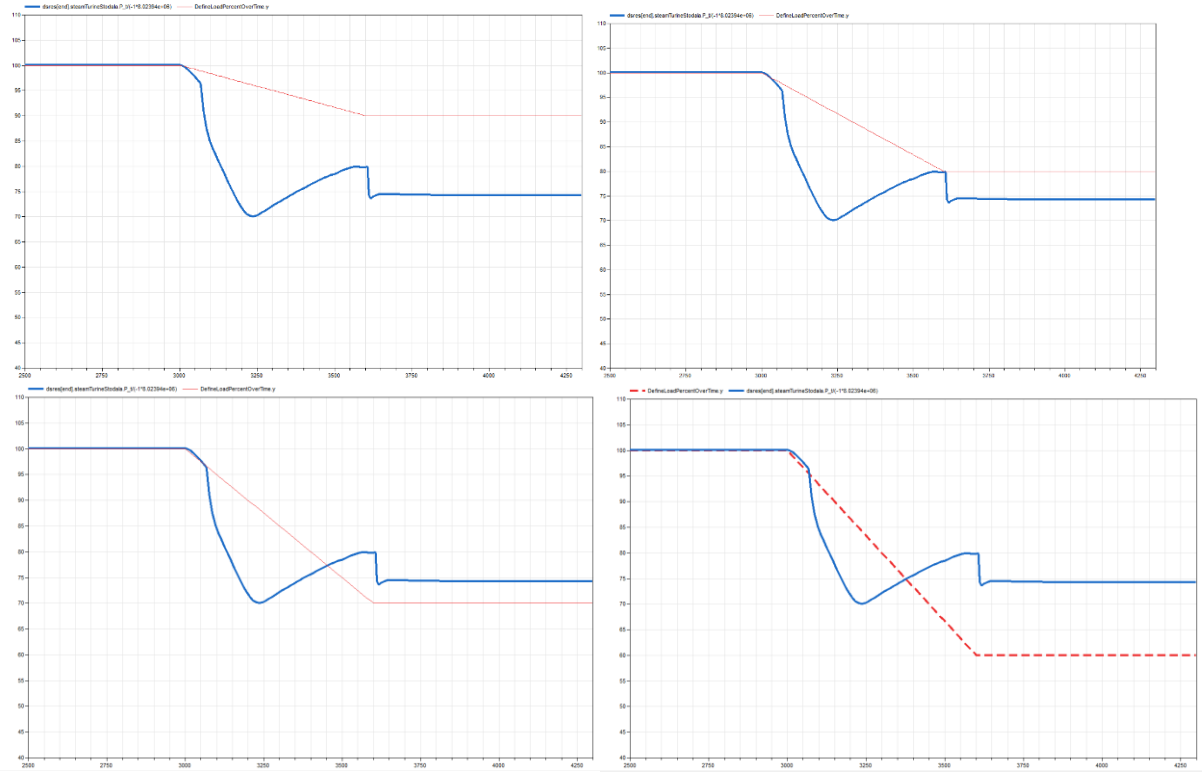

Figure 44: Simulations results from 100 to a) 90% b) 80% c) 70% d) 60%

Removing the separator proves this with the model failing in 90% load in 10 min change. Using the separator as a safety and stabilizer through the simulations is thus advised.

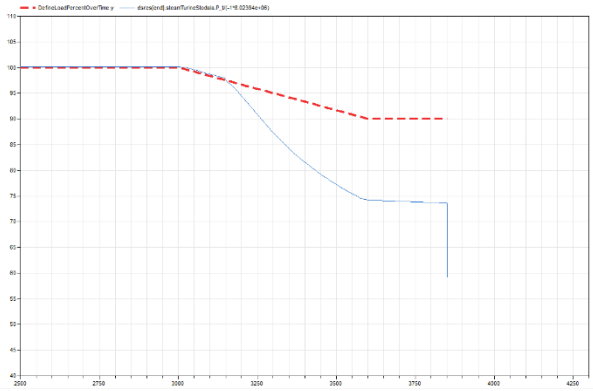

Figure 45: Simulation wihtout seperator. Design-load to 90%

14 Discussion

Although proper methodology has been applied when modelling the steam cycle, the complexity grows with every component, regardless of whether their function is passive or active to the flow. This problem comes apparent in with the ClaRa library where monitoring components visualizing the values of either the gas or steam flow, dictate whether the model will initiate or not when added after a certain point of complexity. Increased number of equations in the initialization after being added reveals that visualization components contribute to the matrix, and thus should be removed from the model if not essential for current debugging.

It is further shown that small disturbances in flows or components can cause the property-functions in the TILMedia flue-gas library to calculate singularities. Ironically these initialization errors occur when adding arbitrary models, like the pThs-visualizer just discussed. Instabilities due to the TILMedia flue-gas has even throughout single-heat exchange modelling been problematic, latest with the initialization of the LTE-HE in the current model.

However, the TILMedia errors could be traced back to the gas side HT-correlations, since modelling the LTE has been a persistent problem both in L2 and L4 heat exchangers. Even though the Næss correlations show good agreement with only 8% error in the total heat transfer of the once-through boiler, there is no guarantee that this level of error will be the same on the other heat exchangers. In fact, the LTE extract only 75% of nominal heat transfer with default numbers. In general - none of the HT-correlations investigated were able to replicate the heat transfer properties of the GT PRO data at their nominal values, even though all geometrical parameters regarding the inside and outside of the tubes were correct. With a permanent gap for averaging 8 percent too low heat transfer in both VDI, K.Shah, Næss and other HT-correlations tested, but not documented, it is suggested that a more detailed analysis of the GT PRO data should be carried out. In the end, the Næss correlations were multiplied with correction factors twice their normal nominal HTC values on the gas side, still without ceiling the GT PRO steam temperature numbers.

It is evident that more valid GT PRO off-design data are needed for the feedwater control system to function as suggested by M.F. Brady in chapter 3.6. The two design-points included in the current feedwater controller does not comply with the offset data at 450°C exhaust temperature and 65 kg/s mass flow according to the temporary curve fit of the Flatebo data. Thus the two points may be tuned to fit a specific load, off design steady-state data with increment at maximum 5 percent should be acquired to improve the controller.

Dynamics of the heat exchanger has been a primary focus throughout the investigation of all the libraries modelled, and ironically, this was the one feature missing in the developed in the custom heat exchanger model. Though balancing on the edge of stability with the model, it is hard to see how the L4 water/steam model could be implemented without simplifying other components in the model. With live-steam temperature, and tank-level control systems still to be implemented, a prioritizing strategy should be laid in to see which components can be set to simpler L2 and L1 levels in order to reduce the number of equations and potential instabilities in the current model.

15 Conclusion

Although open-source libraries have high potential for building a dynamic combined cycle model, only small errors are needed to disrupt the models and inhibit the growth of more complex systems. Homotopy can help the initialization process to certain limits, but proper and consistent initialization methods will be needed when more components are put together.

Since none of the libraries evaluated have been directly tested towards commercial alternatives, it is hard to conclude whether they are recommended or not when taken the workload into account.

Not a single one of the libraries have spawned out of research programs specifically directed towards once-through evaporations systems for gas turbines. Both ThermoSysPro and ClaRa is very close to being viable libraries capable of performing modelling task for others than the developers themselves, and it they both have extensive libraries with content of various quality. Almost all L3 and L4 models

contain multiple lines of code that has been commented out and not documented, which reflect the continuous development and that the models at times are not compatible after updates. This is probably the case with the SiemensPower library which was discontinued long before the latest version of Dymola was released.

Surprisingly, all the heat transfer correlations showed conservative heat transfer values, even when using correction factors to max them out. If the GT PRO data are a result of the assumed ESCOA equations, one could conclude that these equations in general should generate higher heat transfer values than all other HT-correlations, by at least a margin of 8%.

Current experience show that balancing level of detail with the number of components in the system will determine whether further expansion and development of the model is possible. All current models exhibit around 10000 equations, which is more or less the limit to how large the models can get without slowing computing time considerably or evolve unstable conditions in your model.

However, the current control system of the steam cycle works as intended, and with an L4 fluid model and precise off design data for the feedwater-control, the model would be quite applicable of simulating transients to be validated.

16 References

[1] M. Kavanagh, "Offshore fields use power sent from land," *The Financial Times Limited*, April 20, 2015, 2015.

[2] N. P. Directorate, "CO_2 EMISSIONS FROM PETROLEUM ACTIVITIES IN 2015, BY SOURCE," Updated: 06.04.2016.

[3] O. E. Today, "New field start-ups bump petroleum sector emissions in Norway," *Offshore Energy Today*, May 30, 2016, 2016.

[4] "Sysla | Offshore.no- Johan Sverdrup," 16.08.2016, 2016; http://offshore.no/feltdata?navn=JOHAN%20SVERDRUP.

[5] O. N. Lars, "Thermoflow Output data: Half Oseberg D " O. N. Lars, ed., 2015.

[6] ClaRa.com. "ClaRa – Simulation of Clausius-Rankine cycles," 18th April 2016, 2016; http://claralib.com/.

[7] P. d. Milano. "ThermoPower - Open library for thermal power plant simulation," 10th Des 2015, 2015; http://thermopower.sourceforge.net/.

[8] O. Deneux, B. E. Hafni, B. Péchiné *et al.*, "Establishment of a Model for a Combined Heat and Power Plant with ThermosysPro Library," *Procedia Computer Science,* vol. 19, pp. 746-753, //, 2013.

[9] M. Gule, "Dynamic process simulation of thermal power plant on offshore oil and gas installations," March 11th, 2016, 2016.

[10] O. N. Lars, and B. Olav, "Steam bottoming cycles offshore - Challenges and possibilities," *Journal of Power Technologies,* vol. 92, no. 3, pp. 201, 2012.

[11] A. Benato, A. Stoppato, and A. Mirandola, "Dynamic behaviour analysis of a three pressure level heat recovery steam generator during transient operation," *Energy,* vol. 90, Part 2, pp. 1595-1605, 10//, 2015.

[12] Thermoflow.Inc. "Gas turbine combined cycle design program to create cycle heat balance and physical equipment needed to realize it," 08.08.2016, 2016; https://www.thermoflow.com/combinedcycle_GTP.html.

[13] D. S. AB. "Dymola," 29th April 2016, 2016; http://www.modelon.com/products/dymola/.

[14] R. Kehlhofer, F. Hannemann, F. Stirnimann *et al.*, *Combined-cycle gas & steam turbine power plants*, 3rd ed. ed., Tulsa, Okla: PennWell, 2009.

[15] Siemens, "BENSON HRSG Boilers - Reference List," Siemens, ed., 2016.

[16] T. Landon, " Once Through Steam Generators - Design, Operation, and Maintenance Considerations," in McIlvaine Company Hot Topic Hour, 2013.

[17] B. Olav, "Natural Gas Technology, Thermal power generation Autumn 2014," pp. 176, 2014.02.14, 2014.

[18] P. J. D. a. J.-P. Galopin, "ONCE-THROUGH HEAT RECOVERY STEAM GENERATORS WORKING WITH SUB- AND SUPERCRITICAL STEAM CONDITIONS FOR COMBINED CYCLES."

[19] Brady M. F., "Design aspects of once through systems for heat recovery steam generators for base load and cyclic operation," *Materials at High Temperatures,* vol. 18, no. 4, pp. 223-229, 2001.

[20] J. Franke, U. Lenk, R. Taud *et al.*, *Advanced Benson HRSG makes a successful debut*, London, ROYAUME-UNI: Global Trade Media, 2000.

[21] P. Fontaine, "Cycling Tolerance - Natural Circulation Vertical HRSGs," *ASME*, 16-19, 2003, 2003.

[22] V. Ganapathy, "Heat-recovery steam generators: understand the basics," *Chemical engineering progress,* vol. 92, no. 8, pp. 32-45, 1996.

[23] N. Mertens, F. Alobaid, R. Starkloff *et al.*, "Comparative investigation of drum-type and once-through heat recovery steam generator during start-up," *Applied Energy,* vol. 144, pp. 250-260, 4/15/, 2015.

[24] P. Fontaine, "Modélisation Dynamique d'une chaudière de récuparation'," BSc Thesis, Faculty of Applied Sciences, University of Liège, Belgium, 1990.

[25] Ø. Flatebø, "Off-design Simulations of Offshore - Combined Cycles," Master of Science in Mechanical Engineering, Department of Energy and Process Engineering, Norwegian University of Science and Technology, 2012.

[26] A. Rohatgi, "WebPlotDigitizer," *Web based tool to extract data from plots, images, and maps*, Ankit Rohatgi, 2016.

[27] F. David, and A. Souyri, "Modelling Steam Generators for Sodium Fast Reactor with Modelica." pp. 694-701.

[28] G. P. a. Water. "Causes of carryover," 06.09.2016, 2016; http://www.gewater.com/handbook/boiler_water_systems/ch_16_steampurity.jsp.

[29] F. Starr, “Background to the design of HRSG systems and implications for CCGT plant cycling.pdf,” *OMMI,* vol. 2, no. 1, pp. 17, April 2003, 2003.

[30] NEM-Energy, "Vertical OTSG Start-up," N. Energy, ed., 2015.

[31] P. Dechamps, "Modelling the transient behavior of combined cycle plants." pp. V004T10A001-V004T10A001.

[32] M. F. Brady, “Once-through Steam Generators Power Remote Sites,” *POWER ENGINEERING*, no. Innovative Steam Technologies, 06/01/1998, 1998.

[33] D. Lindsley, and I. o. E. Engineers, *Power-plant Control and Instrumentation: The Control of Boilers and HRSG Systems*: Institution of Electrical Engineers, 2000.

[34] ClaRa.com, “Clara Documentation Guide - GettingStarted,” 2015.

[35] K. Jonshagen, and M. Genrup, “Improved load control for a steam cycle combined heat and power plant,” *Energy,* vol. 35, no. 4, pp. 1694-1700, 4//, 2010.

[36] K. C. Cotton, *Evaluating and Improving Steam Turbine Performance*: Cotton Fact, 1998.

[37] P. Dechamps, “Modelling the transient behaviour of heat recovery steam generators,” *Proceedings of the Institution of Mechanical Engineers, Part A: Journal of Power and Energy,* vol. 209, no. 4, pp. 265-273, 1995.

[38] M. Richter, F. M. A. Starinski, G. Oeljeklaus *et al.*, “Flexibilization of coal-fired power plants by Dynamic Simulation,” *Gas,* vol. 20, no. 26.4, pp. 28.2, 2015.

[39] H. K. Versteeg, and W. Malalasekera, *An introduction to computational fluid dynamics: the finite volume method*: Pearson Education, 2007.

[40] H. G. Roos, “Thomas, JW: Numerical Partial Differential Equations. Finite Difference Methods. New York etc., Springer-Verlag 1995. XX, 437 pp., DM 78,-. ISBN 0-387-97999-9 (Texts in Applied Mathematics 22),” *ZAMM-Journal of Applied Mathematics and Mechanics/Zeitschrift für Angewandte Mathematik und Mechanik,* vol. 77, no. 5, pp. 386-386, 1997.

[41] OpenModelica, "Open Modelica Documentation - Homotopy," 2016.

[42] E. R. Følgesvold, “Combined heat and power plant on offshore oil and gas installations,” Master thesis, Department of Energy and Process Engineering, NTNU, Norwegian University of Science and Technology, Faculty of Engineering Science, 2015.

[43] K. Jordal, P. A. M. Ystad, R. Anantharaman *et al.*, “Design-point and part-load considerations for natural gas combined cycle plants with post combustion capture,” *International Journal of Greenhouse Gas Control,* vol. 11, pp. 271-282, 11//, 2012.

[44] T. L. v. 25, "8.1.3.8 Evaporator Circulation Help files," Thermoflow Ltd., 2016.

[45] K. Jonshagen, “Modern Thermal Power Plants-Aspects on Modelling and Evaluation,” Doctor Thesis, Department of Energy Sciences, Lund University, Room M:B, M-building, Ole Römers väg 1, Lund University, Faculty of Engineering, 2011.

[46] V. Ganapathy, “Design and evaluate finned tube bundles,” *Journal Name: Hydrocarbon Processing; Journal Volume: 75; Journal Issue: 9; Other Information: PBD: Sep 1996*, pp. Medium: X; Size: pp. 103-111, 1996.

[47] H. Walter, and R. Hofmann, “How can the heat transfer correlations for finned-tubes influence the numerical simulation of the dynamic behavior of a heat recovery steam generator?,” *Applied Thermal Engineering,* vol. 31, no. 4, pp. 405-417, 3//, 2011.

[48] K. Kawaguchi, K. Okui, and T. Kashi, “Heat transfer and pressure drop characteristics of finned tube banks in forced convection (comparison of the heat transfer characteristics between spiral fin and serrated fin),” *Heat Transfer—Asian Research,* vol. 34, no. 2, pp. 120-133, 2005.

[49] E. Næss, “Experimental investigation of heat transfer and pressure drop in serrated-fin tube bundles with staggered tube layouts,” *Applied Thermal Engineering,* vol. 30, no. 13, pp. 1531-1537, 9//, 2010.

[50] V. Gesellschaft, *VDI Heat Atlas*: Springer Berlin Heidelberg, 2010.

[51] R. Hofmann, F. Frasz, and K. Ponweiser, "Performance evaluation of solid and serrated finned-tube bundles with different fin geometries in forced convection." pp. 1-8.

[52] F. Frass, *Principles of finned-tube heat exchanger design for enhanced heat transfer*: Inst. f. Thermodynamics and Energy Conversion, Vienna University of Technology, 2007.

[53] A. Pop. "Open Source Modelica Consortium," 12/7/2016, 2016; https://www.openmodelica.org/home/consortium.

[54] GiTHUB. "GitHUB OpenModelica OMLibraries," https://github.com/OpenModelica/OMLibraries.

[55] F. Casella, "ThermoPower Modelica Library," Sourceforge.com, 2016.

[56] J. Munch Jensen, and H. Tummescheit, "Moving boundary models for dynamic simulations of two-phase flows," *Modelica'2002 Proceedings*, pp. 235-244, 2002.

[57] B. E. Hefni, "Dynamic Modeling of Concentrated Solar Power Plants with the ThermoSysPro Library (Parabolic Trough Collectors, Fresnel Reflector and Solar-Hybrid)," *Energy Procedia,* vol. 49, pp. 1127-1137, //, 2014.

[58] B. E. Hefni, "Modelling power plants with ThermoSysPro and OpenModelica," in MODPROD 2013, EDF, 2013.

[59] K. Hashizume, R. Morikawa, T. Koyama *et al.*, "Fin Efficiency of Serrated Fins," *Heat Transfer Engineering,* vol. 23, no. 2, pp. 6-14, 2002/03/01, 2002.

[60] R. K. Shah, and D. P. Sekulic, *Fundamentals of heat exchanger design*, p.^pp. page 282-283: John Wiley & Sons, 2003.

[61] R. Hofmann, F. Frasz, and K. Ponweiser, "Heat transfer and pressure drop performance comparison of finned-tube bundles in forced convection," *WSEAS Trans. Heat Mass Transfer,* vol. 2, no. 4, pp. 72-88, 2007.

[62] B. D. El Hefni Baligh, and L. Gregory, "Dynamic modelling of a combined cycle power plant with ThermoSysPro." pp. 365-375.

17 APPENDIX

17.1Appendix: ESCOA implementation by V.Ganapathy

The following implementation of the heat transfer and gas pressured drop with finned tubes is found with V.Ganapathy (ABCO Industries, Abilene, Texas) [46] from 1996. The whole implementation is to be set from imperial units to SI-units, with comments on uncertainties. Not that this model was not validate nor completed in the final work and may only help as a guideline for future work implementing the ESCOA. Furthermore, it is suggested to use the equations directly, and do the conversion later in output numbers.

Unit explanation are found in the original paper by V.Ganapathy [46] from 1996.

Imperial	SI	Case calculations
$h_c = C_1 C_3 C_5 \left[\frac{d+2h}{d}\right]^{0.5} \left(\frac{T_g}{T_{fa}}\right)^{0.25} G \cdot C_p \left(\frac{k}{\mu C_p}\right)^{0.67}$	Same	T_f = ?
$G = \frac{W_g}{N_w L(\frac{S_t}{12} - A_0)}$ [lb/ft^2*hr] $\left[\frac{kg}{s \cdot m^2}\right]$	Remove 12. Inch to feet conv.	W_g = 78.4 kg/s Nw = tube rows wide (28) L = 7.127m St = trans pinch = 0.07142m
$A_0 = \frac{d}{12} + nbh/6$	Remove 12 (inch->feet) Assuming 6 rows, but number is	d = 31.75mm n = 309.7fins/m b = 1.00mm h = 9.525mm

	negligible with this calculation. n:#fins/inch, b:fin thickness, h:fin height	
$s = \left(\frac{1}{n}\right) - b$	Fin spacing	b = 1.00mm n = 309.7fins/m
$Re = Gd/12\mu$	d [inch] -> why div:12	μ = viscosity. Check units.
$\eta = 1 - [(1 - E)A_f/A_t$	Same	E: fin efficiency
$A_f = \pi dn[2h(ws + b) + bws]/12ws$	12: div 12 x – remove. [inch->feet]	
$A_t = A_f + \frac{\pi d(1-nb)}{12ws}$	Remove 12 for inch->feet	
$E = \tanh(mh)/mh$	Same	
$m = \sqrt{\frac{24h_0(b + ws)}{Kbws}}$	Remove 24 for inch->feet conversion	

17.2 Off-design 60 percent GT load

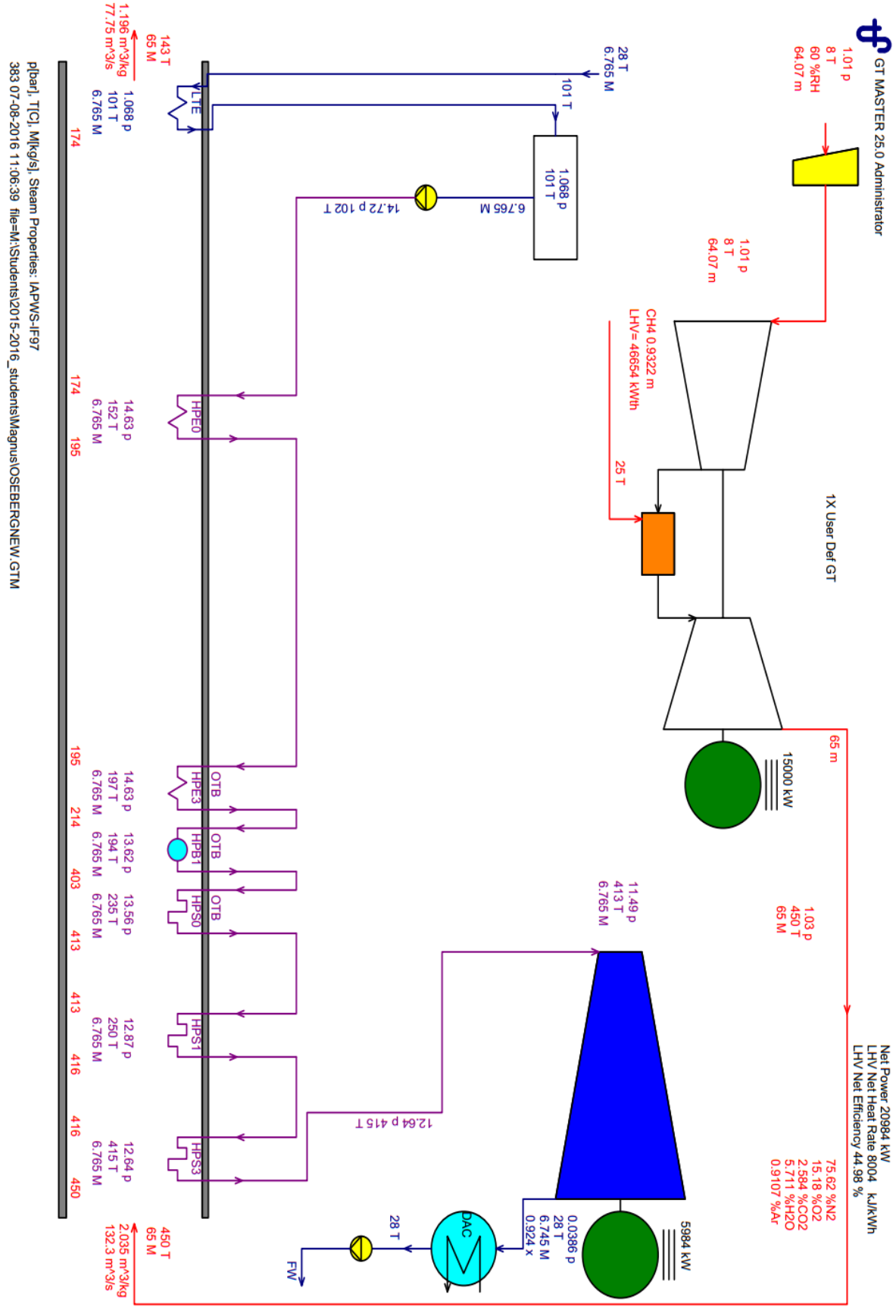

HPS3 Hardware Design (water/steam DP by user)

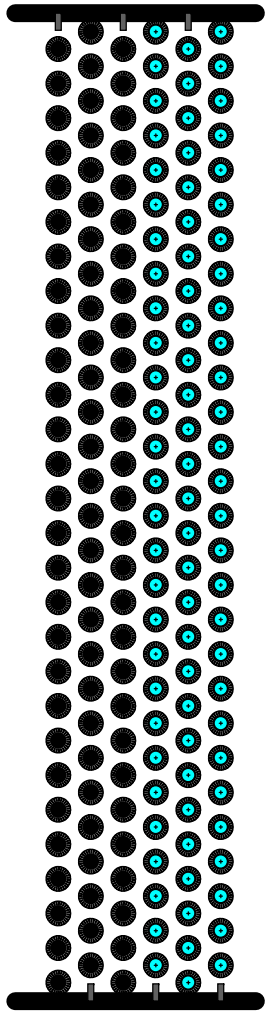

HPS3
6 tube rows
28 tubes per row
Pl = 70 mm
Pt = 71.42 mm

Gas Out
439.9 T
78.4 m

Gas In
480 T
78.4 m

Steam In
16.94 p
250 T
2916.1 h
8.748 m

Steam Out
16.5 p
430.1 T
3319 h
8.748 m

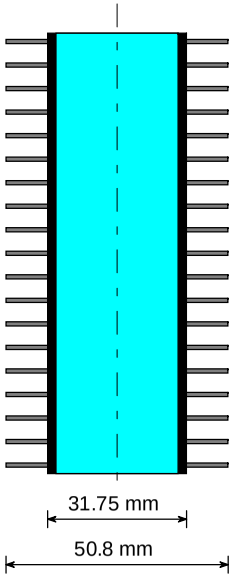

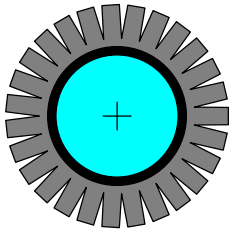

Fin-tube type	Serrated fins
Tube arrangement	Staggered
Fin material	TP409
Tube material	Incoloy
Tube outer diameter	31.75 mm
Tube wall thickness	1.905 mm
Fin height	9.525 mm
Fin spacing	4.373 mm
Fin thickness	1 mm
Number of fins per meter	186.1
Serrated fin segment width	3.97 mm
# of serrated fin segments	26.63
Un-serrated height / fin height	0.2
Longitudinal row pitch	70 mm
Transverse tube pitch	71.42 mm
# of tube rows (longitudinal)	6
# of rows per pass	3
# of tubes per row (transverse)	28
Tube length	7.127 m
Gas path transverse width	2.036 m
Gas path frontal area	14.51 m^2
HX total outside surface area	660.9 m^2
Maximum gas velocity	22.93 m/s
Gas pressure drop	4.295 millibar
Steam side velocity	27.81 m/s
Steam side DP from hardware	0.2842 bar
Heat transfer from gas	3555 kW
Heat transfer to steam	3529 kW

Flow out of drawing
Flow into drawing
p[bar] T[C] m[kg/s] h[kJ/kg]

0 150 mm

0 50 mm

Thermoflow, Inc.	Company: Norwegian University of Science and Technology
	User: Administrator
	HPS3
Date: 11.13.15	
Drawing No:	

HPS1 Hardware Design (water/steam DP by user)

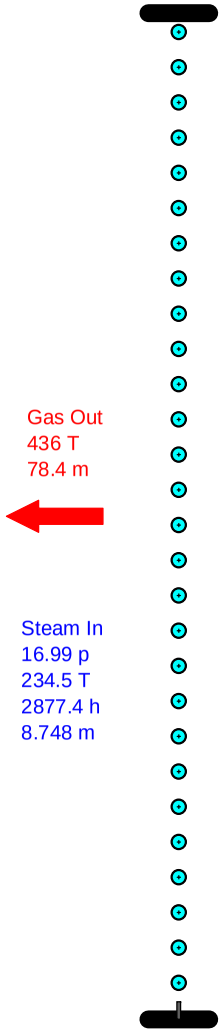

HPS1
1 tube row
28 tubes per row
Pl = 70 mm
Pt = 72.88 mm

Gas Out
436 T
78.4 m

Gas In
439.9 T
78.4 m

Steam In
16.99 p
234.5 T
2877.4 h
8.748 m

Steam Out
16.94 p
250 T
2916.1 h
8.748 m

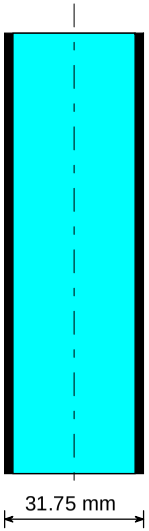

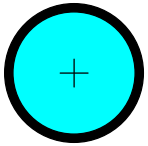

Fin-tube type	Bare
Tube arrangement	Staggered
Fin material	N/A
Tube material	Incoloy
Tube outer diameter	31.75 mm
Tube wall thickness	1.905 mm
Fin height	N/A
Fin spacing	N/A
Fin thickness	N/A
Number of fins per meter	N/A
Serrated fin segment width	N/A
# of serrated fin segments	N/A
Un-serrated height / fin height	N/A
Longitudinal row pitch	70 mm
Transverse tube pitch	72.88 mm
# of tube rows (longitudinal)	1
# of rows per pass	1
# of tubes per row (transverse)	28
Tube length	7.127 m
Gas path transverse width	2.036 m
Gas path frontal area	14.51 m^2
HX total outside surface area	19.86 m^2
Maximum gas velocity	19.58 m/s
Gas pressure drop	0.2623 millibar
Steam side velocity	66.72 m/s
Steam side DP from hardware	0.8659 bar
Heat transfer from gas	341.2 kW
Heat transfer to steam	338.7 kW

Flow out of drawing
Flow into drawing
p[bar] T[C] m[kg/s] h[kJ/kg]

0 150 mm

0 50 mm

Thermoflow, Inc.	Company: Norwegian University of Science and Technology
	User: Administrator
	HPS1
Date: 11.13.15	
Drawing No:	

HPS0 (OTB) Hardware Design (water/steam DP by user)

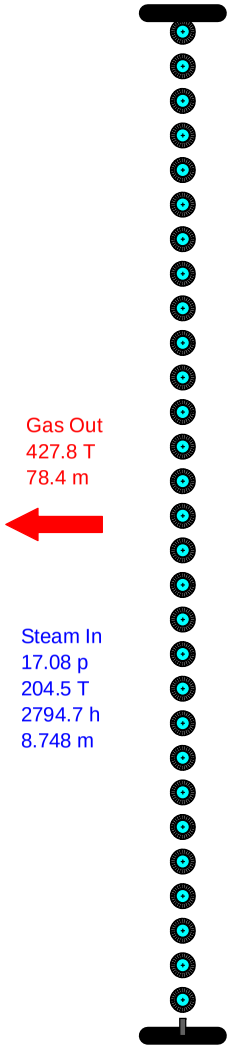

HPS0 (OTB)
0.5095 tube row
29 tubes per row
Pl = 70 mm
Pt = 71.42 mm

Gas Out
427.8 T
78.4 m

Gas In
436 T
78.4 m

Steam In
17.08 p
204.5 T
2794.7 h
8.748 m

Steam Out
16.99 p
234.5 T
2877.4 h
8.748 m

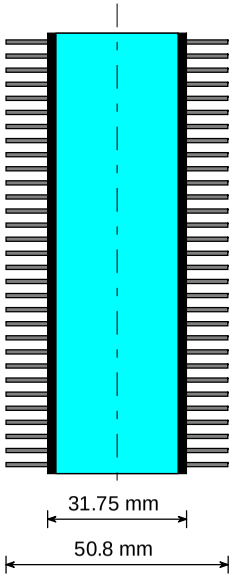

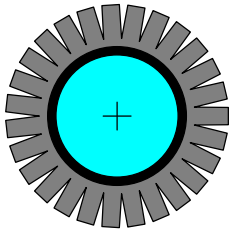

Fin-tube type	Serrated fins
Tube arrangement	Staggered
Fin material	TP409
Tube material	Incoloy
Tube outer diameter	31.75 mm
Tube wall thickness	1.905 mm
Fin height	9.525 mm
Fin spacing	2.229 mm
Fin thickness	1 mm
Number of fins per meter	309.7
Serrated fin segment width	3.97 mm
# of serrated fin segments	26.63
Un-serrated height / fin height	0.2
Longitudinal row pitch	70 mm
Transverse tube pitch	71.42 mm
# of tube rows (longitudinal)	0.5095
# of rows per pass	2
# of tubes per row (transverse)	29
Tube length	7.127 m
Gas path transverse width	2.036 m
Gas path frontal area	14.51 m^2
HX total outside surface area	88.12 m^2
Maximum gas velocity	23.18 m/s
Gas pressure drop	0.5651 millibar
Steam side velocity	30.56 m/s
Steam side DP from hardware	0.0537 bar
Heat transfer from gas	729.1 kW
Heat transfer to steam	723.6 kW

Flow out of drawing
Flow into drawing
p[bar] T[C] m[kg/s] h[kJ/kg]

0 150 mm

0 50 mm

Thermoflow, Inc.	Company: Norwegian University of Science and Technology
	User: Administrator
	HPS0 (OTB)
Date: 11.13.15	
Drawing No:	

HPB1 (OTB) Hardware Design

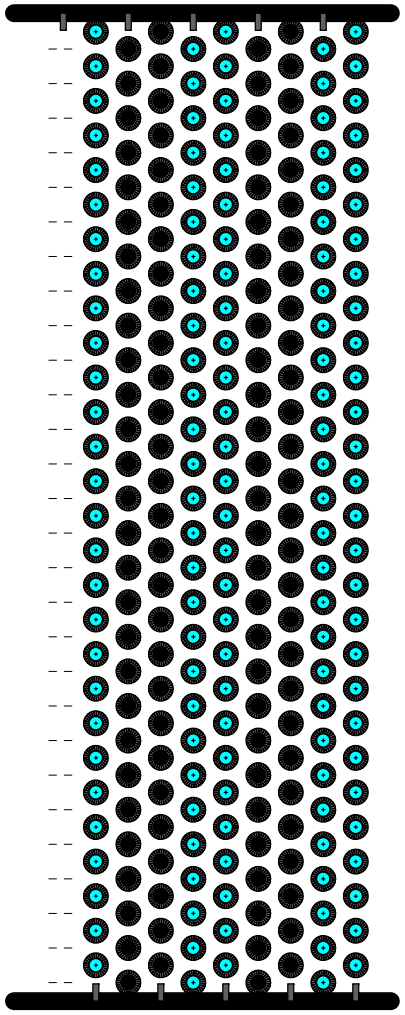

HPB1 (OTB)
15.62 tube rows
28 tubes per row
Pl = 70 mm
Pt = 71.42 mm

Gas Out
231.9 T
78.4 m

Gas In
427.8 T
78.4 m

Water In
17.93 p
206.9 T
883.8 h
8.748 m

Steam Out
17.08 p
204.5 T
2794.7 h
8.748 m

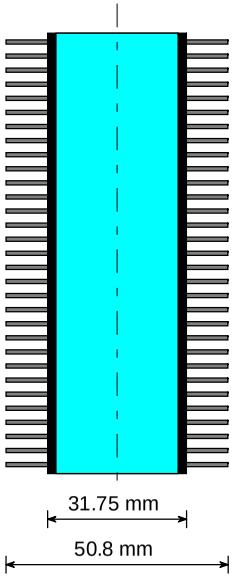

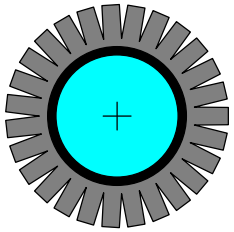

Fin-tube type	Serrated fins
Tube arrangement	Staggered
Fin material	TP409
Tube material	Incoloy
Tube outer diameter	31.75 mm
Tube wall thickness	1.905 mm
Fin height	9.525 mm
Fin spacing	2.229 mm
Fin thickness	1 mm
Number of fins per meter	309.7
Serrated fin segment width	3.97 mm
# of serrated fin segments	26.63
Un-serrated height / fin height	0.2
Longitudinal row pitch	70 mm
Transverse tube pitch	71.42 mm
# of tube rows (longitudinal)	15.62
# of rows per pass	2
# of tubes per row (transverse)	28
Tube length	7.127 m
Gas path transverse width	2.036 m
Gas path frontal area	14.51 m^2
HX total outside surface area	2654.1 m^2
Maximum gas velocity	20.18 m/s
Gas pressure drop	13.26 millibar
Water side velocity	0.2969 m/s
Water side DP from hardware	1.335 bar
Heat transfer from gas	16842 kW
Heat transfer to steam/water	16717 kW

Flow out of drawing
Flow into drawing
p[bar] T[C] m[kg/s] h[kJ/kg]

0 150 mm

0 50 mm

Thermoflow, Inc.	Company: Norwegian University of Science and Technology
	User: Administrator
	HPB1 (OTB)
Date: 11.13.15	
Drawing No:	

HPE3 (OTB) Hardware Design (water/steam DP by user)

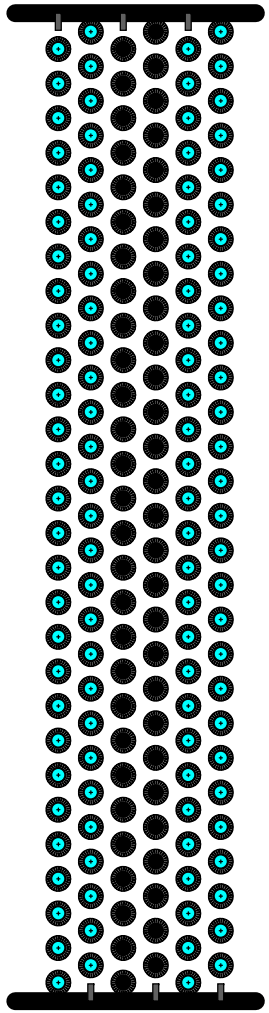

HPE3 (OTB)
5.876 tube rows
28 tubes per row
Pl = 70 mm
Pt = 71.42 mm

Gas Out
206.9 T
78.4 m

Gas In
231.9 T
78.4 m

Water In
18.2 p
152.8 T
645.2 h
8.748 m

Water Out
17.93 p
206.9 T
883.8 h
8.748 m

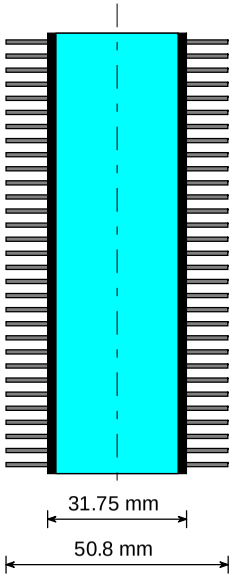

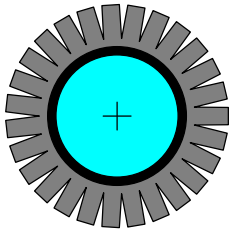

Fin-tube type	Serrated fins
Tube arrangement	Staggered
Fin material	TP409
Tube material	Incoloy
Tube outer diameter	31.75 mm
Tube wall thickness	1.905 mm
Fin height	9.525 mm
Fin spacing	2.229 mm
Fin thickness	1 mm
Number of fins per meter	309.7
Serrated fin segment width	3.97 mm
# of serrated fin segments	26.63
Un-serrated height / fin height	0.2
Longitudinal row pitch	70 mm
Transverse tube pitch	71.42 mm
# of tube rows (longitudinal)	5.876
# of rows per pass	2
# of tubes per row (transverse)	28
Tube length	7.127 m
Gas path transverse width	2.036 m
Gas path frontal area	14.51 m^2
HX total outside surface area	998.5 m^2
Maximum gas velocity	16.48 m/s
Gas pressure drop	4.039 millibar
Water side velocity	0.2869 m/s
Water side DP from hardware	0.008 bar
Heat transfer from gas	2102.7 kW
Heat transfer to water	2087.1 kW

Flow out of drawing
Flow into drawing
p[bar] T[C] m[kg/s] h[kJ/kg]

0 150 mm

0 50 mm

Thermoflow, Inc.	Company: Norwegian University of Science and Technology
	User: Administrator
	HPE3 (OTB)
Date: 11.13.15	
Drawing No:	

HPE0 Hardware Design (water/steam DP by user)

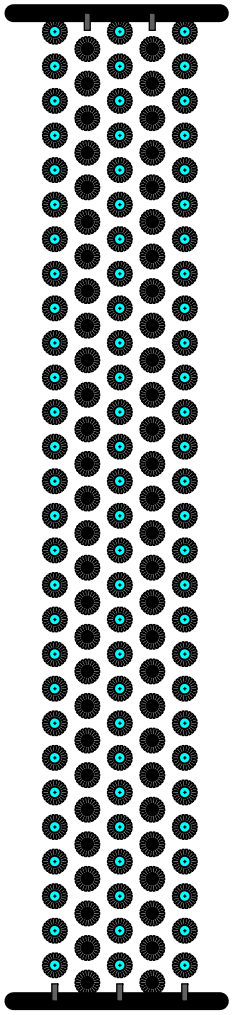

HPE0

5 tube rows
28 tubes per row
Pl = 70 mm
Pt = 71.42 mm

Gas Out
183.8 T
78.4 m

Gas In
206.9 T
78.4 m

Water In
18.44 p
101.5 T
426.7 h
8.748 m

Water Out
18.2 p
152.8 T
645.2 h
8.748 m

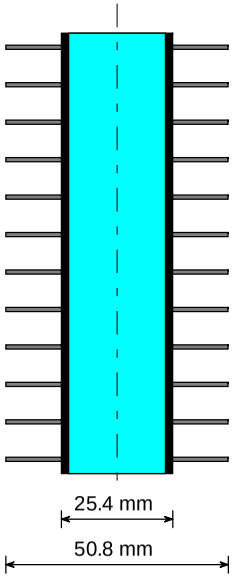

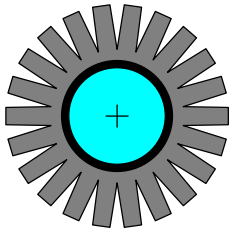

Fin-tube type	Serrated fins
Tube arrangement	Staggered
Fin material	TP409
Tube material	Incoloy
Tube outer diameter	25.4 mm
Tube wall thickness	1.651 mm
Fin height	12.7 mm
Fin spacing	7.557 mm
Fin thickness	1 mm
Number of fins per meter	116.9
Serrated fin segment width	3.97 mm
# of serrated fin segments	22.11
Un-serrated height / fin height	0.2
Longitudinal row pitch	70 mm
Transverse tube pitch	71.42 mm
# of tube rows (longitudinal)	5
# of rows per pass	1
# of tubes per row (transverse)	28
Tube length	7.127 m
Gas path transverse width	2.036 m
Gas path frontal area	14.51 m^2
HX total outside surface area	393.3 m^2
Maximum gas velocity	12.3 m/s
Gas pressure drop	1.384 millibar
Water side velocity	0.868 m/s
Water side DP from hardware	0.1442 bar
Heat transfer from gas	1925.8 kW
Heat transfer to water	1911.4 kW

Flow out of drawing
Flow into drawing
p[bar] T[C] m[kg/s] h[kJ/kg]

0 150 mm

0 50 mm

Thermoflow, Inc.	Company: Norwegian University of Science and Technology
	User: Administrator
	HPE0
Date: 11.13.15	
Drawing No:	

LTE Hardware Design (water/steam DP by user)

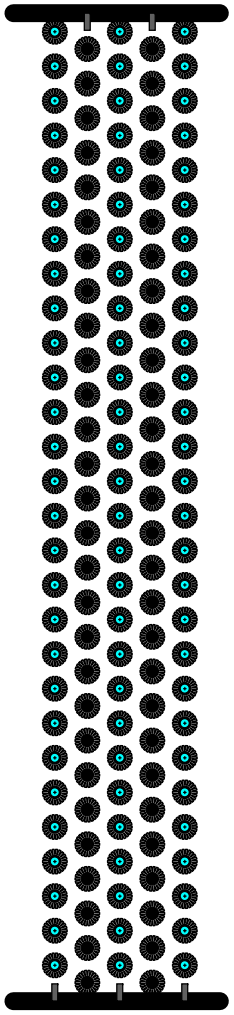

LTE
5 tube rows
28 tubes per row
Pl = 70 mm
Pt = 71.42 mm

Gas Out
153.8 T
78.4 m

Gas In
183.8 T
78.4 m

Water In
1.086 p
33.66 T
141 h
8.748 m

Water Out
1.054 p
101.1 T
423.7 h
8.748 m

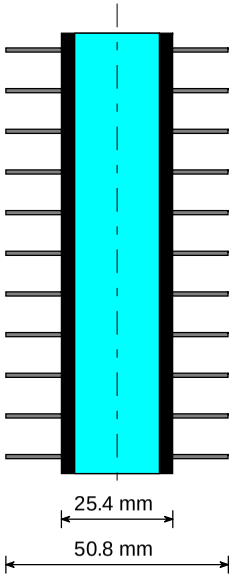

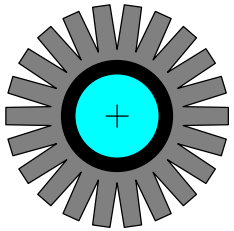

Fin-tube type	Serrated fins
Tube arrangement	Staggered
Fin material	TP409
Tube material	Incoloy
Tube outer diameter	25.4 mm
Tube wall thickness	3.048 mm
Fin height	12.7 mm
Fin spacing	8.303 mm
Fin thickness	1 mm
Number of fins per meter	107.5
Serrated fin segment width	3.97 mm
# of serrated fin segments	22.11
Un-serrated height / fin height	0.2
Longitudinal row pitch	70 mm
Transverse tube pitch	71.42 mm
# of tube rows (longitudinal)	5
# of rows per pass	1
# of tubes per row (transverse)	28
Tube length	7.127 m
Gas path transverse width	2.036 m
Gas path frontal area	14.51 m^2
HX total outside surface area	368.2 m^2
Maximum gas velocity	11.54 m/s
Gas pressure drop	1.209 millibar
Water side velocity	1.09 m/s
Water side DP from hardware	0.2856 bar
Heat transfer from gas	2491 kW
Heat transfer to water	2472.5 kW

Flow out of drawing
Flow into drawing
p[bar] T[C] m[kg/s] h[kJ/kg]

0 150 mm

0 50 mm

Thermoflow, Inc.	Company: Norwegian University of Science and Technology
	User: Administrator
	LTE
Date: 11.13.15	
Drawing No:	